

Assembly of DNA-like Structures Containing Anthraquinone, Tetrathiafulvalene and Perylene Diimide Building Blocks

Inauguraldissertation
der Philosophisch-naturwissenschaftlichen Fakultät
der Universität Bern

vorgelegt von
Nicolas Bouquin
aus Frankreich

Leiter der Arbeit:
Prof. Dr. R. Häner
Departement für Chemie und Biochemie der Universität Bern

Assembly of DNA-like Structures Containing Anthraquinone, Tetrathiafulvalene and Perylene Diimide Building Blocks

Inauguraldissertation
der Philosophisch-naturwissenschaftlichen Fakultät
der Universität Bern

vorgelegt von
Nicolas Bouquin
aus Frankreich

Leiter der Arbeit:
Prof. Dr. R. Häner
Departement für Chemie und Biochemie der Universität Bern

Von der Philosophisch-naturwissenschaftlichen Fakultät angenommen.

Bern, den 23. May 2008

Der Dekan:
Prof. Dr. P. Messerli

This work was supported by the University of Bern and the Swiss National Science Foundation.

Acknowledgements

I would like to thank many people that have marked my life and work in Bern.

First of all, I am very grateful to Prof. Dr. Robert Häner, who not only supervised my work, but also gave me the necessary support to complete it successfully. Our discussion resulted in new ideas and valuable input to my work.

Thanks to Prof. Dr. Silvio Decurtins and Prof. Dr. Jonathan Hall having accepted to carefully read my manuscript and evaluate my work.

The realization of this work would not be possible without the people from MS group and *Ausgabe* whom I would like to thank also. I would like to mention Ms. Rosmarie Rohner, who was always helpful and optimistic about any administrative obstacles.

During my stay in Bern I was accompanied by excellent colleagues Ivan Trkulja, Florent Samain, Dr. Holger Bittermann and Dr. Jean-Paul Bianké. With their support and optimistic attitude they helped me through all the ups and downs. I owe a lot of gratitude to Dr. Vladimir Malinovskii for his guidance and priceless advice. Thanks to: André Mätzener, Daniel Wenger and Luzia Moesch and all the other former members of the Häner group.

I finally also would like to thank my family, my friends and my girl friend who always motivated me during the thesis.

List of Publications:

1. N. Bouquin, V. L. Malinovskii and R. Häner, **Anthraquinones as Artificial DNA Building Blocks**, *E. J. Org. Chem.*, **2008**, in press.

2. N. Bouquin, V. L. Malinovskii, Xavier Guégano, Shi-Xia Liu, Silvio Decurtins and R. Häner, **TTF-Modified DNA**, submitted.

3. N. Bouquin, V. L. Malinovskii and R. Häner, **Highly efficient quenching of excimer fluorescence by perylene diimide in DNA**, *Chem. Comm.*, **2008**, accepted.

« Nothing in life is to be feared, it is only to be understood. Now is the time to understand more, so that we may fear less. »

Marie Curie (1867-1934)

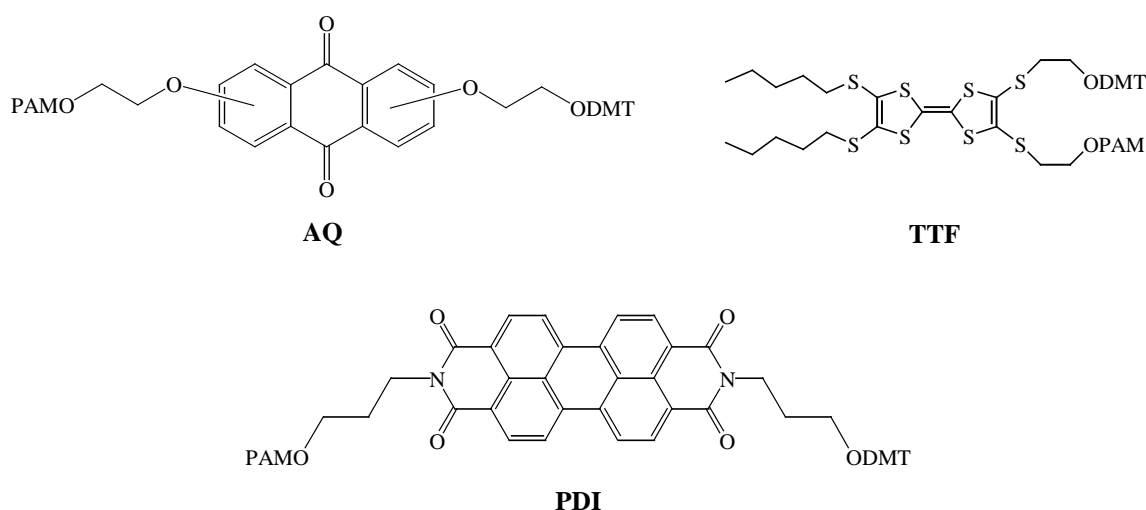
Table of Contents

<i>Summary</i>	1
1. Introduction	3
1.1 History of DNA	3
1.2 Structure of DNA	5
1.3 Stabilisation of DNA by Two Major Interactions	7
1.3.1 Hydrogen Bonds	8
1.3.2 π - π Stacking Interactions	8
1.4 Different DNA Architectures	9
1.4.1 Branched DNA	10
1.4.2 DNA Triplexes	10
1.4.3 DNA Quadruplexes	11
1.5 Chemical Modifications of Nucleotides	12
1.6 New Modified DNA Building Blocks	14
1.6.1 Non-nucleosidic Base Surrogates	14
1.6.2 Interstrand Stacking Building Blocks	14
1.6.3 Fluorophores and Quenchers in DNA	16
1.7 Electron-Acceptor and Electron-Donor Molecules	17
1.7.1 Electron-Acceptor Molecules	17
1.7.2 Electron-Donor Molecules	18
1.7.3 Donor-Acceptor systems with TTF	19
1.7.4 Anthraquinone, TTF and PDI incorporated into DNA	20
1.8 Aim of the work	22
2. Anthraquinones as Artificial DNA Building Blocks	29
2.1 Abstract	29
2.2 Introduction	29
2.3 Results and Discussion	30
2.4 Conclusions	38
2.5 Experimental Part	38

3. TTF-Modified DNA	47
3.1 Abstract	47
3.2 Introduction	47
3.3 Results and Discussion	48
3.4 Conclusions	55
3.5 Experimental Part	55
4. Highly Efficient Quenching of Excimer Fluorescence by Perylene Diimide in DNA	62
4.1 Abstract	62
4.2 Introduction	62
4.3 Results and Discussion	63
4.4 Conclusions	70
4.5 Experimental Part	70
5. Formation of a One- and a Two-Dimensional DNA Scaffold Containing Pyrene Building Blocks	77
5.1 Abstract	77
5.2 Introduction	77
5.3 Results and Discussion	78
5.3.1 One-Dimensional DNA Scaffold	78
5.3.2 Two-Dimensional DNA Scaffold	85
5.4 Conclusions	92
5.5 Experimental part	92
6. Conclusions and Outlook	97
Annexes	99
Annex 1 Chemical Synthesis of Oligonucleotides	99
Annex 2 DNA Single Strands Containing Pyrene Units	103

Summary

Modified oligonucleotides have found widespread applications as diagnostic and research tools. The combination of the natural oligonucleotides with novel, synthetic building blocks leads to a large increase in the number of possible constructs and applications. Our work aimed at the design and synthesis of structural DNA-mimics. We decided to study the properties of several polyaromatic building blocks in DNA-duplexes. These non-nucleosidic base surrogates should be suitable for arrangement in an interstrand stacking mode and for an increase in DNA hybrid stability. We focused our study on electro-donor and electro-acceptor building blocks: tetrathiafulvalene, anthraquinone and perylene diimide (*Scheme 1*).



Scheme 1. AQ, TTF and PDI building blocks used for our study.

In the first part of the work, four isomeric anthraquinone building blocks (AQ) differing in the site of linker attachment were synthesized and incorporated into oligodeoxynucleotides. The site of linker attachment was found to have a strong influence on the stability. Effectively, a pair of the 2,6-isomer shows an increase in stability for DNA duplex. On the other hand, hybrids containing a pair of the 1,4-, 1,5- and 1,8-isomers led to a substantial reduction in stability. Molecular models suggest that the positive effect of the 2,6-isomer is a result of interstrand stacking interaction between the two anthraquinones. All anthraquinone building blocks act as fluorescence quenchers if placed opposite to two pyrenes. These anthraquinone derivatives can be useful building blocks for diagnostic tools or for applications in DNA-based nanomaterials.

In the second part, a tetrathiafulvalene derivative building block (TTF) was synthesized and incorporated into DNA. Its spectroscopical properties and its behaviour on DNA stability were investigated. TTF-modified oligonucleotides form stable hybrids and photo-induced electron transfer was demonstrated by fluorescence quenching in TTF/pyrene modified heterohybrids. Finding shown in this study represent a setting for the development of TTF-oligonucleotide based redox-active and optical sensors.

In the third part of the thesis, a perylene diimide building block (PDI) was synthesized and incorporated into DNA. Oligonucleotides containing one or two non-nucleosidic perylene diimide building blocks form stable duplexes. Fluorescence spectroscopy shows that two PDI opposite to two pyrene units are a powerful quencher for pyrene excimer. It was interesting to observe that a strong fluorophore like the PDI in the presence of DNA and water environment is not fluorescent. On the other hand, in the presence of another fluorophore like the pyrene which is able to form excimer, the PDI is able to quench completely the signal of this excimer. Highly effective excimer quenching is important for many types of DNA based molecular probes. The present system may help in the design of future diagnostic tools.

Chapter 1. Introduction

DNA or deoxyribonucleic acid is a nucleic acid that contains the genetic information for the development and functioning of living organisms. The main role of DNA in the cell is the long-term storage of information. The revelation of the structure of DNA was one of the biggest scientific challenges of the twentieth century.

1.1 History of DNA

F. Miescher, a Swiss biologist discovered nucleic acid in **1869**. He isolated various phosphate-rich chemicals by threatening wounded soldiers during the Franco-Prussian War, which he called nuclein.¹ In **1879**, *A. Kossel*, a German biochemist found that nucleic acids consist of nitrogen-containing bases, such as thymine, cytosine and uracil.² *E. Fischer* received in **1902** the Nobel Prize for basic research on sugars, purines, uric acid, enzymes, nitric acid and ammonia.³ *P. Levene* identified the base, sugar and phosphate nucleotide units in **1929**.⁴ *O. Avery*, *C. MacLeod* and *M. MacCarty* published the first experiment demonstrating that DNA was a genetic material in **1944**.⁵ In the late **1940s**, *E. Chargaff* found that the proportions of purines, adenine (A) and guanine (G) was always equal to the proportion of pyrimidines, thymine (T) and cytosine (C).⁶ In **1952**, *R. Signer* provides a sample of very pure DNA which gave X-ray diffraction of high quality.⁷ In **1953**, the molecular biologists *J. D. Watson*, an American and *F. H. Crick*, an Englishman, proposed that the two DNA strands were coiled in a double helix.⁸ In this model each nucleotide subunit along one strand is bound to a nucleotide subunit on the other strand by hydrogen bonds between the base portions of the nucleotides. The fact that adenine pairs only with thymine (A-T) and guanine pairs only with cytosine (G-C) determines that the strands will be complementary (*Figure 1.1*). In **1955**, *Chargaff and Davidson* published a set of three volumes on “The Nucleic Acids”, describing in great detail their physical properties and characterisation. In **1959**, RNA polymerase was discovered by Severo Ochoa and Arthur

Cornberg.⁹ In **1961**, *Jacob* and *Monod* proved that messenger RNA transfers the genetic informations.¹⁰ The Nobel Price in Medicine was awarded to *Watson*, *Crick* and *M. Wilkins* in **1962** for their accomplishments. It is in **1977** that DNA sequencing was discovered and published by *Maxam* and *Gilbert*.¹¹ In **1990** the the Human Genome Poject started with the goal to identify all of the approximately 30000 genes in human DNA, to determine the sequences of the 3 billion chemical base pairs that make up the human DNA and to store this information in databases within 15 years. In **1997**, *Dolly*, a sheep, was cloned successfully and the *E. coli* genome was sequenced. The Human Genome Project ended in **2003** with the completion of the human genetic sequence.

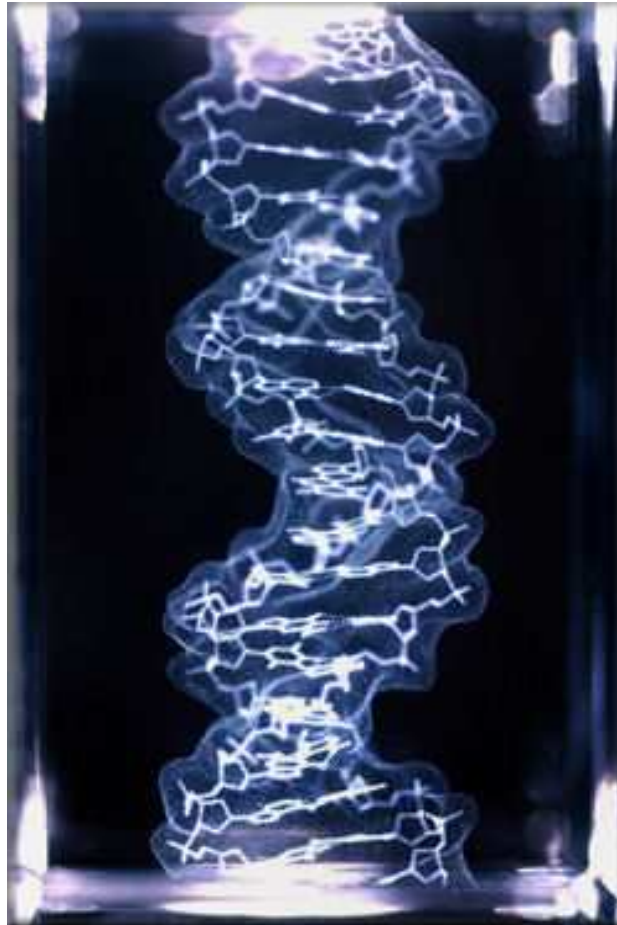


Figure 1.1 DNA double helix model.¹²

1.2 Structure of the DNA Double Helix

DNA is a long polymer of repeating units called nucleotides with a backbone made of sugars and phosphate groups joined by ester bonds. There are four major nucleobases : adenine (A), thymine (T), guanine (G) and cytosine (C). Two of them are called purines (A, G) and the two other one pyrimidines (T, C). These nucleobases are linked at the C(1') position of a pentose sugar (forming nucleosides) and the phosphate ester is attached at the O(3') and the O(5') positions of this sugar. Two DNA single strands are able to form a DNA duplex by Watson-Crick base-pairing (*Figure 1.2*). This base-pairing takes place because purines form hydrogen bonds to pyrimidines with A bonding only to T, and C bonding only to G.

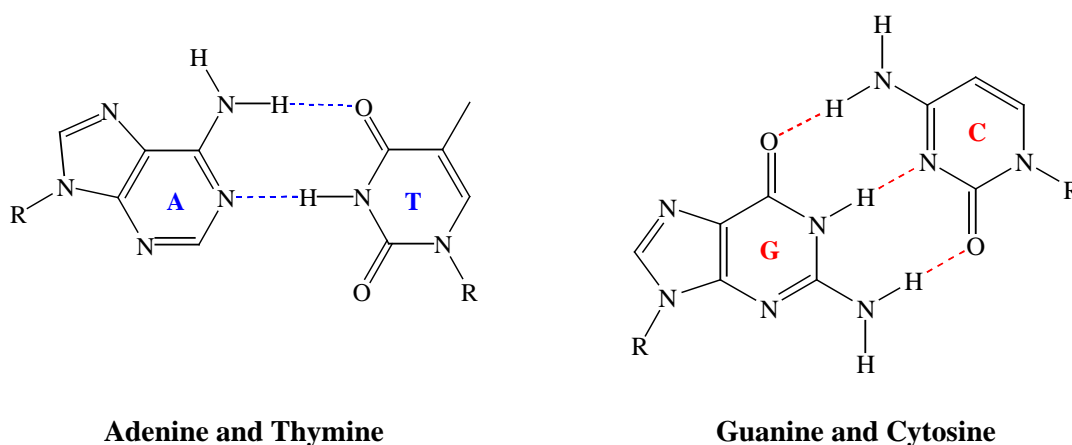


Figure 1.2 Watson-Crick base pairs for A-T and G-C.

As the DNA strands wind around each other, they leave gaps between each set of phosphate backbones, revealing the sides of the bases inside. There are two of these grooves twisting around the surface of the double helix: one groove, the major groove, is 22 Å wide and the other, the minor groove, is 12 Å wide (*Figure 1.3*).¹³ The narrowness of the minor groove means that the edges of the bases are more accessible in the major groove.

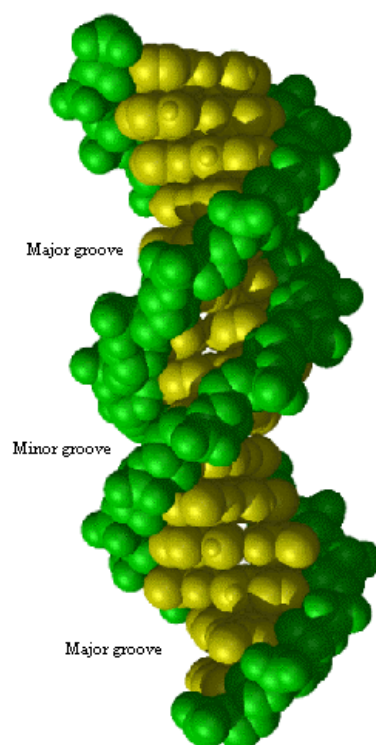


Figure 1.3 Structure of B-DNA showing the location of the major and minor grooves.¹⁴

DNA can adopt three types of major conformations: A-DNA, B-DNA and Z-DNA (*Figure 1.4*).

B-DNA has a right-handed conformation. In fully hydrated form, DNA duplexes will commonly exist in the B-form. This form has 10 bases per turn with a wide major groove and a narrow minor groove. The distance between neighbouring base-pairs is 3.3-3.4 Å. The bases are located near to the axis and the C2'-*endo* sugar pucker is typical for a B-duplex. The dislocation of the base-pairs from the axis varies between 0.2 and 1.8 Å.

A-DNA has also a right-handed conformation and is usually observed when DNA is dehydrated *in vitro*. The helix contains 11 bases per turn and the major groove is narrow and deep and the minor groove is broad and shallow. The distance between the neighbouring base-pairs is 2.9 Å and the axis is pushed away from the base pair. This dislocation base-pairs from the axis is 4.5 Å which is very different from B-DNA. The sugar puckering mode C3'-*endo* is observed for a A-DNA conformation.

Z-DNA has a left-handed conformation and can be formed under high salt concentration with G/C DNA sequences. In Z-DNA, the purines are in a *syn conformation* while pyrimidines are in an anti conformation maintaining Watson-Crick base pairing. The number of bases per turn is 12 and the major groove is shallow and the minor groove is narrow and deep. The distance between the neighbouring base pairs is 3.7 Å. The sugar pucker mode is C2'-*endo* in pyrimidine and C3'-*endo* in purine where the dislocation of the base-pairs from the axis varies between 2 and 3 Å.

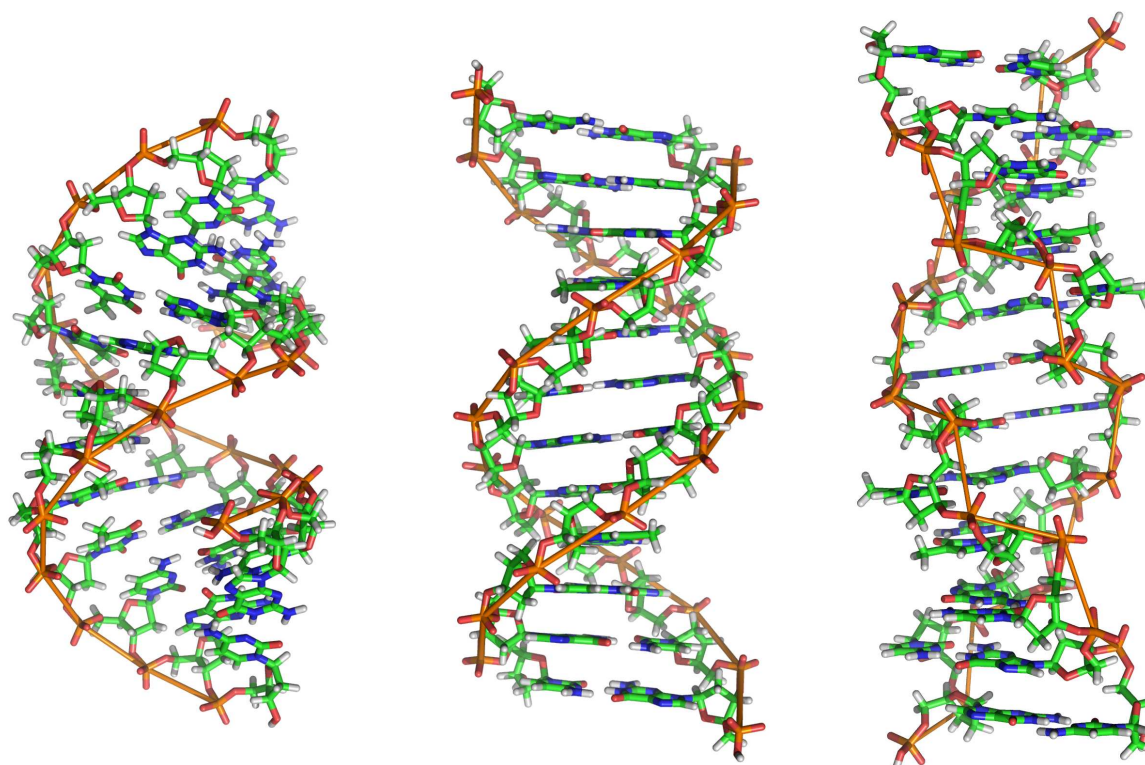


Figure 1.4 A-DNA (left), B-DNA (middle), Z-DNA (right).¹⁵

1.3 Stabilisation of DNA by Two Major Interactions

In DNA duplex conformations, the helix is stabilized by two major interactions: the hydrogen bonds and the stacking interactions between the nucleotide bases.

1.3.1 Hydrogen Bonds

A hydrogen bond is an attractive inter- or intramolecular force that exists between two partial electric charges of opposite polarity: the bond exists between a hydrogen atom and an electronegative heteroatom. The hydrogen bond is much weaker than the ionic or the covalent bonds but stronger than most other intermolecular forces. Hydrogen bonds can be formed between two molecules and the resulting associate can be quite stable. Hydrogen bonds have an important role in the structure of nucleic acids. The Watson-Crick hydrogen bonds are responsible for the A-T and G-C pairing in the duplex.¹⁶ Numerous experimental and theoretical works have been devoted to the study and characterisation of nucleic acid hydrogen bonds.¹⁷⁻²³

1.3.2 π - π Stacking Interactions

Stacking in supramolecular chemistry refers to a stacked arrangement of aromatic molecules, which interact through π - π stacking interactions. One of the most popular examples of a stacked system refers to the DNA base-pairs (*Figure 1.5*). Stacking also occurs in proteins where two aromatic rings have overlapping π -orbitals. The exact nature of such interactions (electrostatic or nonelectrostatic) is a matter of debate but there are several known factors that can contribute to the stacking between the DNA base pairs.²⁴

The first of them is the Van der Waals interactions which correspond to the sum of the dispersion and repulsion energies and is varied with r^{-6} (r = distance between the nuclear positions of the atoms). The second factor is the electrostatic interactions between partial atomic charges where electronegative atoms like nitrogen or oxygen polarize the electron density of heteroaromatic molecules such as nucleobases and so these atoms and neighbouring atoms are associated with partial atomic charges. These interactions vary with r^{-1} according to the Coulomb's law : $V \sim q_i q_j / r_{ij}$ where q_i and q_j are the magnitude of the charges and r_{ij} their separation. The third interaction correspond to the electrostatic interactions between the charge distribution associated to the out-of-plane π -electron density. The nuclei of aromatic molecules have a characteristic charge distribution with a positively charged σ -framework which is sandwiched between two regions of negatively charged π -electron

density. The interactions vary as r^{-5} and strongly depend on geometry. The fourth effect is the electrostatic interactions between charge distribution associated with the out-of-plane π -electron density and the partial atomic charges. This term varies roughly with r^{-4} and is, thus, quite sensitive to geometry. This contribution is relatively high if large partial atomic charges are involved. The last contribution concerns the interaction of aromatic residues and solvent. It is also called solvation-driven force or hydrophobic effect, solvation effect, desolvation, solvophobic force. The contribution of this interaction to the π - π stacking remains a matter of a controversial debate. *Diedrich et al.* found a strong linear relationship between the free enthalpy and the solvent polarity.²⁵⁻²⁷ The most polar solvent which is water was the best for apolar bonding. In a different approach, *Gellman et al.* found no significant solvent-induced interactions.²⁸



Figure 1.5. 3D representation of a B-DNA double helix showing π - π stacking interactions between base pairs along the axis.²⁹

1.4 Different DNA Architectures

DNA is not only able to form a simple double helix, DNA is also able to form different kinds of 2D branched structures and also triplexes or quadruplexes.

1.4.1 Branched DNA

During the last 10 years, there was an important increase interest in the use of DNA for engineering purposes.³⁰ Effectively, DNA is an excellent system for studying molecular self-assembly and nanoconstruction.³¹ One particular interest is to design DNA motifs to grow large, ordered two-dimensional arrays. This is why a variety of simple branched structures have been developed (*Figure 1.6*).³² One of these branched motifs is a linear polymer, a partial DNA duplex which has the possibility to be extended along the same axis by strand complementarity. DNA molecules are joined by sticky ends and can yield longer lines. The second branched structure is a three-way junction which consists in three different strands forming three partial duplexes. The resulting structure is a three branched structure. The third branched junction is a four-way junction (also called a Holliday junction) which consists of four different strands forming four partial duplexes.

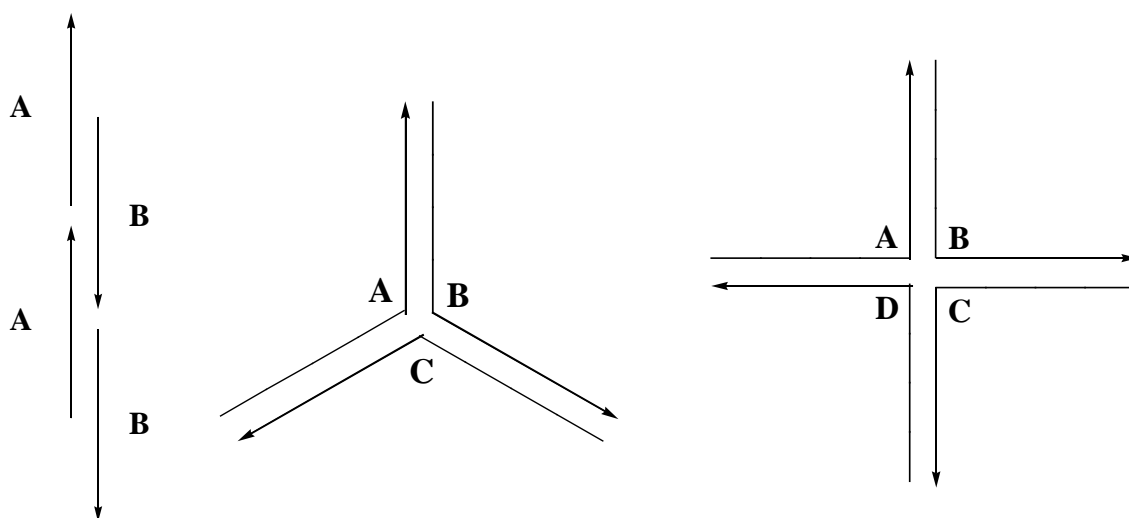


Figure 1.6 Linear polymer (left), three way junction (middle) and four-way junction (right).

1.4.2 DNA Triplexes

Triple helical DNA structures (*Figure 1.7*) have been a subject of vast research in the past 50 years.³³⁻³⁵ In this structure, one strand binds to a B-DNA double helix through Hoogsteen and reverse Hoogsteen hydrogen bonds (*Figure 1.8*). Hoogsteen base pairing takes place in the pyrimidine binding motif when the homopyrimidine triplex-forming oligonucleotide is

parallel to the duplex (C^+ -GC or T-AT base triplets). The reverse Hoogsteen base pairing appears in the purine binding motif when the homopurine triplex-forming is antiparallel to the duplex (G-GC, A-AT or T-AT base triplets). Effectively, the triplex formation is most of the time limited to homopurine/homopyrimidine regions of a DNA duplex. Since triplex formation takes place in a highly specific manner it has found wide interest as a method of selectively targeting DNA for gene-based diagnostic and pharmaceutical applications.³⁶⁻³⁸



Figure 1.7 Structure of a DNA triple helix.³⁹

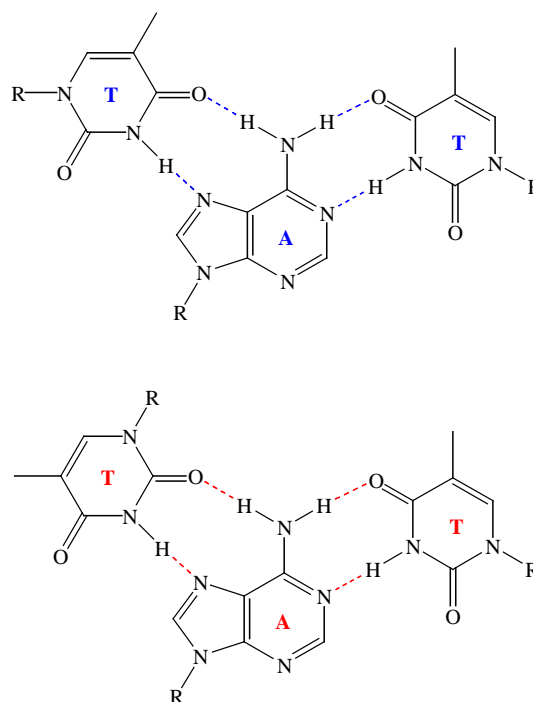


Figure 1.8 T-AT Hoogsteen base pair (top) and T-AT reverse Hoogsteen base pair (bottom).

1.4.3 DNA Quadruplexes

DNA oligonucleotides that have repetitive tracts of guanine bases linked by hydrogen bonds (*Figure 1.9*) can form four-stranded inter- and intramolecular quadruplex structures that may be important for a number of biological processes and disease-related mechanisms.⁴⁰⁻⁴¹ In particular G-quadruplex DNA formed from telomeric sequence repeats (*Figure 1.10*) may be important for telomere maintenance and DNA replication and is a potential target for novel anti-cancer drugs.⁴²⁻⁴⁴ These structures can be further stabilized by interaction between O6 of

guanine with cations, particularly monovalent metal ions. G-quadruplexes are highly polymorphic and a large number of different structures have been observed.⁴⁵

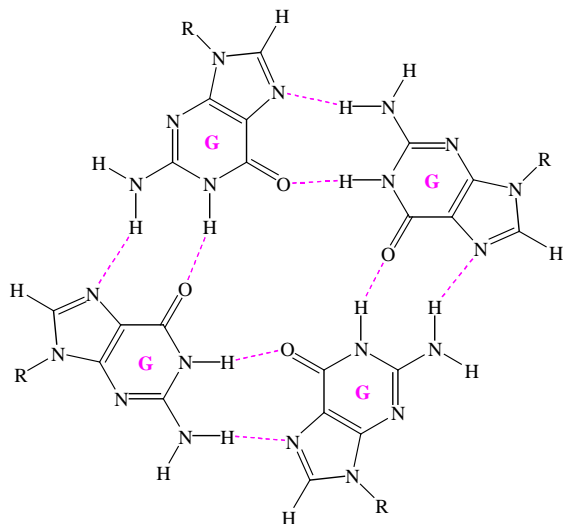


Figure 1.9 Hydrogen bonds formed in GGGG quadruplex.

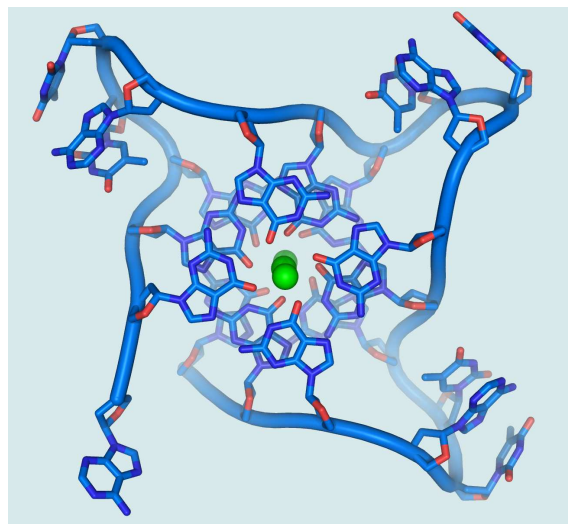


Figure 1.10 Structure of a DNA quadruplex formed by telomere repeats.⁴⁶

1.5 Chemical Modification of Nucleotides

Chemically modified nucleotide building blocks have been a great importance for the understanding of the mechanisms and stereochemical aspects of numerous biochemical reactions and processes nucleic acids are involved in.⁴⁷ Nucleotide modifications can occur at three different places: on the nucleobases, on the sugar backbone or on the phosphate linker (*Figure 1.11*).

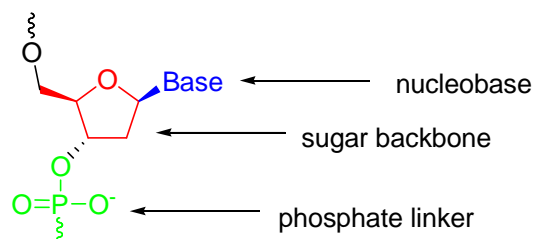


Figure 1.11 Sites of possible modifications of nucleotides.

The modification of the bases leads to the extension of the genetic code, to the analysis of the interactions between DNA/RNA and proteins, to the study of the physical properties of natural bases and to the improvement of binding properties in diagnostic applications.⁴⁸⁻⁴⁹

The modification of the phosphate can be done to show RNase H activity and to increase biological activity.⁵⁰ The two main modified groups for this applications are the phosphorothioate and the phosphorodithioate (*Figure 1.12*).⁵¹

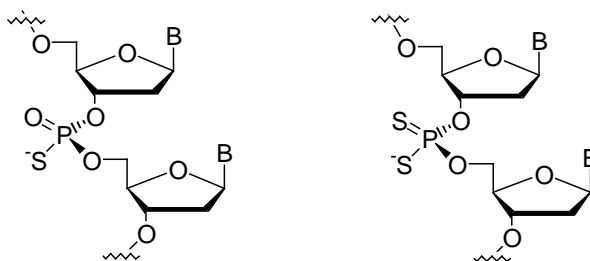


Figure 1.12 Phosphorothioate (left) and phosphorodithioate (right).

The modification of the sugar backbone shows an important interest for the development of diagnostic probes and tools in molecular biology as well as in antisense and antigene therapy.⁵²⁻⁵³ Modification of the sugar backbone can completely change the thermodynamic stability, the helical properties and the selectivity of base pairing. For example, sugar backbone modified nucleotides can be a 4-, 5- or 6-membered ring (*Figure 1.13*).⁵⁴⁻⁵⁶

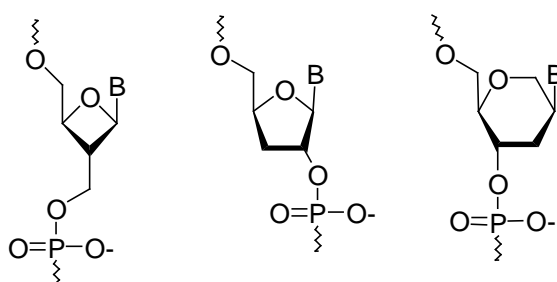


Figure 1.13 A 4-membered ring sugar (left), a 5-membered ring sugar (middle) where the phosphate is linked at the 2' position and a 6-membered ring sugar (right).

1.6 New Modified DNA Building Blocks

1.6.1 Non-nucleosidic Base Surrogates

In the past, most of the efforts on modification of nucleic acids was focused on the sugar-base analogues. Modified oligonucleotides have found widespread applications as diagnostic and research tool.⁵⁷⁻⁵⁸ The generation of defined molecular architectures by using nucleoside-like building blocks is a research topic of increasing interest.⁵⁹⁻⁶³ The repetitive and well-defined structural features of nucleic acids and related types of oligomers renders them valuable building blocks for the nanometre-sized structures.³⁰ The combination of nucleotides with non-natural building block leads to a large increase in possible constructs and applications.⁶⁴⁻⁶⁵ The use of these nucleic acids is famous for five main properties : for their ability of self-organisation, for their chemical and physical stability, for the construction of one-, two- or three-dimensional structures⁶⁶, because they are amenable to a large variety of chemical, physical and biological processes and because their modified building block can be easily incorporated. In our group of research we focused on non-nucleosidic building blocks because it is a domain that was not so explored for the moment.

1.6.2 Interstrand Stacking Building Blocks

In our group, we first decided to study the properties of some polyaromatic building blocks arranged in an interstrand stacking mode. These building blocks were the phenantrene **P**, the phenantroline **Q**.⁶⁷⁻⁶⁸ The phenantrene or the phenantroline (*Figure 1.14*) can serve as base surrogates without destabilising the DNA duplex or altering its overall B-DNA structure. Another building block was also incorporated for its stacking properties and this molecule was the pyrene **S** (*Figure 1.15*).⁶⁹

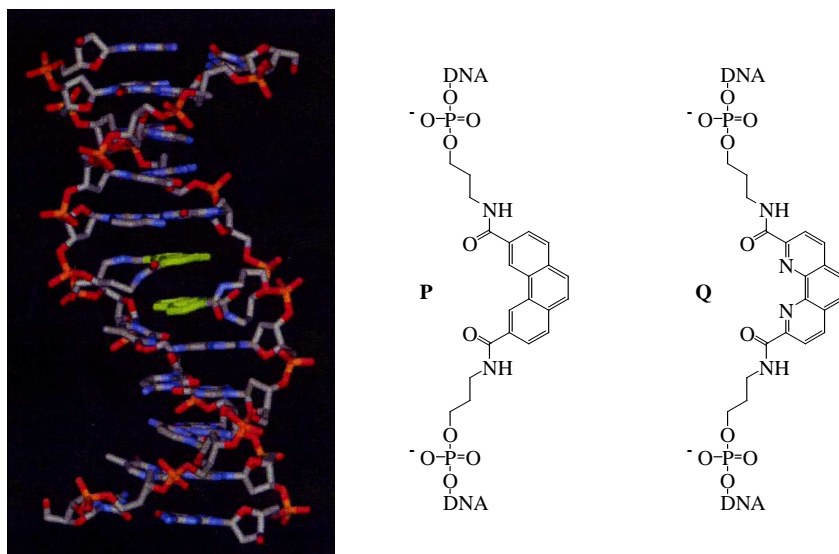


Figure 1.14 Molecular model showing DNA duplex with two interstrand stacked phenantrene (left) and the corresponding phenantrene building block **P** (middle) and the phenantroline building block **Q** (right).⁶⁷⁻⁶⁸

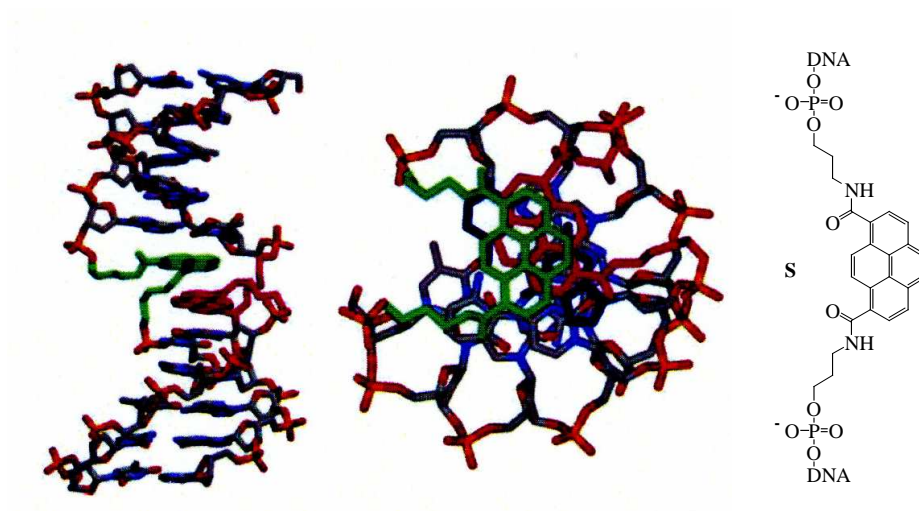


Figure 1.15 Molecular model showing DNA duplex with two interstrand stacked pyrenes (left) with a stacking view of the two pyrene moieties (middle) and the pyrene building block **S** (right).⁶⁹

1.6.3 Fluorophores and Quenchers in DNA

A fluorophore, is a component of a molecule which causes a molecule to be fluorescent. A fluorophore will absorb energy of a specific wavelength and reemit energy at a different (but equally specific) wavelength. The amount and wavelength of the emitted energy depend on both the fluorophore and the chemical environment of the fluorophore. In DNA duplexes, the pyrene building block **S** that we used for its stacking properties is also fluorescent. Pyrene is not only fluorescent but has also the ability to form excimer (*Figure 1.16*).⁶⁹ It was also proved that the pyrene and the phenantrene are forming an exciplex in DNA duplexes.⁷⁰⁻⁷¹

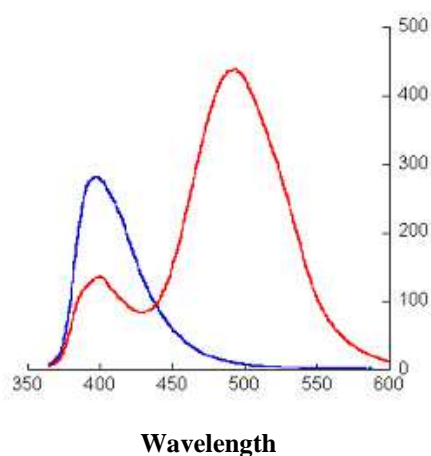


Figure 1.16 Fluorescence emission spectra of single strand (blue) and duplex (red) containing pyrenes in opposite positions.⁶⁹

Quenching refers to any process which decreases the fluorescence intensity of a given substance. A variety of processes can result in quenching, such as excited state reactions, energy transfer, complex formation and collisional quenching. The behaviour of the phenantroline building block **Q** which is important for the stabilisation of DNA was studied in opposite position to two pyrene units in DNA duplexes. A reduction in the signal of the pyrene excimer was observed (signal divided by 10) which is due to the presence of the phenantroline building block.⁷² The change in geometry can be one factor of this reduction in the signal. Another possibility can be that the phenantroline is intercalated between the two pyrene units and the last explanation can be that the phenantroline is able to quench pyrene monomer and/or pyrene excimer.

1.7 Electron-Acceptor and Electron-Donor Molecules

1.7.1 Electron-Acceptor Molecules

An electron acceptor is a chemical entity that accepts electrons transferred to it from another compound. It is an oxidizing agent that, by virtue of its accepting electrons, is itself reduced in the process. Anthraquinones (AQ) are known to be good electron-acceptor molecules⁷³ and can act as fluorescence quenchers.⁷⁴ Electrochemical measurements show that AQ can be reduced twice, reversibly (*Figure 1.17*).⁷⁵ They are investigated as photo-activated nucleases and they can serve as molecular entities for supramolecular assemblies.⁷⁶⁻⁷⁸ Anthraquinones are also known as potential anticancer agents, due to their property to intercalate into DNA.⁷⁹⁻⁸¹

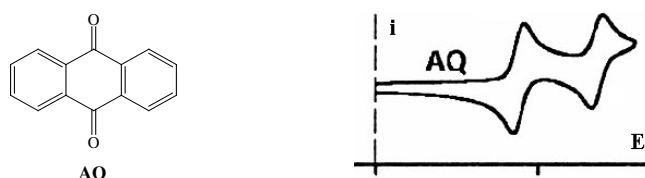


Figure 1.17 The AQ molecule (left) and the cyclic voltammetry of AQ in THF/TBAPF₆ (right).⁷⁵

Another electro-acceptor molecule is the perylene diimide (PDI) (*Figure 1.18*).⁸² PDI are colorants that have received considerable attention in academic as well as industrial dye and pigment research.⁸³⁻⁸⁴ PDI were initially applied for industrial purposes as red vat dyes. More recent applications of perylene bisimide pigments are in the field of electronic materials among which PDI is the best n-type semiconductors available to date.⁸⁵⁻⁸⁶ The n-type semiconductivity is related to the high electron affinity of perylene bisimide dyes.⁸⁷ PDI is also a fluorescent dye with high fluorescence quantum yield and photostability⁸⁸ which constituted a fertile soil for research on light-induced energy and electron transfer processes.⁸⁹⁻⁹¹

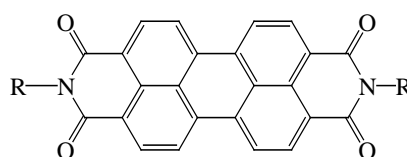


Figure 1.18 Perylene diimide derivative (PDI).

1.7.2 Electron-Donor Molecules

An electron donor is a chemical entity that donates electrons to another compound. It is a reducing agent that, by virtue of its donating electrons, is itself oxidized in the process. One of the famous electron-donor molecule is the tetrathiafulvalene (TTF) (*Figure 1.19*).⁹²

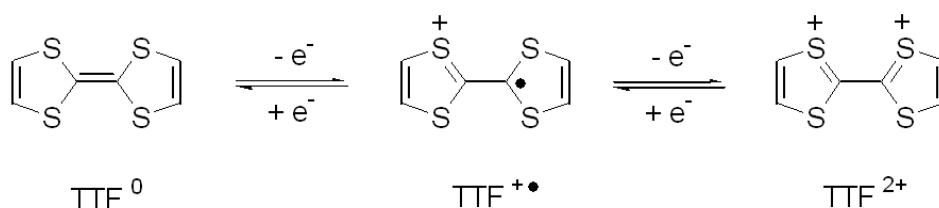


Figure 1.19 TTF molecule showing two reversible oxidation processes.⁹³

TTF is a planar molecule which allows π - π stacking of its oxidized derivatives. It has a high symmetry, which promotes charge delocalization, thereby minimizing coulombic repulsions, and has the ability to undergo oxidation at mild potentials to give a stable radical cation. Electrochemical measurements show that TTF can be oxidized twice reversibly (*Figure 1.19 and 1.20*).⁹³

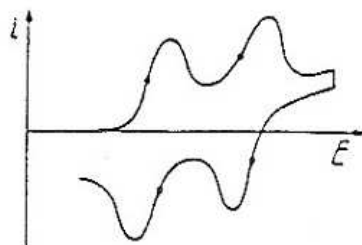


Figure 1.20 Cyclic voltammetry of TTF showing reversible process with $E^1_{1/2}=0.34$ V; $E^2_{1/2}=0.78$ V vs Ag/AgCl in acetonitrile.⁹¹

TTF and its derivatives were originally prepared as strong electron-donor molecules for the development of electrically conducting materials.⁹⁴⁻⁹⁶ TTF and its derivatives offer new and in some cases little-exploited possibilities at the molecular to the supramolecular levels.⁹⁷⁻⁹⁸ TTF is an important building block in supramolecular chemistry, crystal engineering and in systems able to operate as machines.⁹⁹ Important goals have been achieved in the use of TTF at the macromolecular level (TTF-containing oligomers, polymers and dendrimers).¹⁰⁰⁻¹⁰³

1.7.3 Donor-Acceptor Systems with TTF

In an electron-donating process, an electron-donor transfers an electron to an electron-acceptor. During this process the electron donor is oxidized and the electron acceptor is reduced. An example of a donor-acceptor system is the dendrimer¹⁰⁴ containing TTF and anthraquinone units shown in *Figure 1.21*.¹⁰² This molecule undergoes amphoteric redox behaviour as a consequence of the presence of the electron-donating TTF moiety and the electron-accepting anthraquinone system. These types of donor-acceptor systems are specially attractive since the incorporation of stronger π -acceptor group will enable the study of intra-molecular charge-transfer interactions within a dendritic microenvironment.¹⁰⁵⁻¹⁰⁷

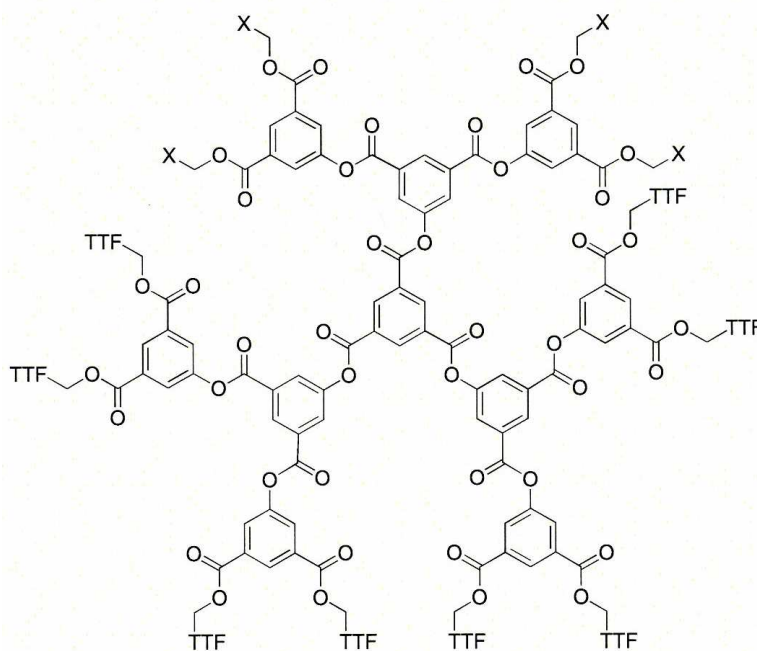


Figure 1.21 A polyester dendrimer containing anthraquinone (X) and TTF units.¹⁰²

A second example of donor-accepting system is a dyad system involving a TTF unit as a non-fluorescent donor and a perylene dicarboximide (PDI) unit as a fluorescent acceptor (*Figure 1.22*). Depending on the oxidation state of the TTF, the emission fluorescence of the dyad in solution can be reversibly modulated by either electron or energy transfer. This dyad could therefore be considered as a new kind of redox molecular switch with delayed optical response.¹⁰⁸

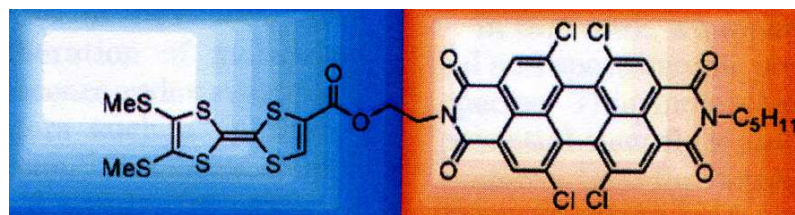


Figure 1.22 A donor-acceptor dyad system involving TTF and PDI.¹⁰⁸

1.7.4 Anthraquinone, TTF and Perylene diimide incorporated into DNA

Anthraquinones were most of the time incorporated or intercalated into DNA for its electronic properties. Long-charge transport in DNA duplex was studied with anthraquinone linked at the 5' end of a DNA strand.¹⁰⁹ Electrochemistry of DNA duplex containing an anthraquionylmethyl group at the 2'-sugar position (*Figure 1.23*) was studied by cyclic voltametry.¹¹⁰ Anthraquinone conjugates were incorporated into DNA by phosphodiester linkage to facilitate triplex formation.¹¹¹ DNA cleavage was examined with porphyrin-anthraquinone hybrids as intercalator.¹¹²

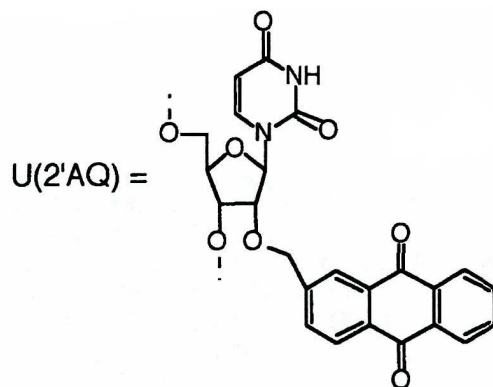


Figure 1.23 Anthraquinone moiety attached at the 2' position of a sugar
Sequence : dACAU(2'AQ)GCAGTGTGAT.¹¹⁰

So far as we know, tetrathiafulvalene was just incorporated one time into oligoribonucleoside and it was used for a system containing redox-active ribonucleoside and oligoribonucleoside (*Figure 1.24*).¹¹³

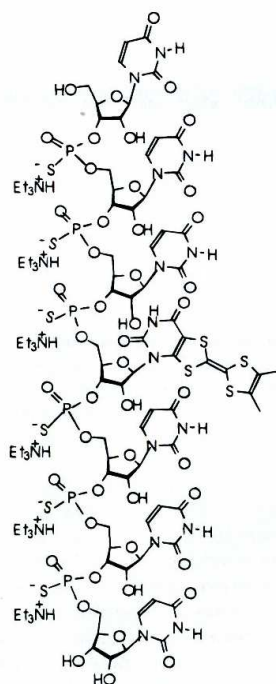


Figure 1.24 Synthesized sequence 5'-UsUsUs(U-TTF)sUsUsU-3'.¹¹³

Many reports describe the incorporation of perylene diimide into DNA.¹¹⁴⁻¹¹⁷ Oligonucleotide conjugates possessing PDI linkers have been reported to form a variety of structures including duplexes (*Figure 1.25*), triplexes, capped hairpins as well as novel structures possessing several PDI chromophores connected by distorted oligonucleotides.¹¹⁸⁻¹²⁰ Perylene diimide is an electron-acceptor¹⁰⁸ but also a well stacking entity, especially in DNA as non-nucleosidic base surrogates. Incorporation of two perylene units in opposite positions in DNA duplex show an increase in stability¹¹⁴ but a strongly reduced fluorescence of the PDI probably due to the quenching by water.¹¹⁶

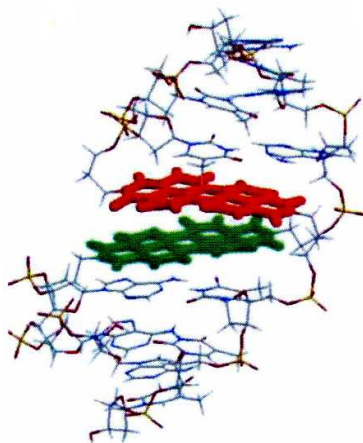


Figure 1.25 Modeling of a DNA duplex containing two perylene units in opposite positions.¹¹²

1.8 Aim of the Work

Our work aimed at the design and synthesis of structural DNA-mimics. We decided to study the properties of some polyaromatic building blocks in DNA-duplexes. These non-nucleosidic base surrogates should be suitable for arrangement in an interstrand stacking mode and for an increase in DNA stabilization. We focused our study on one electro-donor and two electro-acceptor building blocks: tetrathiafulvalene, anthraquinone and perylene diimide (*Figure 1.26*).

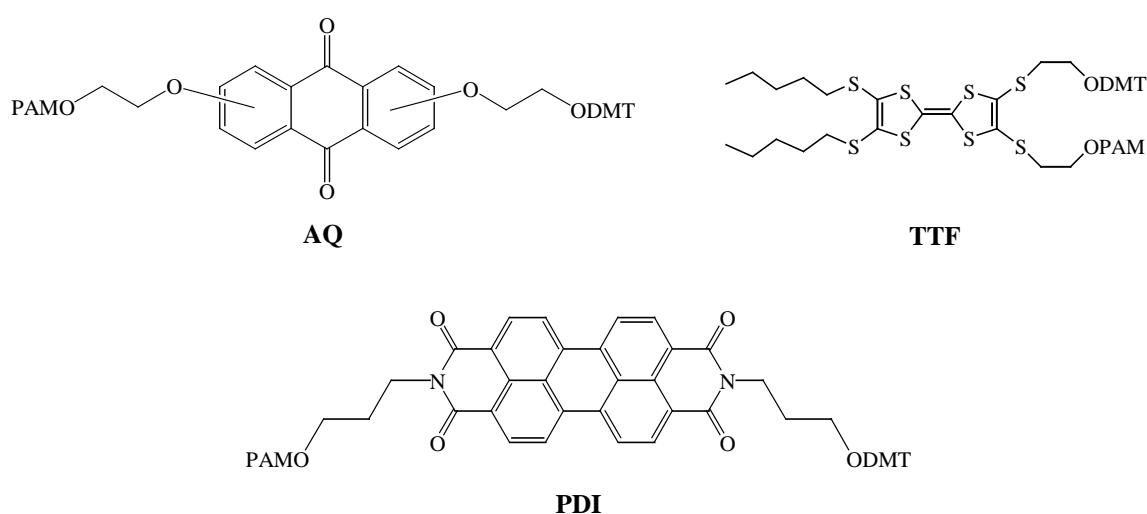


Figure 1.26 AQ, TTF and PDI building blocks used for our study.

The first part of our work was the synthesis and the incorporation of four different anthraquinone isomers into DNA. We were interested in the influence of the geometrical attachment of the linkers on hybrid formation and in their use as fluorescence quenchers. The second part of the work aimed at the synthesis and the incorporation of a tetrathiafulvalene derivative into DNA. Its spectroscopical properties and its behaviour on DNA stability were carried out. The third part of our work was devoted to the synthesis and the incorporation of a perylene diimide building block into DNA. PDI was used for its interesting stacking system which should have a positive effect on DNA stability. We also observed its behaviour opposite to the pyrene moiety that we are using in our group which is also a good fluorophore and able to form excimer in DNA.

Homogeneous duplexes containing all these three building blocks were our first interest, especially the effect on duplex stabilisation and the effect of the non-nucleosidic base surrogate (*Figure 1.27*).



Figure 1.27 Homogeneous duplexes containing TTF, AQ or PDI.

Heterogeneous duplexes were also studied as potential donor-acceptor systems in DNA duplexes (*Figure 1.28*). Redox properties of these moieties can have interesting results on DNA and some applications with TTF-, AQ- or PDI-containing oligonucleotides attached to gold surfaces are feasible.



Figure 1.28 Heterogeneous duplexes containing TTF, AQ or PDI.

Finally, anthraquinones are known to be good quencher molecules and perylene diimide is known to be a strong fluorophore in organic solutions. We decided to study the properties of these two molecules and at the same time also the behaviour of the TTF moiety on pyrene monomer and pyrene excimer fluorescence (*Figure 1.29*).

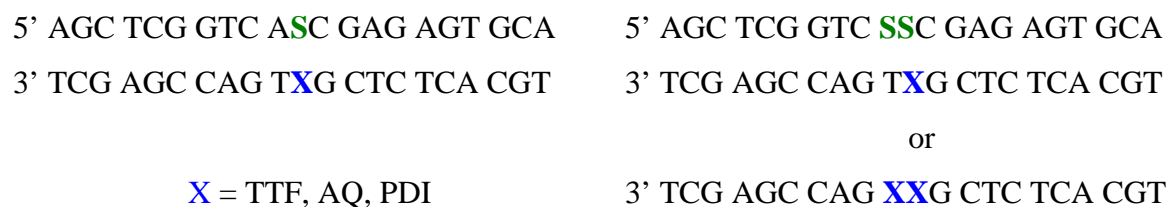


Figure 1.29 Duplexes containing one or two AQ, TTF or PDI units opposite to one or two pyrene units.

References

1. Mirsky A. E. *Scientific American* **1968**, 218, 78.
2. Kossel A. Z. *Physiol. Chem.* **1879**, 3, 284-291.
3. Fischer E. *Ber. Deutsch. Chem. Ges.* **1896**, 29, 1377-1683.
4. Levene P. *J. Biol. Chem.* **1919**, 40, 415.
5. Avery O.T. MacLeod C.M., McCarty M. *J. Exp. Med.* **1944**, 79, 137-158.
6. a) Chargaff E. *Journal of Cellular and Comparative Physiology* **1951**, 38, 41.
b) Chargaff E. *Federation Proceedings* **1951**, 10, 654.
7. Wilkins M. H. F. *Nobel Lecture*, **1962**, 754-755.
8. a) Watson J. D., Crick F. H. C. *Nature* **1953**, 171, 737.
b) Watson J. D., Crick F. H. C. *Nature* **1953**, 171, 964.
9. Kresge N., Simoni R. D., Hill R. L. *J. Biol. Chem.* **2006**, 15, 12-14.
10. Jacob F., Monod J. *Journal of Molecular Biology* **1961**, 3, 318-356.
11. Maxam A. M., Gilbert W. *Proc. Natl. Acad. Sci USA*, **1977**, 74(2), 560-564.
12. <http://www.thednastore.com/dnastuff/crystalcube.html>
13. Wing R., Drew H., Takano T., Broka C., Tanaka S., Itakura K., Dickerson R., *Nature* **1980**, 287, 755.
14. http://www.pharmacy.umaryland.edu/courses/PHAR531/lectures_old/dna.html
15. <http://en.wikipedia.org/wiki/DNA>
16. Saenger W., *Principles of Nucleic Acid Structure*, Springer-Verlag, New York **1984**.
17. Guerra C. F., Bickelhaupt F. M., Snijders J. G., Baerends E. J. *J. Am. Chem. Soc.* **2000**, 122, 4117.
18. Kryachko E. S. *NATO Science Series, II: Mathematics, Physics and Chemistry* **2003**, 116, 539.
19. Ogawa T., Kurita N., Sekino H., Kitao O., Tanaka S., *Chem. Phys. Lett.* **2003**, 374, 271.
20. Sponer J. V., Leszczynski J., Hobza P. *THEOCHEM* **2001**, 573, 43.
21. Rueda M., Luque F. J., Orozco M. *Biopolymers* **2001**, 61, 52.
22. Dingley A. J., Masse J. E., Peterson R. D., Barfield M., Feigon J., Grzesiek S. *J. Am. Chem. Soc.* **1999**, 121, 6019.

23. Gaffney B. L., Kung P.-P., Wang C., Jones R. A. *J. Am. Chem. Soc.* **1995**, *117*, 12281.
24. Langenegger S. M., *Ph.D.Thesis - Department of Chemistry and Biochemistry, University of Bern - 2005.*
25. Smithrud D. B., Diederich F. *J. Am. Chem. Soc.* **1990**, *112*, 339.
26. Smithrud D. B., Wyman T. B., Diederich F. *J. Am. Chem. Soc.* **1991**, *113*, 5420.
27. Meyer E. A., Castellano R. K., Diederich F. *Angew. Chem. Int. Ed.* **2003**, *42*, 1210.
28. Gellman S. H., Haque T. S., Newcomb L. F. *Biophys. J.* **1996**, *71*, 3523.
29. <http://www.thednastore.com/#mouse%20pad>
30. Wengel J. *Org. Biomol. Chem.* **2004**, *2*, 277-280.
31. Seeman N. C. *Nature* **2003**, *421*, 427-431.
32. Gothelf K. V., LaBean T. H. *Org. Biomol. Chem.* **2005**, *2*, 4023-4037.
33. Felsenfeld G., Davies D. R., Rich A. *J. Am. Chem. Soc.* **1957**, *79*, 2023-2024.
34. Moser H. E., Dervan P. B. *Science*, **1992**, *258*, 1463-1466.
35. Roberts R. W., Crothers D. M. *Science* **1992**, *258*, 1463-1466.
36. Hélène C., Toulmé J. J. *Biochim. Biophys. Acta* **1990**, *1049*, 99-125.
37. Mahner L. J. *Cancer Invest.* **1996**, *14*, 66-82.
38. Buchini S., Leumann C. J. *Curr. Opin. Chem. Biol.* **2003**, *7*, 717-726.
39. http://www.farooqhussain.org/projects/paulingdnamodel/document_view
40. Simonsson T. *Biol. Chem.* **2001**, *382*, 621-628.
41. Arthanari H., Bolton P. H. *Chem. Biol.* **2001**, *8*, 221-230.
42. Zahler A. M., Williamson J. R., Cech T. R., Prescott D. M. *Nature* **1991**, *350*, 718-720.
43. Sen D., Gilbert W., *Nature* **1988**, *334*, 364-366.
44. Neidle S., Parkinson G. *Nature Drug Discovery* **2002**, *1*, 383-393.
45. Williamson J. R. *Annu. Rev. Biophys. Biomol. Struct.* **1994**, *23*, 703-730.
46. <http://en.wikipedia.org/wiki/DNA>
47. Mathis G., *Ph.D. Thesis - Department of Chemistry and Biochemistry, University of Bern - 2004.*
48. Kool E. T. *Curr. Opin. Chem. Biol.* **2000**, *4*, 602.
49. Kool E. T. *Biopolymers* **1998**, *48*, 3.
50. Marshall W. S., Beaton G., Stein C. A., Matsukura M., Caruthers M. H. *Proc. Natl. Acad. Sci USA* **1992**, *89*, 6265.

51. Uhlmann E., Peyman A. *Chem. Rev.* **1990**, *90*, 543.
52. De Mesmaeker A., Häner R., Martin P., Moser H. E. *Acc. Chem. Res.* **1995**, *28*, 366.
53. Prevot-Halter I., Leumann C. J. *Bioorg. Med. Chem. Lett.* **1999**, *9*, 2657.
54. Henlin J. M., Jaeke K. Moser P., Rink H., Spiesser E., Baschang G. *Angew. Chem.* **1992**, *104*, 492.
55. Eschenmoser A. *Science* **1999**, *284*, 2118.
56. Hendrix C., Rosemeyer H., Verheggen I., Seela F., Van Aerschot A., Herdewijn P. *Chem. Eur. J.* **1997**, *3*, 110.
57. Verma S., Jager S., Thum O., Famulok M. *Chem. Rec.* **2003**, *3*, 51-60.
58. Kohler O., Jarikote D. V., Singh I., Parmar V. S., Weinhold E., Seitz O., *Pure Appl. Chem.* **2005**, *77*, 327-338.
59. Samori B., Zuccheri G. *Angew. Chem. Int. Ed.* **2005**, *44*, 1166-1181.
60. Shih W. M., Quispe J. D., Joyce G. F. *Nature*, **2004**, *427*, 618-621.
61. Mirkin, C. A. *Inorg. Chem.* **2000**, *39*, 2258-2272.
62. Chworos A., Severcan I., Koyfman A. Y., Weinkam P., Oroudjev E., Hansma H. G., Jaeger L. *Science* **2004**, *306*, 2068-2072.
63. Claridge S. A., Goh S. L., Frechet J. M. J., William S. C., Micheel C. M., Alivisatos A. P. *Chem. Mater.* **2005**, *17*, 1628-1635.
64. Eschenmoser A. *Chimia* **2005**, *59*, 836-850.
65. Herdewijn P. *Biochim. Biophys. Acta, Gene Struct. Expr.* **1999**, *1489*, 167-179.
66. Langenegger S. M., Bianke G., Tona R., Häner R., *Chimia* **2005**, *59*, 794-797.
67. Langenegger S. M., Häner R., *Helv. Chim. Acta* **2002**, *85*, 3414-3421.
68. Langenegger S. M., Häner R., *Tetrahedron Lett.* **2004**, *45*, 9273-9276.
69. Langenegger S. M., Häner R., *Chem. Commun.* **2004**, 2792-2793.
70. Langenegger S. M., Häner R., *Bioorg. Med. Chem. Lett.* **2006**, *16*, 2792-2793.
71. Trkulja I., Häner R., *Bioconjugate Chem.* **2007**, *18*, 289-292.
72. Langenegger S. M., *unpublished results*.
73. Kondo M., Murata M., Nishihara H., Nishibori E., Aoyagi S., Yoshida M., Kinoshita Y., Sakata M. *Angew. Chem. Int. Ed.* **2006**, *118*, 5587-5590.
74. May J. P., Brown L. J., Delft I. Thelwell N., Harley K., Brown T. *Org. Biomol. Chem.* **2005**, *3*, 2534-2542.
75. Gouloumis A., Liu S. *Chem. Commun.* **2001**, 399-400.
76. Breslin, D. T., Schuster, G. B. *J. Am. Chem. Soc.* **1996**, *118*, 2311-2319.

77. Mehta, G., Muthusamy, S., Maiya, B. G., Arounaguiri, S. *Tetrahedron Lett.* **1997**, *38*, 7125-7128.
78. Dzolic, Z., Cametti, M., Cort, A. D., Mandolini, L., Zinic, M. *Chem. Commun.* **2007**, 3535-3537.
79. Agbandje M., Jenkins T. C., McKenna R., Reszka A. P., Neidle S. *J. Med. Chem.* **1992**, *35*, 1418-1429.
80. Murdock K. C., Child R. G., Fabio P. F., Angier R. B. *J. Med. Chem.* **1979**, *9*, 1024-1030.
81. Collier D. A., Neidle S. *J. Med. Chem.* **1988**, *31*, 847-857.
82. Zhou Q. Z., Jiang X. K., Shao X. B., Chen G. J., Jia M. X., Li Z. T. *Org. Lett.* **2003**, *11*, 1955-1958.
83. Zollinger H. *Color Chemistry*, 3rd edn, VCH, Weinheim, **2003**.
84. Herbst W., Hunger K. *Industrial Organic Pigments*, 2nd edn, WILEY-VCH, Weinheim, **1997**.
85. Struijk C. W., Sieval A. B., Dakhorst J. E. J., Van Dijk D. M., Kimkes P., Koehorst R. B. M., Donker H., Schafsma T. J., Picken S. J., van de Craats A. M., Warman J. M., Zuilhof H., Sudhölter E. J. R. *J. Am. Chem. Soc.* **2000**, *122*, 11 057-11 066.
86. Dimitrakopoulos C. D., Malenfant P. R. L. *Adv. Mater.* **2002**, *14*, 99-117.
87. Lee S. K., Zu Y., Hermann A., Geerts Y., Müllen K., Bard A. J. *J. Am. Chem. Soc.* **1999**, *121*, 3513-3520.
88. Geisser G., Remy H. *Ger. Pat. Appl.* DE 1130099, **1959** (*Chem. Abst.* **1962**, *57*, P11346f).
89. O'Neil M. P., Niemczyk M. P., Svec W. A., Gosztda D., Gaines L., Wasielewski M. *R. Science*, **1992**, *257*, 63-66.
90. Prathapan S., Yang S. I., Seth J., Miller M. A., Bocian D. F., Holten D., Lindsey J. S. *J. Phys. Chem. B.* **2001**, *105*, 8237-8248.
91. Serin J. M., Brousmiche D. W., Frechet J. M. *Chem. Commun.* **2002**, 2605-2607.
92. Segura J. L., Martin N. *Angew. Chem. Int. Ed.* **2001**, *40*, 1372-1409.
93. Jeppesen J. O., Becher J. *Eur. J. Org. Chem.* **2003**, 3245-3266.
94. Bryce M. R. *Chem. Soc. Rev.* **1991**, *20*, 355.
95. Day P., Kurmoo M. *J. Mater. Chem.* **1997**, *8*, 1291.
96. Bryce M. R. *Adv. Mater.* **1999**, *11*, 11.
97. Jorgensen T., Hansen T. K., Becher J. *Chem. Soc. Rev.* **1994**, *41*.

-
98. Simonsen K. B., Becher J. *Synlett* **1997**, 1211.
 99. Nielsen M. B., Lomholt C., Becher J. *Chem. Soc. Rev.* **2000**, 29, 153.
 100. Otsubo T., Aso Y., Takimiya *Adv. Mater.* **1996**, 8, 203.
 101. Adam M., Müllen K. *Adv. Mater.* **1994**, 6, 439.
 102. Bryce M. R., Miguel P., Devonport W. *Chem. Commun.* **1998**, 2565-2566.
 103. Huchet L., Akoudad S., Roncali J. *Adv. Mater.* **1998**, 10, 541.
 104. Newkome G. R., Moorefield C. N., Vögtle F. *Dendritic Molecules: Concepts, Synthesis, Perspectives*, VCH, Weinheim, **1996**.
 105. Martin N., Segura J. L., Seoane C. *J. Mater. Chem.* **1997**, 7, 1661.
 106. Kampar V., Neilands O. *Russ. Chem. Rev.* **1986**, 55, 334.
 107. Hünig S. *J. Mater. Chem.* **1995**, 5, 1469.
 108. Leroy-Lhez S., Baffreau J., Perrin L., Levillain E., Allain M., Blesa M. J., Hudhomme P., *J. Org. Chem.*, **2005**, 16, 6313-6320.
 109. Santhosh U., Schuster G. B. *J. Am. Chem. Soc.* **2002**, 37, 10986-10987.
 110. Yamana K., Kumamoto S., Nakano H., Sugie Y. *Nucleic Acids Res. Suppl.* **2001**, 1, 35-36.
 111. Sato M., Moriguchi T., Shinozuka K. *Bioorg. Med. Chem. Lett.* **2004**, 14, 1305-1308.
 112. Mehta G., Muthusamy S., Maiya B. G., Arounaguiri S. *Tetrahedron Lett.* **1997**, 40, 7125-7128.
 113. Neilands O., Leipinsh V., Turovska B. *Org. Lett.* **1999**, 13, 2065-2067.
 114. Zheng Y., Long H., Schatz G. C., Lewis F. D. *Chem. Commun.* **2005**, 4795-4797.
 115. Zheng Y., Long H., Schatz G. C., Lewis F. D. *Chem. Commun.* **2006**, 3830-3832.
 116. Wagner C., Wagenknecht H. A. *Org. Lett.* **2006**, 19, 4191-4194.
 117. Lewis F. D., Zhang L., Kelley R. F., McCamant D., Wasielewski M. R. *Tetrahedron*, **2007**, 63, 3457-3464.
 118. Bevers S., Schutte S., Mclaughlin L. W. *J. Am. Chem. Soc.* **2000**, 122, 5905.
 119. Rahe N., Rinn C., Carell T. *Chem. Commun.* **2003**, 2120.
 120. Wang W., Zhou H., Niu S., Li A. D. Q. *J. Am. Chem. Soc.* **2003**, 125, 5248.

Chapter 2. Anthraquinones as Artificial DNA Building Blocks

Published in: N. Bouquin, V. L. Malinovskii and R. Häner *E. J. Org. Chem.*, **2008**, in press.

2.1 Abstract

Synthesis and properties of oligodeoxynucleotides containing anthraquinone-derived building blocks with flexible linkers are described. Starting from the 1,4-, 1,5-, 1,8- and 2,6-dihydroxy-anthraquinone isomers, the corresponding phosphoramidites were prepared and incorporated into oligonucleotides. The site of linker attachment was found to be of critical importance for hybrid stability. While the 2,6-isomer led to a significant stabilization, all other isomers had a negative effect on duplex stability. Spectroscopic studies showed that the anthraquinones behave as fluorescence quenchers. Models of anthraquinone-modified double stranded hybrids are proposed.

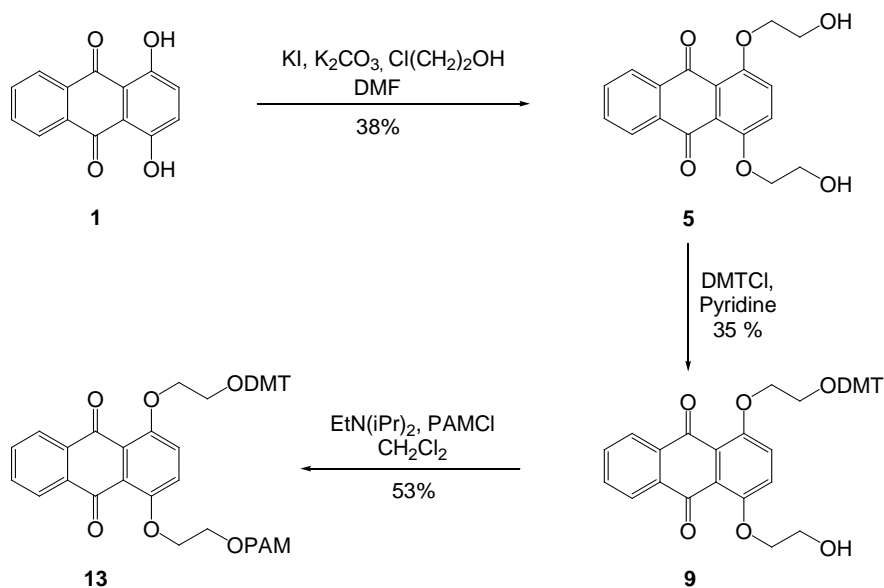
2.2 Introduction

The use of chemically modified nucleic acids is a rapidly growing area. Oligonucleotides containing unnatural building blocks are commonly used in the areas of diagnostics, supramolecular chemistry and materials research.^[1-5] Among the many modifications, building blocks lacking a sugar or a sugar-like moiety are increasingly used as versatile components. In particular, polyaromatic compounds, which often possess interesting electronic and spectroscopic properties, were found to integrate well into DNA without compromising hybrid stability. Typical modifications of this kind include stilbene,^[6,7] phenanthrene,^[8-12] pyrene,^[13-19] perylene,^[20-24] or phenanthroline.^[25,26] One of the primary reasons for the positive effect of the modifications on stability is their tendency to develop stacking interactions among themselves or with the nucleobases.^[16,17,27,28] Anthraquinone and

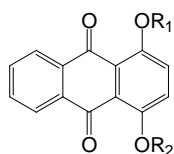
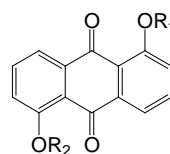
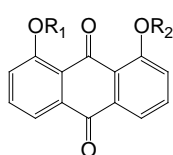
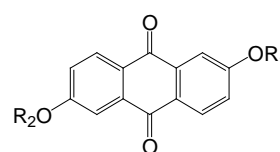
its derivatives are well-known intercalators.^[29,30] They are a frequently found motif in DNA targeting drugs.^[29,31-35] Not surprisingly, conjugation of anthraquinone to oligonucleotides has served as a common strategy for the development of high affinity oligonucleotides.^[36-44] Furthermore, the low reduction potential of anthraquinone derivatives opens possibilities for charge transport through DNA^[45-49] and electrochemical DNA sensing.^[48,50-54] In addition, anthraquinone derivatives can act as fluorescence quenchers,^[37,53,55] they are investigated as photo-activated nucleases^[56,57] and they can serve as molecular entities for supramolecular assemblies.^[58] On this background, we investigated the use of anthraquinone as an elemental building block for the construction of DNA-like structures. In particular, we were interested in the influence of the geometrical attachment of the linkers on hybrid formation and in their properties as fluorescence quenchers. Here, we report the synthesis of four isomeric anthraquinone phosphoramidites, their incorporation into oligonucleotides as well as the properties of the resulting oligomers.

2.3 Results and Discussion

Synthesis of the Phosphoramidite Building Blocks and Oligonucleotides. Incorporation of anthraquinone-derived with different geometries into DNA should give us indications about the effect of the sites of attachment of the linkers on duplex stability. Thus, the four dihydroxy-anthraquinones **1-4** (the 1,4-, 1,5-, 1,8- and the 2,6-isomers) were chosen for the study. Representative for all four isomers, the synthesis of the 1,4-substituted phosphoramidite building block is shown in *Scheme 2.1*. Introduction of the linkers was done by treatment with 2-chloroethanol in the presence of potassium carbonate and potassium iodide following a similar method described in the literature.^[59] The obtained bis-hydroxyethylated compounds **5-8** were converted to the mono-protected derivatives **9-12** by reaction with 4,4'-dimethoxytrityl chloride. Phosphitylation under conventional conditions yielded the phosphoramidite derivatives **13-16**. Structures of all anthraquinone derivatives are shown in *Table 2.1*. The phosphoramidites were subsequently incorporated into oligonucleotides using the phosphoramidite procedure.^[60,61] Deprotection (conc. NH₃, 50°C), followed by HPLC purification yielded oligonucleotides **17-26**. The correct molecular weights of all oligomers were verified by mass spectrometry (*Table 2.7*).

Scheme 2.1. Synthesis of the 1,4-substituted anthraquinone phosphoramidite building block **13**.**Table 2.1.** The 1,4-, 1,5-, 1,8- and 2,6-substituted anthraquinone intermediates and phosphoramidites.

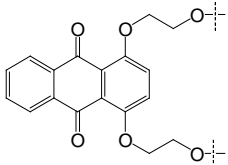
1,4-isomer	1,5-isomer	1,8-isomer	2,6-isomer
1 $\text{R}_1=\text{R}_2=\text{H}$	2 $\text{R}_1=\text{R}_2=\text{H}$	3 $\text{R}_1=\text{R}_2=\text{H}$	4 $\text{R}_1=\text{R}_2=\text{H}$
5 $\text{R}_1=\text{R}_2=$ $(\text{CH}_2)_2\text{OH}$	6 $\text{R}_1=\text{R}_2=$ $(\text{CH}_2)_2\text{OH}$	7 $\text{R}_1=\text{R}_2=$ $(\text{CH}_2)_2\text{OH}$	8 $\text{R}_1=\text{R}_2=$ $(\text{CH}_2)_2\text{OH}$
9 $\text{R}_1=(\text{CH}_2)_2\text{ODMT}$ $\text{R}_2=(\text{CH}_2)_2\text{OH}$	10 $\text{R}_1=(\text{CH}_2)_2\text{ODMT}$ $\text{R}_2=(\text{CH}_2)_2\text{OH}$	11 $\text{R}_1=(\text{CH}_2)_2\text{ODMT}$ $\text{R}_2=(\text{CH}_2)_2\text{OH}$	12 $\text{R}_1=(\text{CH}_2)_2\text{ODMT}$ $\text{R}_2=(\text{CH}_2)_2\text{OH}$
13 $\text{R}_1=(\text{CH}_2)_2\text{ODMT}$ $\text{R}_2=(\text{CH}_2)_2\text{OPAM}$	14 $\text{R}_1=(\text{CH}_2)_2\text{ODMT}$ $\text{R}_2=(\text{CH}_2)_2\text{OPAM}$	15 $\text{R}_1=(\text{CH}_2)_2\text{ODMT}$ $\text{R}_2=(\text{CH}_2)_2\text{OPAM}$	16 $\text{R}_1=(\text{CH}_2)_2\text{ODMT}$ $\text{R}_2=(\text{CH}_2)_2\text{OPAM}$

**1,4-isomer****1,5-isomer****1,8-isomer****2,6-isomer**

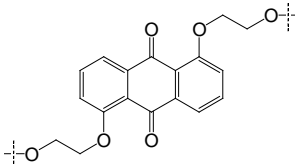
Influence of Anthraquinone Building Blocks on Hybrid Stability. The effect of the four non-nucleosidic building blocks on duplex stability was analyzed by thermal denaturation experiments. As shown in *Table 2.2*, incorporation of a pair of 1,4-, 1,5- or 1,8-derivatives in each strand (**19*20**, **21*22** and **23*24**) results in a considerable decrease in hybrid stability. All three regio-isomeric modifications reduce the melting temperature (T_m) by approximately 5°C ($\Delta T_m = -5.4^\circ\text{C}$, -5.2°C and -5.5°C , respectively).

Table 2.2. Melting temperatures of hybrids containing equal pairs of isomeric anthraquinone building blocks.

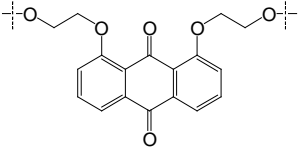
oligonucleotide		T_m [°C]	ΔT_m [°C]
17 18	(5') AGC TCG GTC ATC GAG AGT GCA (3') TCG AGC CAG TAG CTC TCA CGT	71.4	-
19 20	(5') AGC TCG GTC AH ₁₄ C GAG AGT GCA (3') TCG AGC CAG TH ₁₄ G CTC TCA CGT	66.0	- 5.4
21 22	(5') AGC TCG GTC AH ₁₅ C GAG AGT GCA (3') TCG AGC CAG TH ₁₅ G CTC TCA CGT	66.2	- 5.2
23 24	(5') AGC TCG GTC AH ₁₈ C GAG AGT GCA (3') TCG AGC CAG TH ₁₈ G CTC TCA CGT	65.9	- 5.5
25 26	(5') AGC TCG GTC AH ₂₆ C GAG AGT GCA (3') TCG AGC CAG TH ₂₆ G CTC TCA CGT	76.6	+ 5.2



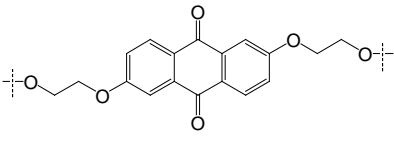
H14



H15



H18

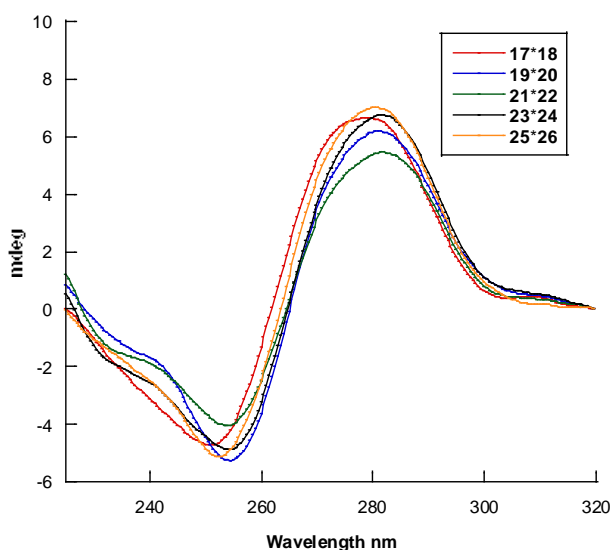


H26

Conditions: 1.0 μM oligonucleotide concentration (each strand), 10 mM phosphate buffer (pH 7.4) and 100 mM NaCl. a) Difference in T_m relative to the reference duplex **17*18**.

On the other hand, incorporation of a pair of the 2,6-isomer in opposite positions results in a significant increase in stability ($\Delta T_m +5.2^\circ\text{C}$). Circular dichroism (CD) spectral analysis of anthraquinone duplexes **19*20**, **21*22**, **23*24** and **25*26** are consistent with an overall B-conformation (Fig. 2.1).

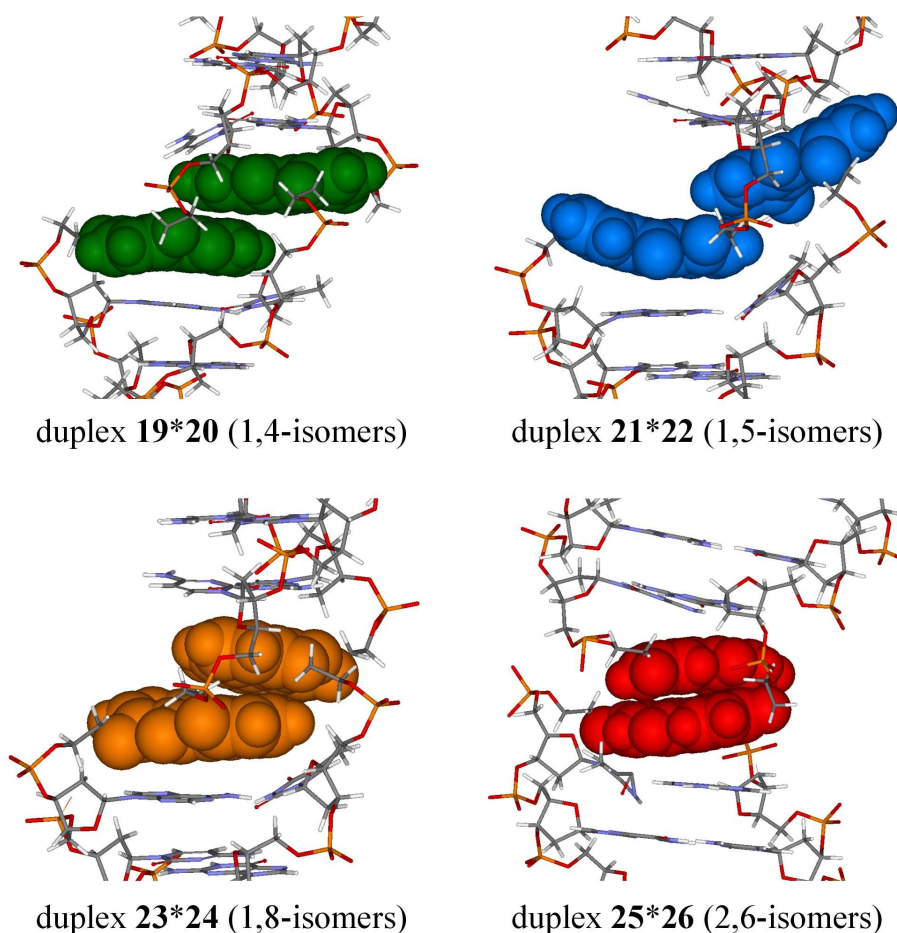
Figure 2.1. CD spectra of hybrids **17*18**, **19*20**, **21*22**, **23*24** and **25*26**.



Conditions: 1.0 μM oligonucleotide concentration (each strand), 10 mM phosphate buffer (pH 7.4) and 100 mM NaCl.

Due to the well-known property of anthraquinones to intercalate into DNA, we calculated possible models containing the building blocks in an interstrand stacked arrangement. The minimization process was done with *amber* force field^[62] considering the two anthraquinone moieties and one base pair on each side. After minimization, the remaining natural bases were attached using B-DNA parameters (see experimental section). The hybrid models thus obtained are depicted in Figure 2.2. As can be seen, only the 2,6-linked anthraquinones are arranged in a face-to-face stacking mode. Stacking of the anthraquinones in the hybrids containing the other isomeric building blocks seems much less favourable. While this would be in agreement with the large differences observed in duplex stabilities, alternative structures can, of course, not be excluded. In fact, a recent crystal structure of a bis-alkoxy-anthraquinone reveals that crystal packing is stabilized by intermolecular C-H \cdots O non-classical hydrogen bonds whereas no π - π stacking interactions were observed.^[63]

Figure 2.2. Amber-minimized models of DNA hybrids containing isomeric anthraquinone building blocks as indicated. Anthraquinones are shown in space filling representation.



We subsequently studied the effect of mixed pairs, in which the most stable 2,6-isomer was placed opposite to one of the other isomeric building blocks. T_m values are shown in *Table 2.3*. For all hybrids (**25*20**, **25*22** and **25*24**) a decrease in stability (ΔT_m respectively -2.8°C, -0.8°C, -5.3°C) compared to the unmodified duplex is observed. The decrease in stability, however, is relatively small for hybrids **25*20** and **25*22** (ΔT_m values of -5.4°C and -5.2°C, see *Table 2.2*, for the respective hybrids with identical anthraquinone modifications), which further illustrated the stabilizing effects of the 2,6-isomer. In agreement with previous observations with non-nucleosidic phenanthrene building blocks,^[11] a significant destabilization was observed with all regio-isomeric anthraquinones if placed opposite to a thymidine (*Table 2.4*). Anthraquinones had no stabilizing effect on DNA with an abasic site (*Table 2.5*). This is surprising since several reports exist in the literature describing a significant structural stabilization of abasic site containing DNA.^[25,64-66]

Table 2.3. Melting temperatures in hybrids containing mixed pairs of anthraquinones.

oligonucleotide		T_m [°C]	ΔT_m [°C]
17 18	(5') AGC TCG GTC ATC GAG AGT GCA (3') TCG AGC CAG TAG CTC TCA CGT	71.4	-
25 20	(5') AGC TCG GTC AH ₂₆ C GAG AGT GCA (3') TCG AGC CAG TH ₁₄ G CTC TCA CGT	68.6	- 2.8
25 22	(5') AGC TCG GTC AH ₂₆ C GAG AGT GCA (3') TCG AGC CAG TH ₁₅ G CTC TCA CGT	70.6	- 0.8
25 24	(5') AGC TCG GTC AH ₂₆ C GAG AGT GCA (3') TCG AGC CAG TH ₁₈ G CTC TCA CGT	66.3	- 5.3

Conditions: 1.0 μ M oligonucleotide concentration (each strand), 10 mM phosphate buffer (pH 7.4) and 100 mM NaCl.

Table 2.4. Hybridization data of the anthraquinone building blocks in opposite position to a thymidine.

oligonucleotide		T_m [°C]	ΔT_m [°C]
17 18	(5') AGC TCG GTC ATC GAG AGT GCA (3') TCG AGC CAG TAG CTC TCA CGT	71.4	-
17 20	(5') AGC TCG GTC ATC GAG AGT GCA (3') TCG AGC CAG TH ₁₄ G CTC TCA CGT	62.7	- 8.7
17 22	(5') AGC TCG GTC ATC GAG AGT GCA (3') TCG AGC CAG TH ₁₅ G CTC TCA CGT	61.7	- 9.7
17 24	(5') AGC TCG GTC ATC GAG AGT GCA (3') TCG AGC CAG TH ₁₈ G CTC TCA CGT	63.6	- 7.8
17 26	(5') AGC TCG GTC ATC GAG AGT GCA (3') TCG AGC CAG TH ₂₆ G CTC TCA CGT	63.8	- 7.6

Conditions : 1.0 μ M oligonucleotide concentration (each strand), 10 mM Phosphate buffer (pH 7.4) and 100 mM NaCl.

Table 2.5. Hybridization data of the anthraquinone building blocks in opposite position to an abasic site.

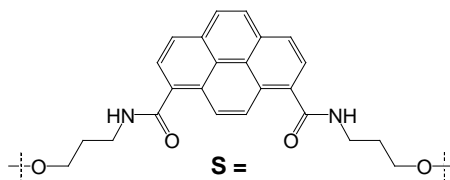
oligonucleotide		T _m [°C]	ΔT _m [°C]
28 18	(5') AGC TCG GTC AΦC GAG AGT GCA (3') TCG AGC CAG TAG CTC TCA CGT	62.6	- 8.8
28 20	(5') AGC TCG GTC AΦC GAG AGT GCA (3') TCG AGC CAG TH ₁₄ G CTC TCA CGT	62.6	- 8.8
28 22	(5') AGC TCG GTC AΦC GAG AGT GCA (3') TCG AGC CAG TH ₁₅ G CTC TCA CGT	61.2	- 10.2
28 24	(5') AGC TCG GTC AΦC GAG AGT GCA (3') TCG AGC CAG TH ₁₈ G CTC TCA CGT	63.0	- 8.4
28 26	(5') AGC TCG GTC AΦC GAG AGT GCA (3') TCG AGC CAG TH ₂₆ G CTC TCA CGT	62.7	- 8.7

Conditions : 1.0 μM oligonucleotide concentration (each strand), 10 mM Phosphate buffer (pH 7.4) and 100 mM NaCl.

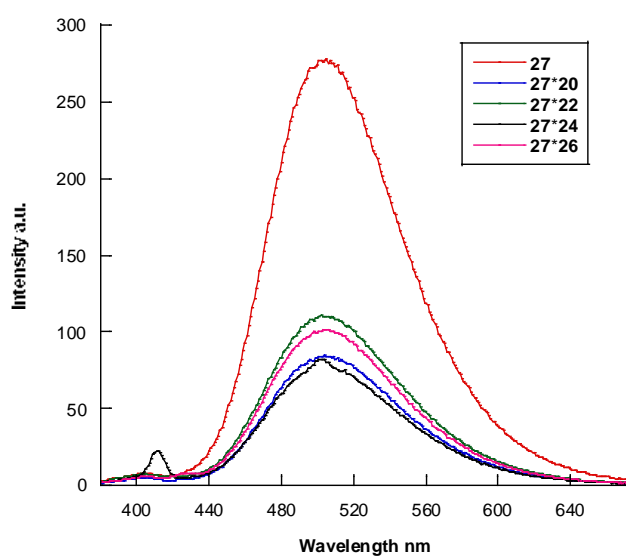
Fluorescence Quenching by Anthraquinone Building Blocks. Anthraquinones have been described as non-fluorescent quenchers and are, therefore, of interest for applications in diagnostic tools.^[37,55] The four different anthraquinone building blocks were investigated for their influence on pyrene excimer fluorescence. As shown in Figure 2.3, all four isomers have a significant quenching effect if placed opposite to two pyrene building blocks. Single strand **27** containing two pyrene moieties next to each other shows pyrene excimer fluorescence with a maximum at 505 nm.^[67] Complementary single strands **20**, **22**, **24** and **26** with the different anthraquinone moieties opposite the two pyrenes lead to a significant reduction (60 to 70%) of the fluorescence signal. The values are given in *Table 2.6* along with the T_m data of the different hybrids. The combination of a fluorophore with a quencher is used in many types of molecular probes. Efficient quenching of excimer fluorescence is difficult to achieve.^[68,69] Excimer quenching upon hybrid formation with interstrand stacking modifications opens a new way for the design of DNA based probes.

Table 2.6. Quenching of pyrene excimer fluorescence by anthraquinone building blocks.

oligonucleotide		T_m [°C]	ΔT_m [°C]	Quenching [%]
27	(5') AGC TCG GTC S S C GAG AGT GCA	64.0	- 7.4	60.3
20	(3') TCG AGC CAG TH₁₄G CTC TCA CGT			
27	(5') AGC TCG GTC S S C GAG AGT GCA	64.6	- 6.8	63.9
22	(3') TCG AGC CAG TH₁₅G CTC TCA CGT			
27	(5') AGC TCG GTC S S C GAG AGT GCA	64.9	- 6.5	69.7
24	(3') TCG AGC CAG TH₁₈G CTC TCA CGT			
27	(5') AGC TCG GTC S S C GAG AGT GCA	66.3	- 5.1	70.8
26	(3') TCG AGC CAG TH₂₆G CTC TCA CGT			



Conditions : 1.0 μ M oligonucleotide concentration (each strand), 10 mM Phosphate buffer (pH 7.4) and 100 mM NaCl.

Figure 2.3. Fluorescence spectra of single strand **27** containing two pyrene units and of hybrids between **27** and complementary strands containing anthraquinone building blocks.

Conditions: 1.0 μ M oligonucleotide concentration (each strand), 10 mM phosphate buffer (pH 7.4) and 100 mM NaCl.

2.4 Conclusions

Four isomeric anthraquinone building blocks differing in the site of linker attachment were synthesized and incorporated into oligodeoxynucleotides. The site of linker attachment was found to have a strong influence on the stability. Hybrids containing a pair of the 1,4-, 1,5- and 1,8-isomers led to a substantial reduction of the T_m value (ΔT_m -5.4°C, -5.2°C and -5.5°C, respectively). On the other hand, the 2,6-isomer resulted in a considerable increase in stability (ΔT_m +5.2°C). Hybrids containing mixed pairs of isomeric anthraquinones show moderate to significant destabilization. Molecular models suggest that the positive effect of the 2,6-isomer is a result of interstrand stacking interactions between the two anthraquinones. In the case of the other isomers investigated, such stacking interactions seem much less favourable. All anthraquinone building blocks act as fluorescence quenchers. If placed opposite to two pyrene building blocks, excimer fluorescence is quenched by 60-70%. The anthraquinone derivatives described here represent, thus, useful building blocks for diagnostic tools or for applications in DNA-based nanomaterials.

2.5 Experimental part

General. - Reactions were carried out under N_2 atmosphere using anhydrous solvents. Flash column chromatography was performed using silica gel 60 (63-32 μ M, *Chemie Brunschwig AG*). If compounds were sensitive to acid, the silica was pre-treated with solvent containing 1% Et_3N . All NMR spectra were measured at room temperature on a *Bruker AC-300* spectrometer. 1H -NMR spectra were recorded at 300 MHz. Chemical shifts (δ) are reported in ppm relative to the residual undeuterated solvent ($CDCl_3$: 7.27 ppm). Multiplicities are abbreviated as follows: *s* = singlet, *d* = doublet, *t* = triplet, *q* = quadruplet, *m* = multiplet. ^{13}C -NMR spectra were recorded at 75 MHz. Chemical shifts are reported in ppm relative to the residual non-deuterated solvent ($CDCl_3$: 77.00 ppm). ^{31}P -NMR spectra were recorded at 122 MHz. Chemical shifts are reported in ppm relative to 85% H_3PO_4 as an external standard. Electron impact mass spectra (EI-MS) was performed.

General method for bis-hydroxyethylation of dihydroxy-anthraquinones (5-8). A solution of 5.0 g (20.0 mmol) of dihydroxy-anthraquinone was dissolved in 100 ml of DMF. Potassium carbonate (27.7 g, 200 mmol) was added to the mixture. The mixture was stirred for 2h at 120°C. 2-Chloroethanol (27 ml, 400 mmol) and potassium iodide (6.65 g, 40.0 mmol) were added to the mixture. The mixture was stirred at 120°C overnight, then cooled to room temperature and concentrated. Water (100 ml) was added to the residue and the mixture was extracted with CH₂Cl₂ + isopropanol (3:1). The organic phase was washed again with water, dried with magnesium sulfate and evaporated under reduced pressure. The crude product was purified by CC (silica gel: AcOEt + 10% MeOH).

1,4-Bis[(hydroxyethyl)oxy]anthraquinone (5). Yield: 2.54 g (38%). ¹H-NMR (CDCl₃, 300 MHz): 3.99 (t, 4 H), 4.29 (t, 4 H), 7.37 (s, 2 H), 7.74 (dd, 2 H), 8.18 (dd, 2 H). ¹³C-NMR (CDCl₃, 75 MHz): 61.16, 73.34, 124.23, 126.90, 127.11, 134.07, 134.37, 154.79, 184.36. EI-MS: m/z = 328 (M⁺); MW = 328.09; C₁₈H₁₆O₆.

1,5-Bis[(hydroxyethyl)oxy]anthraquinone (6). Yield: 1.82 g (27%). ¹H-NMR (CDCl₃, 300 MHz): 4.02 (t, 4 H), 4.31 (t, 4 H), 7.30 (dd, 2H), 7.70 (t, 2 H), 7.93 (dd, 2 H). ¹³C-NMR (CDCl₃, 75 MHz): 60.77, 72.11, 119.34, 120.17, 120.79, 135.26, 136.96, 159.36, 182.8. EI-MS: m/z = 328 (M⁺); MW = 328.09; C₁₈H₁₆O₆.

1,8-Bis[(hydroxyethyl)oxy]anthraquinone (7). Yield: 1.93 g (29%). ¹H-NMR (CDCl₃, 300 MHz): 4.03 (t, 4 H), 4.32 (t, 4 H), 7.34 (dd, 2 H), 7.68 (t, 2 H), 7.91 (dd, 2 H). ¹³C-NMR (CDCl₃, 75MHz): 60.77, 72.53, 119.61, 120.17, 121.20, 134.47, 135.02, 159.00, 182.82, 184.15. EI-MS: m/z = 328 (M⁺); MW = 328.09; C₁₈H₁₆O₆.

2,6-Bis[(hydroxyethyl)oxy]anthraquinone (8). Yield: 1.98 g (30%). ¹H-NMR (CDCl₃, 300 MHz): 4.04 (t, 4 H), 4.29 (t, 4 H), 7.29 (dd, 2 H), 7.74 (d, 2 H), 8.26 (d, 2 H). EI-MS: m/z = 328 (M⁺); MW = 328.09; C₁₈H₁₆O₆.

General method for 4,4'-dimethoxytrityl (DMT) protection of bis[(hydroxyethyl)oxy]anthraquinones (9-12). The diol (1.0 g, 3.0 mmol) was dissolved in absolute pyridine (8 ml). 4,4'-Dimethoxytrityl chloride (1 g, 3.0 mmol) dissolved in absolute pyridine (8 ml) was added dropwise. After stirring at room temperature for 6 hours, saturated aqueous sodium

bicarbonate solution was added. After extraction with dichloromethane and concentration under reduced pressure, the product was purified by CC (silica gel: AcOEt + 1% TEA).

1,4-({(4,4'-Dimethoxytrityl)oxy}ethyl)oxy)-(hydroxyethyl)oxy]-anthraquinone (9). Yield: 0.66 g (35%). ¹H-NMR (CDCl₃, 300 MHz): 3.78 (s, 6 H), 3.98 (m, 4 H), 4.28 (m, 4 H), 6.83 (m, 4 H), 7.18 (m, 2 H), 7.28 (m, 3 H), 7.37 (m, 4 H), 7.48 (m, 2 H), 7.73 (m, 2 H), 8.18 (m, 2 H).

1,5-({(4,4'-Dimethoxytrityl)oxy}ethyl)oxy)-(hydroxyethyl)oxy]-anthraquinone (10). Yield: 0.59 g (31%). ¹H-NMR (CDCl₃, 300 MHz): 3.79 (s, 6 H), 4.01 (m, 4 H), 4.31 (m, 4 H), 6.84 (m, 4 H), 7.15 (m, 1 H), 7.30 (m, 4 H), 7.42 (m, 4 H), 7.50 (m, 2 H), 7.70 (m, 2 H), 7.95 (m, 2 H).

1,8-({(4,4'-Dimethoxytrityl)oxy}ethyl)oxy)-(hydroxyethyl)oxy]-anthraquinone (11). Yield: 0.70 g (37%). ¹H-NMR (CDCl₃, 300 MHz): 3.78 (s, 6 H), 3.82 (m, 4 H), 4.26 (m, 4 H), 6.85 (m, 4 H), 7.15 (m, 1 H), 7.30 (m, 4 H), 7.38 (m, 4 H), 7.48 (m, 2 H), 7.62 (m, 2 H), 7.88 (m, 2 H).

2,6-({(4,4'-Dimethoxytrityl)oxy}ethyl)oxy)-(hydroxyethyl)oxy]-anthraquinone (12). Yield: 0.49 g (26%). ¹H-NMR (CDCl₃, 300 MHz): 3.78 (s, 6 H), 4.05 (m, 4 H), 4.28 (m, 4 H), 6.82 (m, 4 H), 7.20 (m, 1 H), 7.28 (m, 4 H), 7.35 (m, 4 H), 7.46 (m, 2 H), 7.74 (m, 2 H), 8.25 (m, 2 H).

General method for the phosphorylation of monoprotected anthraquinones 9-12. The alcohol (0.50 g, 0.79 mmol) and ethyldiisopropylamine (0.25 g, 2.0 mmol) were dissolved in 10 ml of dichloromethane. 2-Cyanoethyl-diisopropylaminochloridophosphite (0.225 g, 0.95 mmol) dissolved in 5 ml of dichloromethane was added dropwise. The reaction was stirred at room temperature for 2 hours. The resulting mixture was directly applied on a silica column for purification (eluent: AcOEt + 1% TEA).

1,4-({(Diisopropylamino)(2-cyanoethyl)phosphinoxy}ethyl)oxy)-({(4,4'-dimethoxytrityl)oxy}ethyl)oxy]-anthraquinone (13). Yield: 0.35 g (53%). ¹H-NMR (CDCl₃, 300 MHz): 1.17 (m, 12 H), 2.64 (t, 2 H), 3.58 (t, 2 H), 3.59 (m, 2 H), 3.69 (m, 2 H), 3.79 (s, 6 H), 3.86 (m, 2

H), 4.35 (m, 4 H), 6.83 (m, 4 H), 7.24 (m, 1 H), 7.28 (m, 4 H), 7.39 (m, 4 H), 7.50 (m, 2 H), 7.65 (m, 2 H), 7.87 (m, 2 H). ^{31}P -NMR (CDCl_3 , 122 MHz): 149.11.

1,5-(((Diisopropylamino)(2-cyanoethyl)phosphinoxy)ethyl)oxy)-(((4,4'-dimethoxytrityl)oxy)ethyl)oxy)-anthraquinone (14). Yield: 0.39 g (60%). ^1H -NMR (CDCl_3 , 300 MHz): 1.18 (m, 12 H), 2.64 (m, 2 H), 3.59 (m, 4 H), 3.70 (m, 2 H), 3.79 (s, 6 H), 3.89 (m, 2 H), 4.33 (m, 4 H), 6.84 (m, 4 H), 7.24 (m, 1 H), 7.28 (m, 4 H), 7.40 (m, 4 H), 7.51 (m, 2 H), 7.66 (m, 2 H), 7.87 (m, 2 H). ^{31}P -NMR (CDCl_3 , 122 MHz): 149.10.

1,8-(((Diisopropylamino)(2-cyanoethyl)phosphinoxy)ethyl)oxy)-(((4,4'-dimethoxytrityl)oxy)ethyl)oxy)-anthraquinone (15). Yield: 0.35 g (53%). ^1H -NMR (CDCl_3 , 300 MHz): 1.18 (m, 12 H), 2.64 (m, 2 H), 3.59 (m, 4 H), 3.70 (m, 2 H), 3.79 (s, 6 H), 3.89 (m, 2 H), 4.33 (m, 4 H), 6.84 (m, 4 H), 7.24 (m, 1 H), 7.28 (m, 4 H), 7.40 (m, 4 H), 7.51 (m, 2 H), 7.66 (m, 2 H), 7.87 (m, 2 H). ^{31}P -NMR (CDCl_3 , 122 MHz): 148.86.

2,6-(((Diisopropylamino)(2-cyanoethyl)phosphinoxy)ethyl)oxy)-(((4,4'-dimethoxytrityl)oxy)ethyl)oxy)-anthraquinone (16). Yield: 0.25 g (38%). ^1H -NMR (CDCl_3 , 300 MHz): 1.19 (m, 12 H), 2.65 (m, 2 H), 3.55 (m, 2 H), 3.61 (m, 2 H), 3.78 (s, 6 H), 3.79 (m, 2 H), 4.01 (m, 2 H), 4.33 (m, 4 H), 6.84 (m, 4 H), 7.22 (m, 1 H), 7.28 (m, 4 H), 7.34 (m, 4 H), 7.46 (m, 2 H), 7.73 (m, 2 H), 8.25 (m, 2 H). ^{31}P -NMR (CDCl_3 , 122 MHz): 148.86.

Synthesis and analysis of oligonucleotides. Cyanoethyl phosphoramidites from *Transgenomic* (Glasgow, UK) were used for oligonucleotide synthesis. Oligonucleotides **17-27** were prepared via automated oligonucleotide synthesis by a standard synthetic procedure ('trityl-off' mode) on a 394-DNA/RNA synthesizer (*Applied Biosystems*). Cleavage from the solid support and final deprotection was done by a treatment with 33% aqueous NH_3 at 55°C overnight. All oligonucleotides were purified by ion exchange HPLC (*Tricorn column SOURCE 15Q 4.6/100 PE 100 15 μm , Merck, L-6250 Intelligent Pump*); eluent A = Na_2HPO_4 (20 mM), pH 11.5; eluent B = Na_2HPO_4 (20 mM) + NaCl (2 M), pH 11.5; gradient 0-60% B over 30 min at 25°C. ESI-MS (negative mode, $\text{CH}_3\text{CN}/\text{H}_2\text{O}/\text{TEA}$) of oligonucleotides was performed with a *Sciex QSTAR pulsar*, (hybrid quadrupole time-of-flight mass spectrometer, *Applied Biosystems*); data of oligomers **17-26** and **28** are given *Table 2.7*.

Thermal denaturation experiments were carried out on a *Varian Cary-100 Bio-UV/VIS* spectrometer equipped with a *Varian Cary-block* temperature controller and data were collected with *Varian WinUV* software at 260 nm (cooling-heating-cooling cycles in the temperature range of 10-90°C, temperature gradient of 0.5°C/min). Experiments were carried out for 1.0 µM oligonucleotide concentration (each strand), 10 mM phosphate buffer and 100 mM NaCl at pH 7.4. Data were analyzed with *Kaleidagraph software* from *Synergy software*. Melting temperature (T_m) values were determined as the maximum of the first derivative of the smoothed melting curve.

Fluorescence data were collected for 1.0 µM oligonucleotide solutions (1.0 µM of each strand in case of double strands) in phosphate buffer (10 mM) and NaCl (100 mM) at pH 7.4 on a *Varian Cary Eclipse* fluorescence spectrophotometer equipped with a *Varian Cary-block* temperature controller (excitation at 354 nm, excitation and emission slit width 10 and 5nm, respectively).

CD spectra were recorded on a *JASCO J-715* spectrophotometer using quartz cuvettes with an optical path of 1 cm.

Modeling: structures of DNA hybrids containing anthraquinone units were minimized using the *Amber* force field (*Hyperchem 7.0*). Initial energy minimization was carried out with two stacked anthraquinones. Subsequently, two natural base pairs were added on both ends of the anthraquinones. After minimization, the remaining natural bases were attached using B-DNA parameters.

Table 2.7. Mass spectrometry data (molecular formula, calc. average mass, and obtained).

<i>Oligo.</i>		<i>Molecular formula</i>	<i>calc. mass</i>	<i>found</i>
17	(5') AGC TCG GTC ATC GAG AGT GCA	C ₂₀₅ H ₂₅₇ N ₈₃ O ₁₂₃ P ₂₀	6471.3	6470.4
18	(3') TCG AGC CAG TAG CTC TCA CGT	C ₂₀₃ H ₂₅₈ N ₇₆ O ₁₂₅ P ₂₀	6382.2	6383.9
19	(5') AGC TCG GTC AH ₁₄ C GAG AGT GCA	C ₂₁₃ H ₂₅₉ N ₈₁ O ₁₂₄ P ₂₀	6557.1	6557.5
20	(3') TCG AGC CAG TH ₁₄ G CTC TCA CGT	C ₂₁₁ H ₂₆₁ N ₇₁ O ₁₂₈ P ₂₀	6459.0	6459.4
21	(5') AGC TCG GTC AH ₁₅ C GAG AGT GCA	C ₂₁₃ H ₂₅₉ N ₈₁ O ₁₂₄ P ₂₀	6557.1	6557.0
22	(3') TCG AGC CAG TH ₁₅ G CTC TCA CGT	C ₂₁₁ H ₂₆₁ N ₇₁ O ₁₂₈ P ₂₀	6459.0	6458.5
23	(5') AGC TCG GTC AH ₁₈ C GAG AGT GCA	C ₂₁₃ H ₂₅₉ N ₈₁ O ₁₂₄ P ₂₀	6557.1	6556.3
24	(3') TCG AGC CAG TH ₁₈ G CTC TCA CGT	C ₂₁₁ H ₂₆₁ N ₇₁ O ₁₂₈ P ₂₀	6459.0	6458.4
25	(5') AGC TCG GTC AH ₂₆ C GAG AGT GCA	C ₂₁₃ H ₂₅₉ N ₈₁ O ₁₂₄ P ₂₀	6557.1	6556.0
26	(3') TCG AGC CAG TH ₂₆ G CTC TCA CGT	C ₂₁₁ H ₂₆₁ N ₇₁ O ₁₂₈ P ₂₀	6459.0	6458.4
28	(5') AGC TCG GTC AΦC GAG AGT GCA	C ₂₀₀ H ₂₅₃ N ₈₁ O ₁₂₁ P ₂₀	6347.1	6949.0

References

1. A. J. A. Cobb, *Org.Biomol.Chem.* **2007**, *5*, 3260-3275.
2. S. Verma, S. Jager, O. Thum, M. Famulok, *Chemical Record* **2003**, *3*, 51-60.
3. C. M. Niemeyer, *Nano Today* **2007**, *2*, 42-52.
4. F. Kukulka, C. M. Niemeyer, *Org.Biomol.Chem.* **2004**, *2*, 2203-2206.
5. E. T. Kool, J. C. Morales, K. M. Guckian, *Angew.Chem.Int.Ed Engl.* **2000**, *39*, 990-1009.
6. F. D. Lewis, Y. S. Wu, X. Y. Liu, *J.Am.Chem.Soc.* **2002**, *124*, 12165-12173.
7. F. D. Lewis, T. F. Wu, E. L. Burch, D. M. Bassani, J. S. Yang, S. Schneider, W. Jager, R. L. Letsinger, *J.Am.Chem.Soc.* **1995**, *117*, 8785-8792.
8. F. D. Lewis, E. L. Burch, *Journal of Photochemistry and Photobiology A-Chemistry* **1996**, *96*, 19-23.
9. D. Ackermann, R. Häner, *Helv.Chim.Acta* **2004**, *87*, 2790-2804.

10. A. Stutz, S. M. Langenegger, R. Häner, *Helv.Chim.Acta* **2003**, *86*, 3156-3163.
11. S. M. Langenegger, R. Häner, *Helv.Chim.Acta* **2002**, *85*, 3414-3421.
12. S. M. Langenegger, R. Häner, *ChemBioChem* **2005**, *6*, 2149-2152.
13. U. B. Christensen, M. Wamberg, F. A. El Essawy, A. Ismail, C. B. Nielsen, V. V. Filichev, C. H. Jessen, M. Petersen, E. B. Pedersen, *Nucleosides Nucleotides Nucleic Acids* **2004**, *23*, 207-225.
14. V. V. Filichev, K. M. H. Hilmy, U. B. Christensen, E. B. Pedersen, *Tetrahedron Lett.* **2004**, *45*, 4907-4910.
15. U. B. Christensen, E. B. Pedersen, *Nucl.Acids Res.* **2002**, *30*, 4918-4925.
16. S. M. Langenegger, R. Häner, *Chem.Commun.* **2004**, 2792-2793.
17. I. Trkulja, R. Häner, *Bioconjug.Chem.* **2007**, *18*, 289-292.
18. V. L. Malinovskii, F. Samain, R. Häner, *Angew.Chem.Int.Ed.Engl.* **2007**, *46*, 4464-4467.
19. I. Trkulja, R. Häner, *J.Am.Chem.Soc.* **2007**, *129*, 7982-7989.
20. W. Wang, W. Wan, H. H. Zhou, S. Q. Niu, A. D. Q. Li, *J.Am.Chem.Soc.* **2003**, *125*, 5248-5249.
21. F. D. Lewis, L. G. Zhang, R. F. Kelley, D. McCamant, M. R. Wasielewski, *Tetrahedron* **2007**, *63*, 3457-3464.
22. Y. Zheng, H. Long, G. C. Schatz, F. D. Lewis, *Chem.Commun.* **2005**, 4795-4797.
23. C. Wagner, H. A. Wagenknecht, *Org.Lett.* **2006**, *8*, 4191-4194.
24. F. D. Lewis, L. G. Zhang, X. B. Zuo, *J.Am.Chem.Soc.* **2005**, *127*, 10002-10003.
25. S. M. Langenegger, R. Häner, *ChemBioChem* **2005**, *6*, 848-851.
26. S. M. Langenegger, R. Häner, *Tetrahedron Lett.* **2004**, *45*, 9273-9276.
27. C. B. Nielsen, M. Petersen, E. B. Pedersen, P. E. Hansen, U. B. Christensen, *Bioconjug.Chem.* **2004**, *15*, 260-269.
28. I. V. Astakhova, A. D. Malakhov, I. A. Stepanova, A. V. Ustinov, S. L. Bondarev, A. S. Paramonov, V. A. Korshun, *Bioconjug.Chem.* **2007**, *18*, 1972-1980.
29. M. Agbandje, T. C. Jenkins, R. Mckenna, A. P. Reszka, S. Neidle, *J.Med.Chem* **1992**, *35*, 1418-1429.
30. R. E. McKnight, J. G. Zhang, D. W. Dixon, *Bioorg.Med.Chem.Lett.* **2004**, *14*, 401-404.
31. A. D. Sill, E. R. Andrews, F. W. Sweet, J. W. Hoffman, P. L. Tiernan, J. M. Grisar, R. W. Fleming, G. D. Mayer, *J.Med.Chem.* **1974**, *17*, 965-968.

32. K. C. Murdock, R. G. Child, P. F. Fabio, R. B. Angier, R. E. Wallace, F. E. Durr, R. V. Citarella, *J.Med.Chem.* **1979**, *22*, 1024-1030.
33. R. K. Y. Zeecheng, C. C. Cheng, *J.Med.Chem.* **1978**, *21*, 291-294.
34. D. A. Collier, S. Neidle, *J.Med.Chem.* **1988**, *31*, 847-857.
35. A. P. Krapcho, M. J. Maresch, M. P. Hacker, L. Hazelhurst, E. Menta, A. Oliva, S. Spinelli, G. Beggiolin, F. C. Giuliani, G. Pezzoni, S. Tognella, *Curr.Med.Chem.* **1995**, *2*, 803-824.
36. K. Yamana, T. Mitsui, J. Yoshioka, T. Isuno, H. Nakano, *Bioconjug.Chem.* **1996**, *7*, 715-720.
37. J. P. May, L. J. Brown, I. van Delft, N. Thelwell, K. Harley, T. Brown, *Org.Biomol.Chem.* **2005**, *3*, 2534-2542.
38. K. Mori, C. Subasinghe, J. S. Cohen, *Febs Letters* **1989**, *249*, 213-218.
39. K. Y. Lin, M. Matteucci, *Nucleic Acids Res.* **1991**, *19*, 3111-3114.
40. A. Ono, A. Dan, A. Matsuda, *Bioconjug.Chem.* **1993**, *4*, 499-508.
41. A. Garbesi, S. Bonazzi, S. Zanella, M. L. Capobianco, G. Gianni, F. Arcamone, *Nucleic Acids Res.* **1997**, *25*, 2121-2128.
42. M. Sato, T. Moriguchi, K. Shinozuka, *Bioorg.Med.Chem.Lett.* **2004**, *14*, 1305-1308.
43. T. H. Keller, R. Häner, *Nucl.Acids Res.* **1993**, *21*, 4499-4505.
44. T. H. Keller, R. Häner, *Helv.Chim.Acta* **1993**, *76*, 884-892.
45. D. Ly, L. Sani, G. B. Schuster, *J.Am.Chem.Soc.* **1999**, *121*, 9400-9410.
46. U. Santhosh, G. B. Schuster, *J.Am.Chem.Soc.* **2002**, *124*, 10986-10987.
47. Y. Z. Kan, G. B. Schuster, *J.Am.Chem.Soc.* **1999**, *121*, 11607-11614.
48. A. A. Gorodetsky, O. Green, E. Yavin, J. K. Barton, *Bioconjug.Chem.* **2007**, *18*, 1434-1441.
49. F. W. Shao, K. Augustyn, J. K. Barton, *J.Am.Chem.Soc.* **2005**, *127*, 17445-17452.
50. V. Kertesz, N. A. Whittemore, G. B. Inamati, M. Manoharan, P. D. Cook, D. C. Baker, J. Q. Chambers, *Electroanalysis* **2000**, *12*, 889-894.
51. K. Yamana, S. Kumamoto, H. Nakano, Y. Matsuo, Y. Sugie, *Chem.Lett.* **2001**, 1132-1133.
52. K. Yamana, S. Kumamoto, T. Hasegawa, H. Nakano, Y. Sugie, *Chem.Lett.* **2002**, 506-507.
53. S. D. Wettig, G. A. Bare, R. J. S. Skinner, J. S. Lee, *Nano Letters* **2003**, *3*, 617-622.

54. M. Nakamura, M. Ueda, S. Watanabe, S. Kumamoto, K. Yamana, *Tetrahedron Lett.* **2007**, *48*, 6159-6162.
55. S. Kodama, S. Asano, T. Moriguchi, H. Sawai, K. Shinozuka, *Bioorg.Med.Chem.Lett.* **2006**, *16*, 2685-2688.
56. D. T. Breslin, G. B. Schuster, *J.Am.Chem.Soc.* **1996**, *118*, 2311-2319.
57. G. Mehta, S. Muthusamy, B. G. Maiya, S. Arounagui, *Tetrahedron Lett.* **1997**, *38*, 7125-7128.
58. Z. Dzolic, M. Cametti, A. D. Cort, L. Mandolini, M. Zinic, *Chem.Commun.* **2007**, 3535-3537.
59. J. A. Valderrama, H. Leiva, R. Tapia, *Synth.Comm.* **2000**, *30*, 737-749.
60. S. L. Beaucage, M. H. Caruthers, *Tetrahedron Lett.* **1981**, *22*, 1859-1862.
61. N. D. Sinha, J. Biernat, J. McManus, H. Koster, *Nucleic Acids Res.* **1984**, *12*, 4539-4557.
62. HyperChem(TM), Hypercube, Inc., 1115 NW 4th Street, Gainesville, Florida 32601, USA; Release 7.5; 2005.
63. L. P. Cao, Y. Z. Wang, M. Gao, B. H. Zhou, *Acta Crystallographica Section E-Structure Reports Online* **2007**, *63*, O1876-O1877.
64. I. Singh, W. Hecker, A. K. Prasad, S. P. A. Virinder, O. Seitz, *Chem.Commun.* **2002**, 500-501.
65. S. M. Langenegger, R. Häner, *Chem.Biodiv.* **2004**, *1*, 259-264.
66. S. Smirnov, T. J. Matray, E. T. Kool, C. los Santos, *Nucleic Acids Res.* **2002**, *30*, 5561-5569.
67. F. Samain, V. L. Malinovskii, S. M. Langenegger, R. Häner, *Bioorg.Med.Chem.* **2008**, *16*, 27-33.
68. P. Conlon, C. J. Yang, Y. Wu, Y. Chen, K. Martinez, Y. Kim, N. Stevens, A. A. Marti, S. Jockusch, N. J. Turro, W. Tan, *J.Am.Chem.Soc.* **2008**, *130*, 336-342.
69. J. N. Wilson, Y. N. Teo, E. T. Kool, *J.Am.Chem.Soc.* **2007**, *129*, 15426-15427.

Chapter 3. TTF-Modified DNA

Published in: N. Bouquin, V. L. Malinovskii, Xavier Guégano, Shi-Xia Liu, Silvio Decurtins and R. Häner, submitted.

3.1 Abstract

A non-nucleosidic tetrathiafulvalene (TTF) building block and its incorporation into DNA are described. TTF-modified oligonucleotides form stable double strands. Exciton coupling reveals a high degree of structural organization in the modified region of a hetero-duplex formed by TTF and perylene diimide-containing strands. Photo-induced electron transfer is demonstrated by fluorescence quenching in TTF/pyrene modified hetero-hybrids. The results presented are important for the development of redox-active, oligonucleotide-based diagnostics or optical sensors.

3.2 Introduction

Ever since its first description,^[1] tetrathiafulvalene (TTF) has taken an eminent role in the field of materials sciences. Due to their specific π -donor properties, TTFs have been incorporated into a number of macrocyclic, molecular and supramolecular systems in order to create multifunctional materials with desired structure, stability and physical properties.^[2-8] As a consequence, they are frequently used as donor units in donor-acceptor (D-A) ensembles which are of prime interest due to their potential applications in molecular electronics and optoelectronics.^[9-12] In addition, their tendency to form π -stacked aggregates renders them attractive objects for the construction of supramolecular assemblies with applications in liquid crystalline materials and organogels.^[13,14] DNA represents a highly developed, yet very practical scaffold for the construction of complex assemblies.^[15] Due to the existence of well-

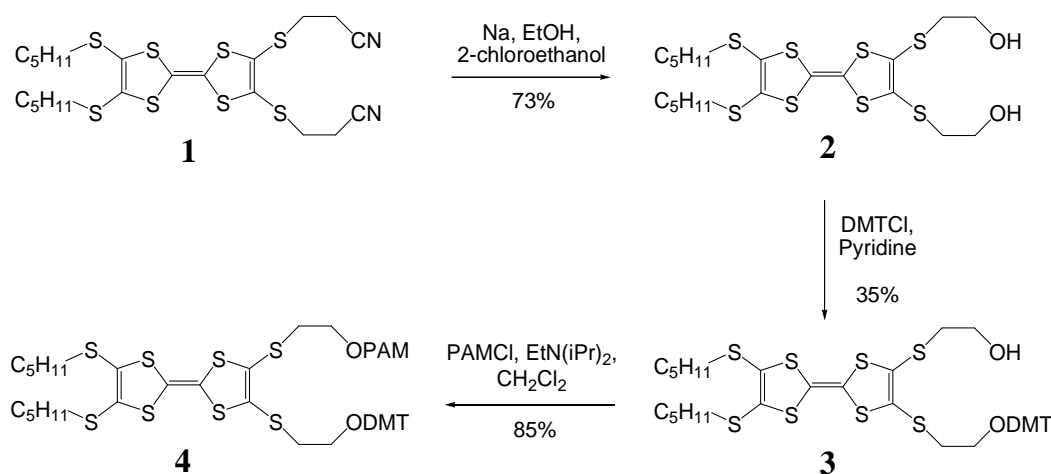
developed and versatile methods for oligonucleotide synthesis, the use of modified nucleic acids has become an attractive way for the generation of functionalized nanostructures.^[16] During the past decade, non-nucleosidic aromatic hydrocarbons, such as phenanthrene,^[17-19] pyrene^[20-27] and perylene,^[28-32] have been developed as building blocks for modified nucleic acids.^[33-36] They were explored as hairpin replacements,^[37-43] as units for conformational control in DNA^[44-46] or as replacements of the natural nucleotides maintaining helical organization.^[47,48] Further efforts aim at the development of advanced functional building blocks with a high level of structural organization. Interest in TTF-oligonucleotide conjugates is documented in patents describing the use of redox-active labels for the development of oligonucleotide-based sensors.^[49] So far, however, a single report on the preparation of such a construct exists, in which *Neilands* and coworkers describe the introduction of pyrimido-TTF nucleosides into a phosphorothioate oligoribonucleotide.^[50] Due to the interesting electronic properties of TTF and its excellent stacking properties, we have explored the generation of TTF-modified DNA. Here, we present the synthesis of a non-nucleosidic TTF building block (**F**, see Table 1), its incorporation into oligonucleotides, as well as the properties of several modified hybrids.

3.3 Results and Discussion

Synthesis of the tetrathiafulvalene phosphoramidite building block is shown in *Scheme 3.1*. Starting from the known 2,3-bis(2-cyanoethylthio)-6,7-bis(pentylthio)tetrathiafulvalene (**1**),^[51] bis-diol **2** was prepared by treatment with sodium in ethanol followed by alkylation with 2-chloroethanol. Reaction with 4,4'-dimethoxytrityl chloride gave the mono-protected intermediate **3**, which was subsequently converted into the phosphoramidite derivative **4**.

Building block **4** was used for the synthesis of modified oligonucleotides. Despite the known susceptibility of TTF towards strong acids and oxidants, the standard phosphoramidite protocol^[52] was successfully applied. Although some fragmentation of the TTF-modified oligonucleotides was observed during ammonia deprotection, oligomers **7-9** were easily purified by reverse phase HPLC.^[53]

Scheme 3.1. Synthesis of TTF phosphoramidite 4; DMT = 4,4'-dimethoxytrityl; PAM = 2-cyanoethyl N,N-diisopropyl-phosphoramidite.

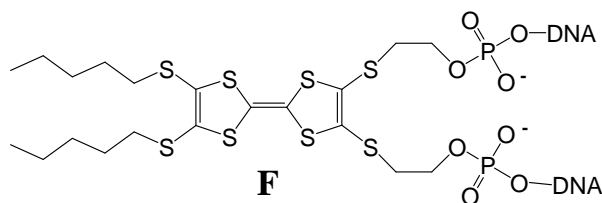


The effect of TTF incorporation on duplex stability was analyzed by thermal denaturation experiments (*Table 3.1*). Incorporation of one TTF moiety in each strand (duplex **7*8**) results in a considerable increase in stability ($\Delta T_m = + 4.9^\circ\text{C}$) in comparison to the unmodified duplex **5*6**. The increase in stability can be due to stacking interactions between the TTF units with the neighbouring nucleobases as well as to hydrophobic interactions of the pentyl chains. Cooperativity of the melting process in the natural and the modified part of duplex **7*8** was shown by monitoring the denaturation process at 290 as well as at 330 nm (hyperchromicity of TTF absorption, *Figure 3.1*).

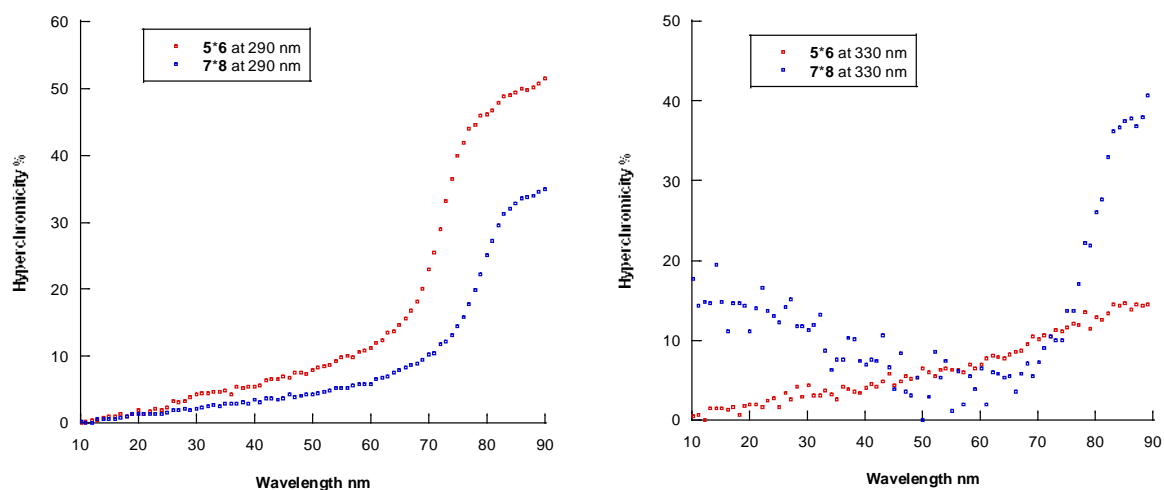
The circular dichroism (CD) spectrum of the duplex **7*8** (*Figure 3.2*) is consistent with an overall *B*-conformation with a maximum at 280 nm and a minimum at 251 nm, indicating that the TTF units are structurally well integrated into a *B*-type DNA. Despite the high duplex stability, no signs of exciton coupling were detected in the TTF region from 300 - 400 nm. A weak CD signal was observed, which is explained by chiral induction by the nucleic acid environment. This signal disappears upon duplex melting (*Figure 3.2*, inset).

Table 3.1. Hybridization data of TTF-modified DNA duplex.

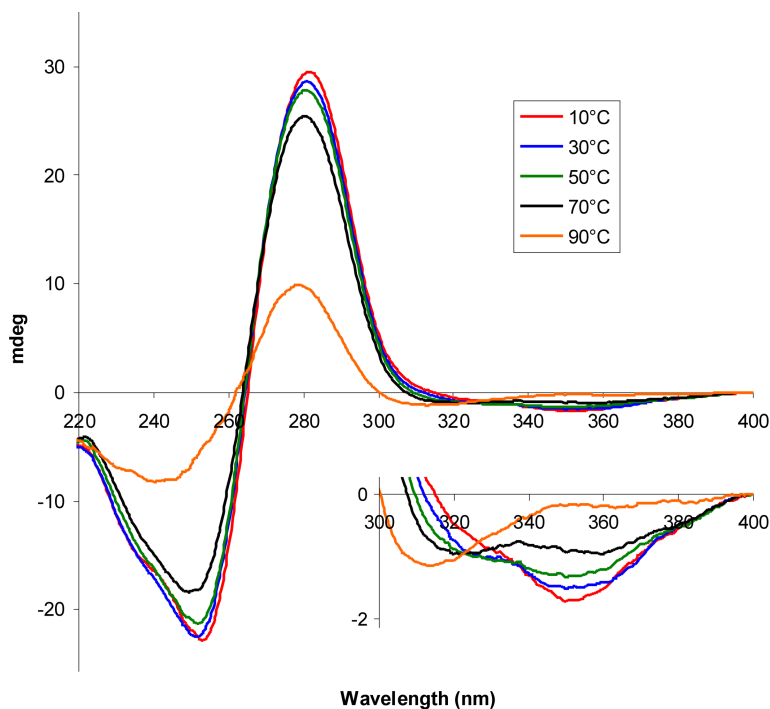
hybrid	T_m [°C]	ΔT_m [°C]
5 (5') AGC TCG GTC ATC GAG AGT GCA	72.5	-
6 (3') TCG AGC CAG TAG CTC TCA CGT		
7 (5') AGC TCG GTC AFC GAG AGT GCA	77.4	+4.9
8 (3') TCG AGC CAG TFG CTC TCA CGT		



Conditions: 1.0 μM oligonucleotide concentration (each strand), 10 mM phosphate buffer (pH 7.4) and 100 mM NaCl.

Figure 3.1. Thermal denaturation experiments with hybrids **5*6** and **7*8** at 290 and 330 nm.

Conditions: 5.0 μM oligonucleotide concentration (each strand), 10 mM phosphate buffer (pH 7.4) and 100 mM NaCl.

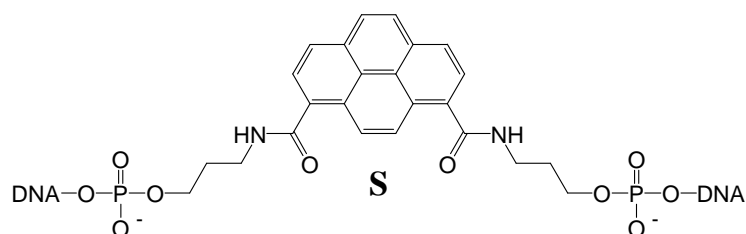
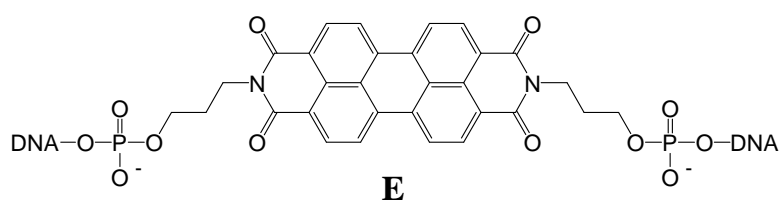
Figure 3.2. Temperature-dependent CD spectrum of TTF-modified duplex **7*8**.

Conditions: 5.0 μM oligo concentration (each strand), 10 mM phosphate buffer (pH 7.4) and 100 mM NaCl; inset shows enlarged view of the region from 300-400 nm.

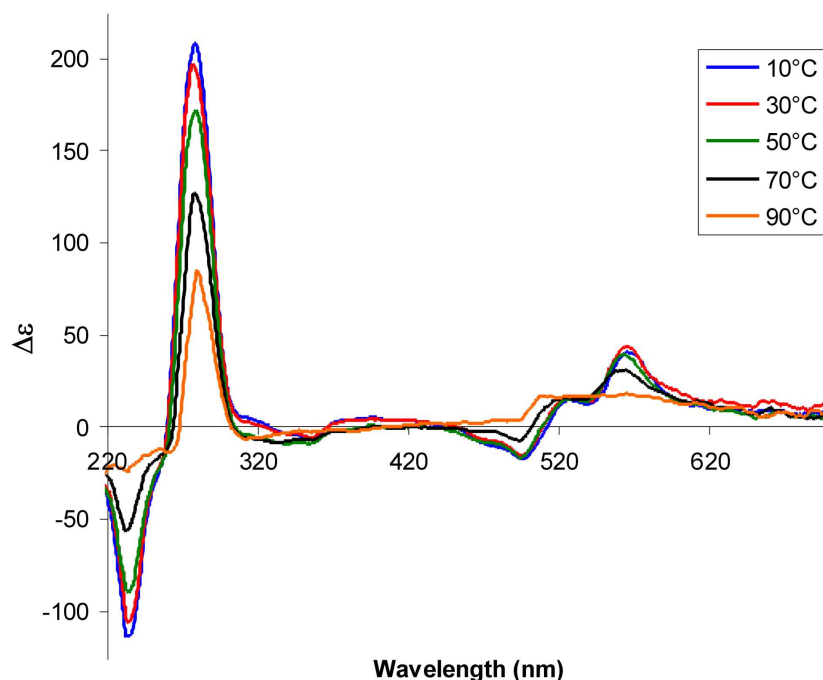
The structural and electronic effects resulting from TTF modification were further studied in mixed DNA hybrids (*Table 3.2*). Non-nucleosidic perylene diimide (PDI, building block **E**) or pyrene (**S**) units were placed opposite TTF. PDI was selected due to its high sensitivity towards conformational changes in CD spectroscopy,^[28] and pyrene for its diverse fluorescence properties.^[54] TTF modified strands form stable hybrids with all other modified strands. T_m values are generally somewhat lower than the one of the reference duplex **5*6** (72.5°C, *Table 3.1*), except for the PDI/TTF-mixed hybrid **9*10**, which has a comparable T_m (72.1°C). In the same duplex, CD spectroscopy (*Figure 3.3*) revealed strong exciton coupling of the PDI chromophores. This shows that the PDI units are oriented in a twisted conformation and that a well-ordered helical structure is maintained in the modified region of the duplex.^[55]

Table 3.2. Hybridization data of mixed DNA hybrids.

hybrid	T_m [°C]
9 (5') AGC TCG GTC FFC GAG AGT GCA	72.1
10 (3') TCG AGC CAG EEG CTC TCA CGT	
9 (5') AGC TCG GTC FFC GAG AGT GCA	67.5
11 (3') TCG AGC CAG SSG CTC TCA CGT	
12 (5') AGC TCG GTC ASC GAG AGT GCA	69.3
8 (3') TCG AGC CAG TFG CTC TCA CGT	
13 (5') AGC TCG GTC SSC GAG AGT GCA	66.7
8 (3') TCG AGC CAG TFG CTC TCA CGT	



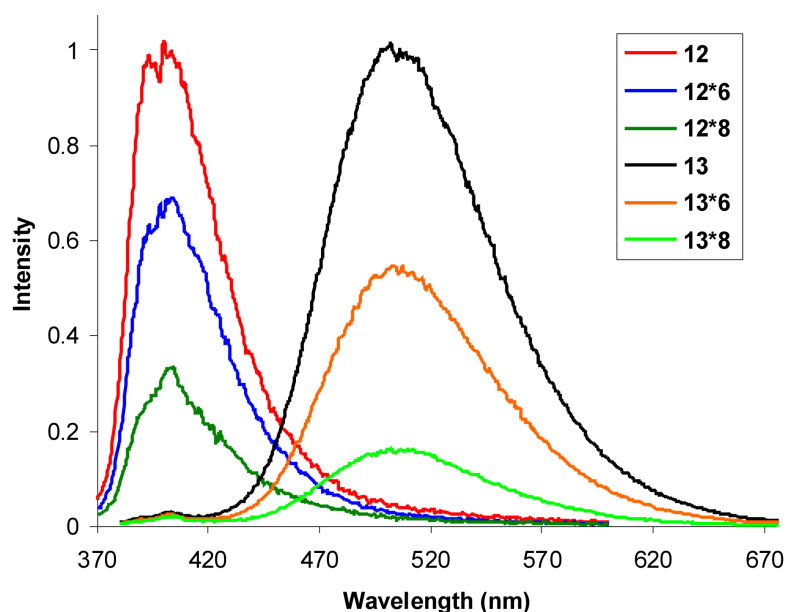
Conditions: 1.0 μ M oligonucleotide concentration (each strand), 10 mM phosphate buffer (pH 7.4) and 100 mM NaCl.

Figure 3.3. Temperature-dependent CD spectra of duplex **9*10**.

Conditions: 2.5 μM oligonucleotide concentration (each strand), 10 mM phosphate buffer (pH 7.4) and 100 mM NaCl; $\Delta\epsilon$ ($\text{mol}^{-1}\cdot\text{dm}^3\cdot\text{cm}^{-1}$).

As expected for a neutral form of tetrathiafulvalene,^[3,51,56,57] no fluorescence was observed for single stranded TTF-modified oligonucleotides (**7**, **8**) nor duplex **7*8**. On the other hand, the low oxidation potential of TTF may, in principle, favour fluorescence quenching *via* photo-induced electron transfer, as recently applied in construction of switchable fluorescent systems.^[51,56,57] Indeed, quenching of pyrene fluorescence by TTF was observed in hybrids **12*8** and **13*8** containing one and two pyrenes, respectively (*Figure 3.4* and *Table 3.3*). The fluorescence spectrum of **13** shows pyrene excimer emission with a maximum at 505 nm. This signal was decreased by 85% in duplex **13*8**, which is considerably more than observed by a non-modified complementary strand (duplex **13*6**). A slightly lower - but still significant - quenching effect (~70%) was observed in the case of monomer fluorescence (duplex **12*8**). These data show that TTF can act as a quencher within a DNA duplex.

Figure 3.4. Normalized fluorescence spectra of pyrene modified single strands **12** and **13** and the respective hybrids formed with an unmodified single strand (**6**) and a TTF-containing strand (**8**).



Conditions: 1.0 μM oligonucleotide concentration (each strand), 10 mM phosphate buffer (pH 7.4) and 100 mM NaCl; λ_{ex} at 354 nm.

Table 3.3. Quenching properties of TTF-modified oligonucleotide **8** in pyrene containing hybrids.

oligonucleotides	ϕ	quenching in %
12 (5') AGC TCG GTC ASC GAG AGT GCA	0.014	-
13 (5') AGC TCG GTC SSC GAG AGT GCA	0.094	-
12 (5') AGC TCG GTC ASC GAG AGT GCA 6 (3') TCG AGC CAG TAG CTC TCA CGT	0.008	35.6
12 (5') AGC TCG GTC ASC GAG AGT GCA 8 (3') TCG AGC CAG TFG CTC TCA CGT	0.004	70.5
13 (5') AGC TCG GTC SSC GAG AGT GCA 6 (3') TCG AGC CAG TAG CTC TCA CGT	0.062	46.0
13 (5') AGC TCG GTC SSC GAG AGT GCA 8 (3') TCG AGC CAG TFG CTC TCA CGT	0.014	85.1

Conditions: see Table 3.1; quinine sulphate was used as standard for quantum yield (ϕ) determination.

3.4 Conclusions

In conclusion, a non-nucleosidic tetrathiafulvalene building block suitable for incorporation into DNA has been described. TTF-modified oligonucleotides form stable hybrids, which were characterized by thermal denaturation, fluorescence and CD spectroscopy. Exciton coupling revealed a high degree of structural organization in the modified region of a heteroduplex formed by TTF and perylene diimide-containing strands. Furthermore, photo-induced electron transfer was demonstrated by fluorescence quenching in TTF/pyrene modified hetero-hybrids. The finding presented here may help in the development of optical sensors or redox-active, oligonucleotide-based diagnostics.

3.5 Experimental part

General. - Reactions were carried out under N₂ atmosphere using anhydrous solvents. Flash column chromatography was performed using silica gel 60 (63-32 μM, *Chemie Brunschwig AG*). If compounds were sensitive to acid, the silica was pre-treated with solvent containing 1% Et₃N. All NMR spectra were measured at room temperature on a *Buher AC-300* spectrometer. ¹H-NMR spectra were recorded at 300 MHz. Chemical shifts (δ) are reported in ppm relative to the residual undeuterated solvent (CDCl₃: 7.27 ppm). ¹³C-NMR spectra were recorded at 75 MHz. Chemical shifts are reported in ppm relative to the residual non-deuterated solvent (CDCl₃: 77.00 ppm). ³¹P-NMR spectra were recorded at 122 MHz. Chemical shifts are reported in ppm relative to 85% H₃PO₄ as an external standard. Electron impact mass spectra (EI-MS) was performed.

Synthesis of 2,3-Bis(2-hydroxyethylthio)-6,7-bis(pentyl-thio)tetrathiafulvalene (2). A solution of sodium (0.17 g, 7.35 mmol) in ethanol (20 ml) was added to a suspension of the cyanoethyl-protected compound **1** (0.85 g, 1.47 mmol) in anhydrous degassed ethanol (80 ml) under nitrogen. After being stirred at room temperature for 4 hours, the red-brown mixture was treated with 2-chloroethanol (1.78 g, 22.05 mmol). After a few minutes, the solution turned orange and a precipitate started to form. The mixture was then stirred overnight after which it was treated with water (50 ml) and extracted with dichloromethane. The extract was

washed with water, dried with magnesium sulfate and concentrated. The resulting solid was chromatographed (silica gel: CH₂Cl₂/EtOAc, 8:2) to give compound **2** with a yield of 73% (0.60 g, 1.08 mmol). ¹H-NMR (CDCl₃, 300 MHz): 0.90 (t, 6H), 1.36 (m, 8H), 1.65 (m, 4H), 2.81 (t, 4H), 3.01 (t, 4H), 3.76 (t, 4H); EI-MS: m/z = 560 (M⁺), C₂₀H₃₂O₂S₈, MW = 560.02; R_f (CH₂Cl₂/EtOAc, 4:1) = 0.15.

Synthesis of 2-{2-[(4,4'-Dimethoxytrityl)oxy]ethylthio}-3-(2-hydroxyethylthio)-6,7-bis(pentylthio)-tetrathiafulvalene (3). The diol **2** (0.50 g, 0.89 mmol) was dissolved in 7.5 ml of absolute pyridine and 4,4'-dimethoxytrityl chloride (0.30 g, 0.89 mmol) in 2.5 ml of absolute pyridine was added dropwise. After stirring at room temperature for 6 hours, a solution of sodium bicarbonate (25 ml) was added. The crude product was isolated by extraction with dichloromethane and dried with magnesium sulfate and concentrated. To avoid decomposition of the product on silica gel, the column was prepared with 1% triethylamine containing solvent. The crude was purified by chromatography (silica gel: hexane/EtOAc, 2:1) to give compound **3** with a yield of 35% (0.27 g, 0.31 mmol). ¹H-NMR (CDCl₃, 300 MHz): 0.87 (t, 3H), 0.90 (t, 3H), 1.30 (m, 8H), 1.63 (m, 4H), 2.76 (t, 2H), 2.82 (t, 2H), 2.87 (t, 2H), 3.02 (t, 2H), 3.34 (t, 2H), 3.62 (t, 2H), 3.79 (s, 6H), 6.83 (m, 4H), 7.19 (m, 1H), 7.28 (m, 2H), 7.31 (m, 4H), 7.43 (m, 2H); EI-MS: m/z = 862 (M⁺); C₄₁H₅₀O₄S₈, MW = 862.15; R_f (hexane/EtOAc 2:1) = 0.4.

Synthesis of 2-{2-[(Diisopropylamino)(2-cyanoethyl)-phosphinoxy]ethylthio}-3-{2-[(4,4'-dimethoxytrityl)oxy]-ethylthio}-6,7-bis(pentylthio)tetrathiafulvalene (4). The alcohol **3** (0.26 g, 0.30 mmol) and ethyldiisopropylamine (0.096 g, 0.75 mmol) were dissolved in 7.5 ml of absolute dichloromethane. 2-Cyanoethyl N,N-diisopropylchlorophosphoramidite (0.078 g, 0.33 mmol) dissolved in 2.5 ml of absolute dichloromethane were added dropwise. The reaction was stirred at room temperature for 2 hours. The crude product was directly purified by chromatography (silica gel: hexane/EtOAc, 2:1 +1% triethylamine). The fractions were combined, evaporated under high vacuum to furnish compound **4** with a yield of 85% (0.27 g, 0.25 mmol). ¹H-NMR (CDCl₃ 300 MHz): 0.88 (t, 3H), 0.90 (t, 3H), 1.16 (m, 12H), 1.33 (m, 8H), 1.64 (m, 4H), 2.59 (m, 2H), 2.79 (t, 2H), 2.82 (t, 2H), 2.96 (t, 2H), 2.99 (t, 2H), 3.32 (t, 2H), 3.61 (m, 4H), 3.79 (s, 6H), 3.80 (m, 2H), 6.83 (m, 4H), 7.19 (m, 1H), 7.28 (m, 2H), 7.31 (m, 4H), 7.43 (m, 2H). ³¹P-NMR (CDCl₃, 122 MHz) : 148.46. EI-MS: m/z = 1063 (M⁺), C₅₀H₆₇N₂O₅PS₈, MW= 1062.26; R_f (hexane/EtOAc, 2:1) = 0.9.

Synthesis and analysis of oligonucleotides. Cyanoethyl phosphoramidites from *Transgenomic* (Glasgow, UK) were used for oligonucleotide synthesis. Oligonucleotides **5, 6** were obtained from *Microsynth* (Switzerland) and were used without additional purification. Oligonucleotides **7-9** (Table 3.4) were prepared via automated oligonucleotide synthesis by a standard synthetic procedure ('trityl-off' mode) on a 394-DNA/RNA synthesizer (Applied Biosystems). Cleavage from the solid support and final deprotection was done by a treatment with 33% aqueous NH_3 at 55°C overnight. Oligonucleotides **7-9** were purified by reverse phase HPLC (LiChrospher 100 RP-18, 5 μm , Merck, *Bio-Tek instrument Autosampler 560*); eluent A = $(\text{Et}_3\text{NH})\text{OAc}$ (0.1 M, pH 7.4); eluent B = 80 % MeCN and 20% eluent A; gradient 5-80% B over 20 min at 25°C. ESI-MS (negative mode, $\text{CH}_3\text{CN}/\text{H}_2\text{O}/\text{TEA}$) of oligonucleotides was performed with a *Sciex QSTAR pulsar* (hybrid quadrupole time-of-flight mass spectrometer, *Applied Biosystems*). Oligomers **10**^[58] and **11-13**^[21] were synthesized as described.

Thermal denaturation experiments were carried out on a *Varian Cary-100 Bio-UV/VIS* spectrometer equipped with a Varian Cary-block temperature controller and data were collected with Varian WinUV software at 260 nm (cooling-heating-cooling cycles in the temperature range of 10-90°C, temperature gradient of 0.5°C/min). Experiments were carried out for 1.0 μM oligonucleotide concentration (each strand) or 5.0 μM (cooperative melting experiment), 10 mM phosphate buffer and 100 mM NaCl at pH 7.4. Data were analyzed with Kaleidagraph software from Synergy software. Melting temperature (T_m) values were determined as the maximum of the first derivative of the smoothed melting curve.

Fluorescence data were collected for 1.0 μM oligonucleotide solutions (1.0 μM of each strand in case of double strands) in phosphate buffer (10 mM) and NaCl (100 mM) at pH 7.4 on a Varian Cary Eclipse fluorescence spectrophotometer equipped with a Varian Cary-block temperature controller. Pyrene fluorescence: excitation at 354 nm, excitation and emission slit width 5 nm and 5 nm respectively, PMT detector voltage at medium sensitivity, 600 V.

CD spectra were recorded on a JASCO J-715 spectrophotometer using quartz cuvettes with an optical path of 1 cm.

Temperature dependent UV-vis spectra were collected in the range of 220-450 nm at 10-90°C with a 10 °C interval on *Varian Cary-100 Bio-UV/VIS* spectrophotometer equipped with a *Varian Cary-block* temperature controller. All experiments were carried out for 5.0 μM oligonucleotide concentration (each strand) in phosphate buffer (10 mM) and NaCl (100 mM) at pH=7.4. The cell compartment was flushed with N₂ to avoid the water condensation at low temperature.

Table 3.4. Mass spectrometry data (molecular formula, calc. average mass, and obtained).

<i>Oligo.</i>		<i>Molecular formula</i>	<i>Calc. aver.mass</i>	<i>Found</i>
7	(5') AGC TCG GTC AFC GAG AGT GCA	C ₂₁₅ H ₂₇₅ N ₈₁ O ₁₂₀ P ₂₀ S ₈	6790.0	6790
8	(3') TCG AGC CAG TFG CTC TCA CGT	C ₂₁₃ H ₂₇₇ N ₇₁ O ₁₂₄ P ₂₀ S ₈	6692.0	6689
9	(5') AGC TCG GTC FFC GAG AGT GCA	C ₂₂₅ H ₂₉₄ N ₇₆ O ₁₁₉ P ₂₀ S ₁₆	7099.9	7098

References

1. F. Wudl, G. M. Smith, E. J. Hufnagel, *J.Chem.Soc., Chem.Commun.* **1970**, 1453-1454.
2. J. Yamada, T. Sugimoto, *TTF Chemistry. Fundamentals and Applications of Tetrathiafulvalene*, Springer Verlag, Berlin **2004**.
3. J. L. Segura, N. Martin, *Angew.Chem.Int.Ed.* **2001**, *40*, 1372-1409.
4. see also the *special issue on molecular conductors* in *Chem. Rev.* **2004**, *104*, 4887-5056.
5. M. B. Nielsen, C. Lomholt, J. Becher, *Chem.Soc.Rev.* **2000**, *29*, 153-164.
6. C. Goze, C. Leiggener, S. X. Liu, L. Sanguinet, E. Levillain, A. Hauser, S. Decurtins, *Chemphyschem* **2007**, *8*, 1504-1512.
7. F. Dumur, N. Gautier, N. Gallego-Planas, Y. Sahin, E. Levillain, N. Mercier, P. Hudhomme, M. Masino, A. Girlando, V. Lloveras, J. Vidal-Gancedo, J. Veciana, C. Rovira, *J.Org.Chem.* **2004**, *69*, 2164-2177.
8. M. R. Bryce, *J.Mater.Chem.* **2000**, *10*, 589-598.

9. C. Y. Jia, S. X. Liu, C. Tanner, C. Leiggener, L. Sanguinet, E. Levillain, S. Leutwyler, A. Hauser, S. Decurtins, *Chem. Commun.* **2006**, 1878-1880.
10. G. Ho, J. R. Heath, M. Kondratenko, D. F. Perepichka, K. Arseneault, M. Pezolet, M. R. Bryce, *Chemistry-A European Journal* **2005**, *11*, 2914-2922.
11. E. Tsiperman, J. Y. Becker, V. Khodorkovsky, A. Shames, L. Shapiro, *Angew.Chem.Int.Ed.* **2005**, *44*, 4015-4018.
12. J. Wu, S. X. Liu, A. Neels, F. Le Derf, M. Salle, S. Decurtins, *Tetrahedron* **2007**, *63*, 11282-11286.
13. J. Puigmarti-Luis, V. Laukhin, A. P. del Pino, J. Vidal-Gancedo, C. Rovira, E. Laukhina, D. B. Amabilino, *Angew.Chem.Int.Ed.* **2007**, *46*, 238-241.
14. C. Wang, D. Q. Zhang, D. B. Zhu, *J.Am.Chem.Soc.* **2005**, *127*, 16372-16373.
15. N. C. Seeman, *Molecular Biotechnology* **2007**, *37*, 246-257.
16. U. Feldkamp, C. M. Niemeyer, *Angew.Chem.Int.Ed.* **2006**, *45*, 1856-1876.
17. F. D. Lewis, E. L. Burch, *Journal of Photochemistry and Photobiology A-Chemistry* **1996**, *96*, 19-23.
18. S. M. Langenegger, R. Häner, *Bioorg.Med.Chem.Lett.* **2006**, *16*, 5062-5065.
19. S. M. Langenegger, R. Häner, *Helv.Chim.Acta* **2002**, *85*, 3414-3421.
20. M. Nakamura, Y. Ohtoshi, K. Yamana, *Chem. Commun.* **2005**, 5163-5165.
21. F. Samain, V. L. Malinovskii, S. M. Langenegger, R. Häner, *Bioorg.Med.Chem.* **2008**, *16*, 27-33.
22. S. M. Langenegger, R. Häner, *Chem. Commun.* **2004**, 2792-2793.
23. U. B. Christensen, E. B. Pedersen, *Helv.Chim.Acta* **2003**, *86*, 2090-2097.
24. I. Trkulja, R. Häner, *Bioconjug.Chem.* **2007**, *18*, 289-292.
25. I. Trkulja, R. Häner, *J.Am.Chem.Soc.* **2007**, *129*, 7982-7989.
26. A. Okamoto, T. Ichiba, I. Saito, *J.Am.Chem.Soc.* **2004**, *126*, 8364-8365.
27. A. D. Malakhov, M. V. Skorobogaty, I. A. Prokhorenko, S. V. Gontarev, D. T. Kozhich, D. A. Stetsenko, I. A. Stepanova, Z. O. Shenkarev, Y. A. Berlin, V. A. Korshun, *Eur.J.Org.Chem.* **2004**, 1298-1307.
28. Y. Zheng, H. Long, G. C. Schatz, F. D. Lewis, *Chem. Commun.* **2005**, 4795-4797.
29. N. Rahe, C. Rinn, T. Carell, *Chem Commun.* **2003**, 2119-2121.
30. C. Wagner, H. A. Wagenknecht, *Org.Lett.* **2006**, *8*, 4191-4194.
31. S. Bevers, S. Schutte, L. W. McLaughlin, *J.Am.Chem.Soc.* **2000**, *122*, 5905-5915.

32. W. Wang, W. Wan, H. H. Zhou, S. Q. Niu, A. D. Q. Li, *J.Am.Chem.Soc.* **2003**, *125*, 5248-5249.
33. U. B. Christensen, E. B. Pedersen, *Nucl.Acids Res.* **2002**, *30*, 4918-4925.
34. S. M. Langenegger, G. Bianké, R. Tona, R. Häner, *Chimia* **2005**, *59*, 794-797.
35. H. Kashida, H. Asanuma, M. Komiyama, *Angew.Chem.Int.Ed.* **2004**, *43*, 6522-6525.
36. W. Wang, A. D. Q. Li, *Bioconjug.Chem.* **2007**, *18*, 1036-1052.
37. F. D. Lewis, X. Liu, Y. Wu, S. E. Miller, M. R. Wasielewski, R. L. Letsinger, R. Sanishvili, A. Joachimiak, V. Tereshko, M. Egli, *J.Am.Chem.Soc.* **1999**, *121*, 9905-9906.
38. A. Stutz, S. M. Langenegger, R. Häner, *Helv.Chim.Acta* **2003**, *86*, 3156-3163.
39. G. Bianké, R. Häner, *Nucleosides, Nucleotides & Nucleic Acids* **2007**, *26*, 949-952.
40. G. Bianké, R. Häner, *ChemBioChem* **2004**, *5*, 1063-1068.
41. F. D. Lewis, L. G. Zhang, R. F. Kelley, D. McCamant, M. R. Wasielewski, *Tetrahedron* **2007**, *63*, 3457-3464.
42. M. Nakamura, M. Ueda, S. Watanabe, S. Kumamoto, K. Yamana, *Tetrahedron Lett.* **2007**, *48*, 6159-6162.
43. V. Looser, S. M. Langenegger, R. Häner, J. S. Hartig, *Chem.Commun.* **2007**, 4357-4359.
44. K. Yamana, A. Yoshikawa, H. Nakano, *Tetrahedron Lett.* **1996**, *37*, 637-640.
45. H. Asanuma, T. Ito, T. Yoshida, X. G. Liang, M. Komiyama, *Angew.Chem.Int.Ed.* **1999**, *38*, 2393-2395.
46. F. D. Lewis, Y. S. Wu, X. Y. Liu, *J.Am.Chem.Soc.* **2002**, *124*, 12165-12173.
47. V. L. Malinovskii, F. Samain, R. Häner, *Angew.Chem.Int.Ed.* **2007**, *46*, 4464-4467.
48. . Kashida, M. Tanaka, S. Baba, T. Sakamoto, G. Kawai, H. Asanuma, M. Komiyama, *Chem.Eur.J.* **2006**, *12*, 777-784.
49. See e.g.: a) Pace, S.J.; Man, P.F.; Patil, A.P.; Tan, K.F., CNT-based sensors: devices, processes and uses thereof, PCT Int. Appl. (2007), WO 2007089550; b) Flechsig, G.-U., Reske, T., Selective Labeling of single-stranded regions of nucleic acid hybrids in the electrochemical detection of hybrids, Ger. (2007), DE 102005039726.
50. O. Neilands, V. Liepinsh, B. Turovska, *Org.Lett.* **1999**, *1*, 2065-2067.
51. S. Leroy-Lhez, J. Baffreau, L. Perrin, E. Levillain, M. Allain, M. J. Blesa, P. Hudhomme, *J.Org.Chem.* **2005**, *70*, 6313-6320.
52. S. L. Beaucage, M. H. Caruthers, *Tetrahedron Lett.* **1981**, *22*, 1859-1862.

-
53. High coupling yields were obtained during oligonucleotide synthesis. Some fragmentation of the oligomers at the site of the tetrathiafulvalene building block during ammonia deprotection was observed, however.
54. F. M. Winnik, *Chem.Rev.* **1993**, *93*, 587-614.
55. N. Berova, L. Di Bari, G. Pescitelli, *Chem.Soc.Rev.* **2007**, *36*, 914-931.
56. C. Loosli, C. Y. Jia, S. X. Liu, M. Haas, M. Dias, E. Levillain, A. Neels, G. Labat, A. Hauser, S. Decurtins, *J.Org.Chem.* **2005**, *70*, 4988-4992.
57. S. Delahaye, C. Loosli, S. X. Liu, S. Decurtins, G. Labat, A. Neels, A. Loosli, T. R. Ward, A. Hauser, *Adv.Funct.Mater.* **2006**, *16*, 286-295.
58. N. Bouquin, V. Malinovskii, R. Häner, *Chem.Commun.* **2008**, accepted.

Chapter 4. Highly Efficient Quenching of Excimer Fluorescence by Perylene Diimide in DNA

Published in: N. Bouquin, V. L. Malinovskii and R. Häner *Chem. Comm.*, **2008**, accepted.

4.1 Abstract

Single stranded DNA containing adjacent pyrenes gives rise to strong excimer fluorescence. Pairing with a complementary strand containing two perylene diimide building blocks opposite to the pyrenes results in powerful quenching. The efficiency of the process is attributed at least partly to interstrand stacking of pyrene and PDI units.

4.2 Introduction

Fluorescence labeling of biopolymers has become an indispensable tool in many areas of biomedical research.¹⁻³ The functionalization of proteins, nucleic acids and other biomolecules with fluorescent dyes enables their structural and functional elucidation,^{4;5} their cellular localization,^{6;7} as well as their quantitation.^{3;8;9} The use of two or more fluorescent labels brings additional benefits.¹⁰ Interaction of the dyes through fluorescence resonance energy transfer (FRET)¹¹ can be used for applications such as signal amplification,¹²⁻¹⁵ wavelength shifting¹⁶ or fluorescence quenching.⁹ The combination of a fluorophore with a quencher is used in many types of molecular probes. In general, these probes are designed to fluoresce in the presence of a target molecule, whereas in the absence of the target fluorescence is suppressed by the nearby quencher.^{9;17} The sensitivity of the probe critically depends on the degree of signal suppression in the absence of the target. Since quenching is often not complete the use of multiple quenchers has been proposed.^{18;19} Especially in the case of pyrene excimer fluorescence, entire quenching is difficult to achieve.^{19;20} Excimer signals offer advantages, such as a large *Stokes*-shift and long fluorescence lifetimes.²¹ Not surprising, interest in excimer forming oligonucleotide probes is high.^{15;22-36} We described the

generation of excimers by non-nucleosidic pyrene building blocks in single and double stranded nucleic acids.^{25;27;37-39} During our search for building blocks that allow proper control of the fluorescence in such hybrids we found that 3,4,9,10-perylenetetracarboxylic diimide (PDI, building block **E**, see *Table 4.1*) is a highly efficient quencher of pyrene excimer fluorescence. PDI and its derivatives have a long-standing history in dye and pigment research. More recently, they have attracted significant interest as electronic materials. Excellent chemical stability and high quantum yields render them attractive for applications in highly fluorescent materials.⁴⁰⁻⁴² Since PDI derivatives have a remarkable propensity to form self-assembled dimers and aggregates, they have been widely used as building blocks for supramolecular architectures.^{41;43;44} PDI-modified oligonucleotide were shown to adopt a variety of structures, including duplex, hairpins, triplex, quadruplex, as well as larger structures.^{30;43;45-49} It was noted that fluorescence of PDI is significantly reduced upon attachment to DNA.^{45;46;50} However, to the best of our knowledge perylene diimide has not been described as a fluorescence quencher. Here we report the use of PDI as a highly potent quencher of pyrene excimer fluorescence.

4.3 Results and Discussion

The PDI-building block was prepared according to the published procedure (see Experimental part *Scheme 4.1*).⁴⁹ Modified oligonucleotides were prepared by conventional means.⁵¹ Melting temperatures (T_m) are shown in *Table 4.1*. In comparison to the unmodified duplex **1*2**, hybrid **3*4** containing one PDI in each strand showed a remarkable increase in hybrid stability ($\Delta T_m = 11.3^\circ\text{C}$), which is in agreement with the literature and can be attributed to favorable stacking properties of the perylene diimides.⁴⁶ Addition of a second PDI in each strand (**5*6**) resulted in a further stabilization of the duplex ($\Delta T_m = 13.5^\circ\text{C}$).

The fluorescence spectra of single strands **3-6**, as well as hybrids **3*4** and **5*6** were measured. No significant emission was observed (*Figure 4.1*), rendering PDI rather uninteresting as a fluorescent building block in the current context. Circular dichroism (CD) spectra of both hybrids are consistent with an overall *B*-DNA conformation. For both hybrids, **3*4** and **5*6**, exciton coupled CD (EC-CD)^{52;53} was observed (*Figure 4.2*). Bisignate signals

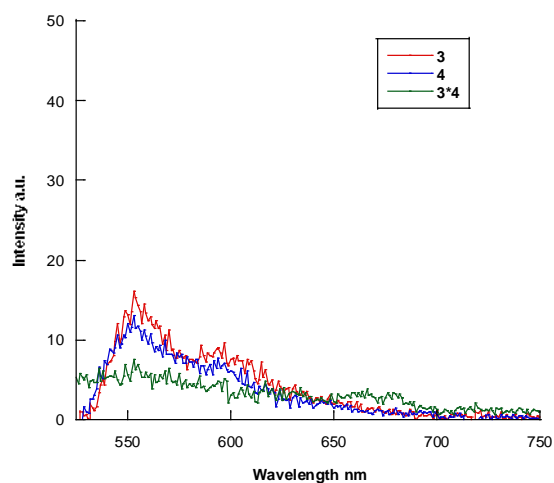
for the perylene band are centered at 531 nm ($A = 95$)⁵² and 525 nm ($A = 77$), respectively, revealing a twisted arrangement of the PDI units.

Table 4.1. Melting temperatures of DNA hybrids containing two and four perylene diimide-derived building blocks.

	oligonucleotide	T_m [°C] ¹	ΔT_m [°C]
1	(5') AGC TCG GTC ATC GAG AGT GCA	72.8	-
2	(3') TCG AGC CAG TAG CTC TCA CGT		
3	(5') AGC TCG GTC AEC GAG AGT GCA	84.1	+11.3
4	(3') TCG AGC CAG TEG CTC TCA CGT		
5	(5') AGC TCG GTC EEC GAG AGT GCA	86.3	+13.5
6	(3') TCG AGC CAG EEG CTC TCA CGT		

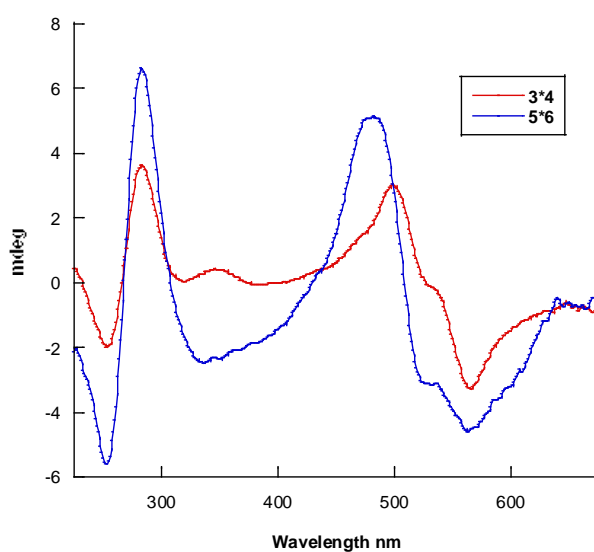
¹Conditions: 1.0 μ M oligonucleotide (each strand), 10 mM phosphate buffer (pH 7.4) and 100 mM NaCl.

Figure 4.1. Fluorescence spectra of PDI containing single strands **3**, **4** and hybrid **3*4**.



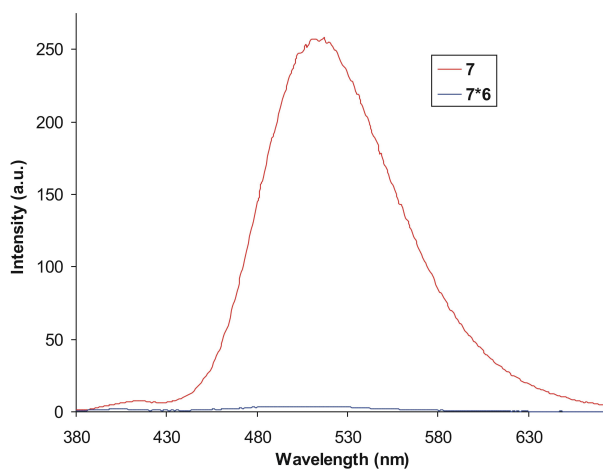
Conditions: 1 μ M oligonucleotide concentration (each strand), 10 mM phosphate buffer (pH 7.4) and 100 mM NaCl; excitation at 505 nm.

Figure 4.2. CD spectra of hybrids 3*4 and 5*6.



Conditions : 1 μ M oligonucleotide concentration (each strand), 10 mM Phosphate buffer (pH 7.4) and 100 mM NaCl.

Figure 4.3. Fluorescence spectra of single strand 7 and of hybrid 7*6.

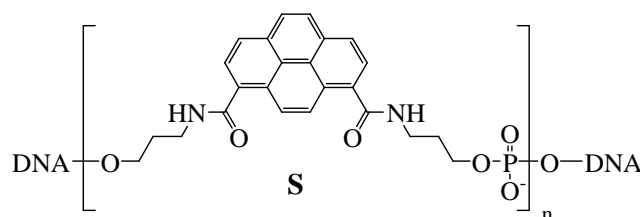


Conditions: 1.0 μ M oligonucleotide (each strand), 10 mM phosphate buffer (pH 7.4) and 100 mM NaCl; excitation: 354 nm.

Analysis of hetero-duplicates (i.e. hybrids formed by a perylene- and a pyrene-modified strand, see *Table 4.2*) led to a rather unexpected finding: duplex formation is accompanied by highly efficient quenching of the pyrene fluorescence (*Figure 4.3*). The excimer signal of the pyrenes^{38;54-57} in **7** is completely suppressed by oligomer **6**, which has two PDI building blocks opposite to the pyrenes. Additionally, it is important to note that the mixed hybrids **7*4** and **7*6** possess high thermal stabilities. The stabilizing effect of a PDI building block is comparable to the one found in the hybrids containing only PDI modifications (see *Table 4.1*).

Table 4.2. Fluorescence quenching by perylene diimide with one or two incorporations in opposite positions to two pyrene building blocks in DNA hybrids.

	oligonucleotide	T_m [°C] ¹	Q% ²
7	(5') AGC TCG GTC SSC GAG AGT GCA		
7 2	(5') AGC TCG GTC SSC GAG AGT GCA (3') TCG AGC CAG TAG CTC TCA CGT	64.6	46
7 4	(5') AGC TCG GTC SSC GAG AGT GCA (3') TCG AGC CAG TEG CTC TCA CGT	73.5	56
7 6	(5') AGC TCG GTC SSC GAG AGT GCA (3') TCG AGC CAG EEG CTC TCA CGT	75.5	98.6



¹Conditions: 1 μ M oligonucleotide (each strand), 10 mM phosphate buffer (pH 7.4) and 100 mM NaCl. ²Quenching effect, measured as the ratio of the excimer signals: $Q\% = 100\% \times \{1 - [F(\text{hybrid})/F(\text{single strand})]\}$.

The observed quenching effect can not simply be explained by the nearby located guanines, which are known for their quenching properties.⁵⁸ Control experiments showed that the unmodified oligonucleotide **2**, containing two guanines, has a quenching effect in the order of 46% (or roughly 23% per guanine base). We assume that the quenching effect is a result of

the formation of a non-fluorescent complex between the pyrene and PDI units and/or energy transfer from pyrene to PDI. Due to a good spectral overlap of PDI absorbance and pyrene excimer emission (Figure 4.5), energy transfer can readily take place. On the other hand, a single PDI unit in the complementary strand (hybrid **7*4**) has a relatively moderate quenching effect (~10% increase compared to the unmodified complementary strand **2**). Thus, the quenching caused by oligomer **6** is not simply explained by the sum of the individual contributions. Reduction of the excimer signal can take place by electronic quenching of the excited monomer or of the excimer. Additionally, it may be due to inhibition of excited dimer formation by steric interference with the PDI units. An interesting observation in this regard is the change in exciton chirality in the CD spectra (Figure 4.4). While the PDI-modified hybrids **3*4** and **5*6** both show a negative chirality, the couplet of the perylene signal in the mixed hybrid **7*6** is of opposite chirality. The switch indicates a fundamental change in the way the perylenes interact. In addition, the amplitude of the CD signal is significantly reduced in the mixed hybrid ($A = 30$ in **7*6** vs. 95 and 77 in **3*4** and **5*6**). Since exciton coupling is considerably distance dependent (\propto to r^{-2})⁵² this suggests a larger separation of the perylenes in hybrid **7*6** than in **3*4** and **5*6**, suggesting an interstrand stacking arrangement of the pyrene and perylene units. Stacking interactions are further supported by UV/VIS absorption spectra (Figure 4.6), which show bathochromic shifts for both the pyrene (16 nm) and the perylene (3-4 nm) absorption bands. Concluding, thus, that the pyrene and PDI residues are arranged in an interstrand stacking mode, four possibilities (-SSEE-, -SEES-, -SESE-, -ESSE-) exist. Of these, only the alternating, zipper-like arrangement of pyrene and PDI units (-SESE-) is compatible with the observations (i.e. no excimer signal, separation of PDI units and pyrene-PDI stacking interactions).

Figure 4.4. CD spectra of hybrids **3*4**, **5*6**, **7*6** at 30°C.

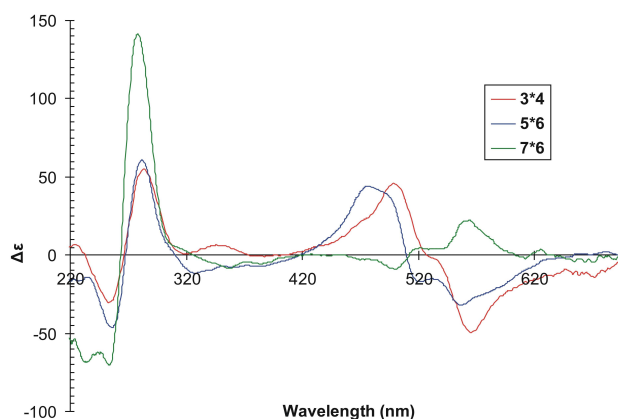


Figure 4.5. Normalized absorbance spectra of PDI-containing strand **6** and fluorescence spectra of pyrene monomer and excimer in oligonucleotides **8** and **7**, respectively.

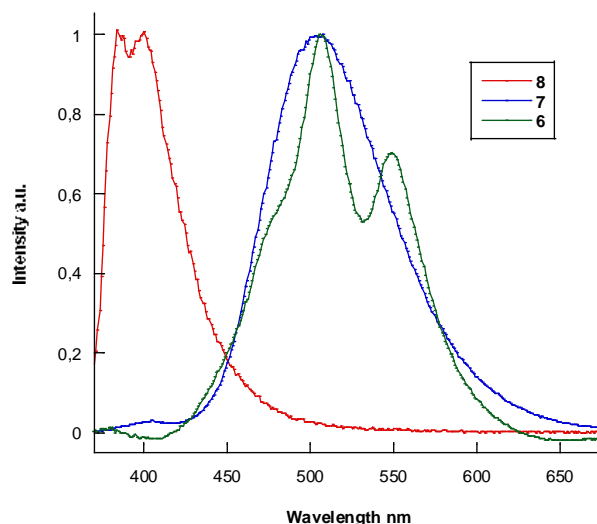
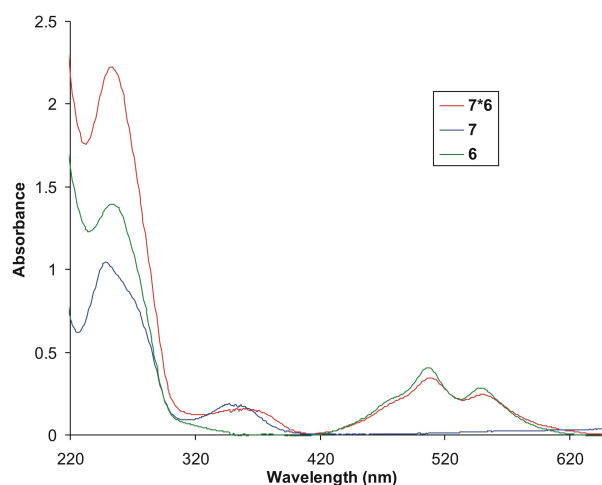


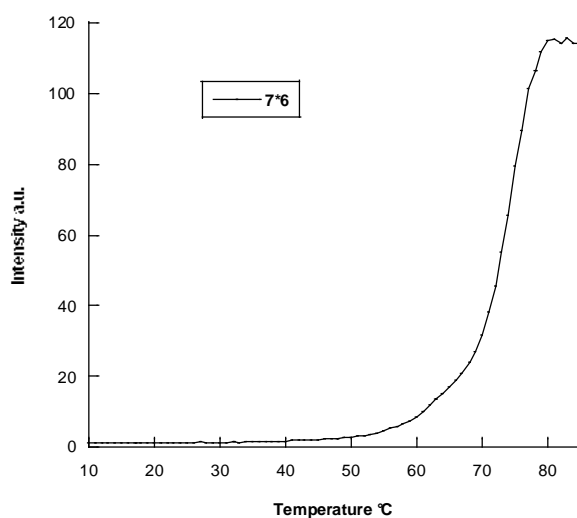
Figure 4.6. UV/VIS spectra of hybrid **7*6** and the corresponding single strands.



Conditions: 2.5 μM oligonucleotide concentration (each strand), 10 mM phosphate buffer (pH 7.4) and 100 mM NaCl.

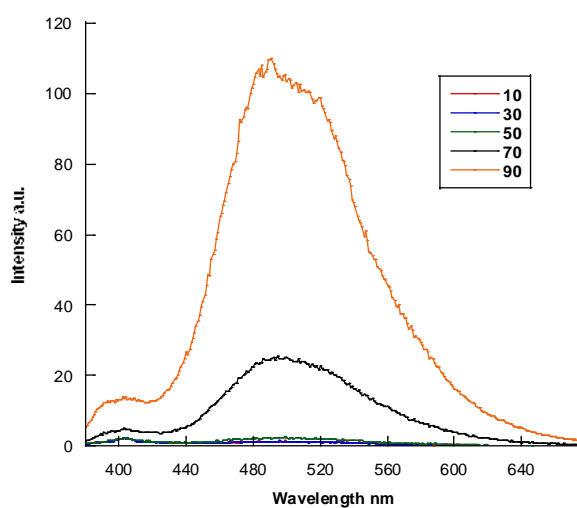
The efficiency of the quenching process is additionally illustrated in *Figure 4.7*, in which the thermal denaturation of hybrid **7*6** is monitored by the emission at 500nm. Below 50°C, the excimer signal is entirely absent. An increase of the temperature above this value is accompanied by a very sharp transition and maximum fluorescence is obtained after melting of the duplex. Temperature-dependent fluorescence shows the same behaviour in *Figure 4.8*.

Figure 4.7. Temperature-dependent fluorescence of hybrid 7*6.



Conditions: 2.5 μM oligonucleotide (each strand), 10 mM phosphate buffer (pH 7.4) and 100 mM NaCl ($T_m = 74.7^\circ\text{C}$).

Figure 4.8. Temperature-dependent fluorescence of hybrid 7*6.



Conditions: 2.5 μM oligonucleotide concentration (each strand), 10 mM phosphate buffer (pH 7.4) and 100 mM NaCl.

4.4 Conclusions

In conclusion, pyrene excimer fluorescence is efficiently quenched by a pair of non-nucleosidic perylene diimide (PDI) building blocks in a DNA duplex. Two factors may account for the quenching effect. Firstly, an excellent spectral overlap between PDI excitation and pyrene excimer emission allows efficient energy transfer. Secondly, pairs of pyrene and PDI units were found to interact *via* interstrand stacking. Thus, the PDI building blocks can physically interfere with the formation of the pyrene excimer leading to a non-fluorescent pyrene-PDI complex. Of course, the observed quenching may also be the result of a combination of these factors. Highly effective excimer quenching is important for many types of molecular probes. The present system may help in the design of future diagnostic tools.

4.5 Experimental part

General. - Reactions were carried out under N₂ atmosphere using anhydrous solvents. Flash column chromatography was performed using silica gel 60 (63-32 μM, *Chemie Brunschwig AG*). If compounds were sensitive to acid, the silica was pre-treated with solvent containing 1% Et₃N. All NMR spectra were measured at room temperature on a *Bruker AC-300* spectrometer. ¹H-NMR spectra were recorded at 300 MHz. Chemical shifts (δ) are reported in ppm relative to the residual undeuterated solvent (CDCl₃: 7.27 ppm). Multiplicities are abbreviated as follows: *s* = singlet, *d* = doublet, *t* = triplet, *q* = quadruplet, *m* = multiplet. ¹³C-NMR spectra were recorded at 75 MHz. Chemical shifts are reported in ppm relative to the residual non-deuterated solvent (CDCl₃: 77.00 ppm). ³¹P-NMR spectra were recorded at 122 MHz. Chemical shifts are reported in ppm relative to 85% H₃PO₄ as an external standard. Electron impact mass spectra (EI-MS) was performed.

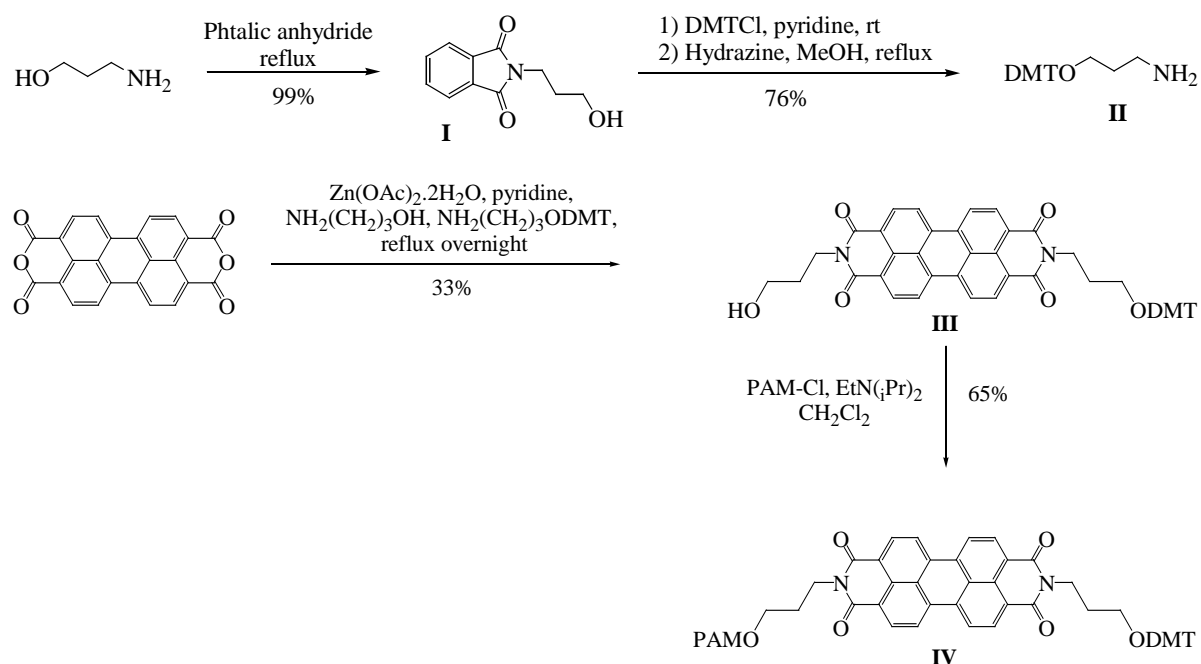
Synthesis of the 3-Phthalimidopropan-1-ol (I). A mixture of 3-aminopropan-1-ol (2 g, 26.62 mmol) and phthalic anhydride (3.95 g, 26.62 mmol) was kept at 145°C for 2 hours. The water which was formed was then removed under vacuum to give compound **I**. Yield: 99% (5.43 g, 26.48 mmol). ¹H-NMR (DMSO, 300 MHz): 1.73 (m, 2H), 3.43 (q, 2H), 3.62 (t, 2H), 4.50 (t, 1H), 7.84 (m, 4H). M_w = 205.07; C₁₁H₁₁NO₃.

Synthesis of the 3-[(4,4'-Dimethoxytrityl)oxy]propanamine (II). The alcohol **I** (1 g, 4.87 mmol) was dissolved in 20 ml of absolute pyridine and 4,4'-dimethoxytrityl chloride (1.82 g, 5.36 mmol) was added dropwise. After stirring at room temperature for 2 hours, the solution was diluted with EtOAc/Hexane 1:1, washed twice with a sodium bicarbonate solution, dried with magnesium sulfate and concentrated. The remaining solid was dissolved in methanol (15 ml) together with hydrazine (0.82 g, 16.45 mmol). The solution was stirred at 40°C for 4h. Then the precipitate was filtered off and the filtrate was reduced to 10 ml. This solution was diluted with dichloromethane, washed with 2_M Na₂CO₃, dried with magnesium sulfate and evaporated to give product as a yellow oil. To avoid decomposition of the product on silica gel, the column was prepared with 1% triethylamine containing solvent. The crude was purified by chromatography (silica gel : CH₂Cl₂ + 3 % Methanol) to give compound **II**. Yield: 76% (1.40 g, 3.71 mmol). ¹H-NMR (DMSO, 300 MHz): 1.72 (m, 2H), 2.79 (t, 2H), 3.11 (t, 2H), 3.76 (s, 6H), 6.79 (m, 4H), 7.15 (m, 1H), 7.28 (m, 2H), 7.31 (m, 4H), 7.41 (m, 2H). ¹³C-NMR (CDCl₃, 75 MHz): 34.09, 39.86, 53.57, 55.34, 61.42, 85.99, 113.18, 126.78, 127.89, 128.32, 129.30, 130.15, 136.69, 145.42, 158.52. R_f (CH₂Cl₂ / MeOH 8:1) : 0.6. M_w = 377.20; C₂₄H₂₇NO₃.

Synthesis of the N-{3-[(4,4'-Dimethoxytrityl)oxy]propyl}-N'-(3-hydroxypropyl)perylene diimide (III). 3,4,9,10-perylenetetracarboxylicdianhydride (1 g, 2.55 mmol) and zinc acetate (0.56 g 2.55 mmol) were dissolved in 10 ml of absolute pyridine. 3-aminopropan-1-ol (0.19 g, 2.55 mmol) and compound **II** (0.96 g, 2.55 mmol) were dissolved in 5 ml of absolute pyridine and were added dropwise. After stirring 150°C overnight, a solution of sodium bicarbonate was added. The crude product was isolated by extraction with dichloromethane and dried with magnesium sulfate and concentrated. To avoid decomposition of the product on silica gel, the column was prepared with 1% triethylamine containing solvent. The crude was purified by chromatography (silica gel : CH₂Cl₂ + MeOH 5%) to give compound **III**. Yield: 40% (1.26 g, 1.02 mmol). ¹H-NMR (CDCl₃, 300 MHz): 2.05 (m, 4H), 3.23 (t, 2H), 3.69 (t, 2H), 3.70 (s, 6H), 4.35 (m, 4H), 6.73 (m, 4H), 7.10 (m, 1H), 7.12 (m, 2H), 7.28 (m, 4H), 7.40 (m, 2H), 8.34 (m, 4H), 8.44 (m, 2H), 8.56 (m, 2H). R_f (CH₂Cl₂ + MeOH 5%) : 0.30. M_w = 808.28; C₅₁H₄₀N₂O₈.

Synthesis of the *N*-{3-[(Diisopropylamino)(2-cyanoethyl)phosphinoxy]propyl}-*N'*-{3-[(4,4'-dimethoxytrityl)oxy]propyl}perylene diimide (IV). The alcohol **III** (0.40 g, 0.50 mmol) and ethyldiisopropylamine (0.161 g, 1.25 mmol) were dissolved in 10 ml of absolute dichloromethane. PAM-Cl (0.13 g, 0.55 mmol) dissolved in 5 ml of absolute dichloromethane were added dropwise. The reaction was stirred at room temperature for 2 hours. The crude product was directly purified by chromatography (silica gel : Hexane / EtOAc 1:1 +1% triethylamine). The fractions were combined, evaporated under high vacuum to furnish compound **IV**. Yield: 82% (0.42 g, 0.41 mmol). ¹H-NMR (CDCl₃, 300 MHz): 1.16 (m, 12H), 2.10 (t, 4H), 2.67 (t, 2H), 3.23 (t, 2H), 3.59 (m, 2H), 3.70 (s, 6H), 3.88 (m, 4H), 4.33 (m, 4H), 6.73 (m, 4H), 7.10 (m, 1H), 7.17 (m, 2H), 7.28 (m, 4H), 7.40 (m, 2H), 8.58-8.66 (m, 8H). ³¹P-NMR (CDCl₃ 122 MHz) : 147.86. R_f (EtOAc) : 0.95. M_w = 1008.39; C₆₀H₅₇N₄O₉P.

Scheme 4.1. Synthesis of the perylene diimide-derived phosphoramidite building block **IV**.



Synthesis and analysis of oligonucleotides. Cyanoethyl phosphoramidites from *Transgenomic* (Glasgow, UK) were used for oligonucleotide synthesis. Oligonucleotides **1, 2** were obtained from *Microsynth* (Switzerland) and were used without additional purification. Oligonucleotides **3-6** (Table 4.3) were prepared via automated oligonucleotide synthesis by a standard synthetic procedure ('trityl-off' mode) on a 394-DNA/RNA synthesizer (Applied

Biosystems). Cleavage from the solid support and final deprotection was done by a treatment with 33% aqueous NH_3 at 55°C overnight. All oligonucleotides were purified by reverse phase HPLC (LiChrospher 100 RP-18, 5 μm , Merck, *Bio-Tek instrument Autosampler 560*); eluent A = $(\text{Et}_3\text{NH})\text{OAc}$ (0.1 M, pH 7.4); eluent B = 80 % MeCN and 20% eluent A; gradient 5-35% B over 20 min at 25°C . ESI-MS (negative mode, $\text{CH}_3\text{CN}/\text{H}_2\text{O}/\text{TEA}$) of oligonucleotides was performed with a *Sciex QSTAR pulsar* (hybrid quadrupole time-of-flight mass spectrometer, *Applied Biosystems*).

Thermal denaturation experiments were carried out on a *Varian Cary-100 Bio-UV/VIS* spectrometer equipped with a Varian Cary-block temperature controller and data were collected with Varian WinUV software at 260 nm (cooling-heating-cooling cycles in the temperature range of $10\text{-}90^\circ\text{C}$, temperature gradient of $0.5^\circ\text{C}/\text{min}$). Experiments were carried out for 1.0 μM oligonucleotide concentration (each strand), 10 mM phosphate buffer and 100 mM NaCl at pH 7.4. Data were analyzed with Kaleidagraph software from Synergy software. Melting temperature (T_m) values were determined as the maximum of the first derivative of the smoothed melting curve.

Fluorescence data were collected for 1.0 μM oligonucleotide solutions (1.0 μM of each strand in case of double strands) in phosphate buffer (10 mM) and NaCl (100 mM) at pH 7.4 on a Varian Cary Eclipse fluorescence spectrophotometer equipped with a Varian Cary-block temperature controller (a) pyrene fluorescence: excitation at 354 nm, excitation and emission slit width 5 nm and 5 nm respectively, PMT detector voltage at medium sensitivity, 600 V; b) perylene diimide: excitation at 505 nm, ex. slit 10 nm, em. slit. 10 nm, PMT detector voltage at high sensitivity, 800 V).

CD spectra were recorded on a JASCO J-715 spectrophotometer using quartz cuvettes with an optical path of 1 cm.

UV-Vis data were collected in the range of 220-700 nm at 30°C on *Varian Cary-100 Bio-UV/VIS* spectrophotometer equipped with a *Varian Cary-block* temperature controller. All experiments were carried out for 2.5 μM oligonucleotide concentration (each strand) in phosphate buffer (10 mM) and NaCl (100 mM) at pH=7.4.

Table 4.3. Mass spectrometry data (molecular formula, calc. average mass and found mass).

<i>Oligo.</i>		<i>Molecular formula</i>	<i>Calc. aver.mass</i>	<i>Found</i>
3	(5') AGC TCG GTC AEC GAG AGT GCA	C ₂₂₅ H ₂₆₅ N ₈₃ O ₁₂₄ P ₂₀	6735.6	6735
4	(3') TCG AGC CAG TEG CTC TCA CGT	C ₂₂₃ H ₂₆₇ N ₇₃ O ₁₂₈ P ₂₀	6637.5	6638
5	(5') AGC TCG GTC EEC GAG AGT GCA	C ₂₄₅ H ₂₇₄ N ₈₀ O ₁₂₇ P ₂₀	6990.9	6992
6	(3') TCG AGC CAG EEG CTC TCA CGT	C ₂₄₃ H ₂₇₅ N ₇₃ O ₁₂₉ P ₂₀	6901.8	6903

References

1. R. Hovius, P. Vallotton, T. Wohland, H. Vogel, *TIPS*, 2000, **21**, 266-273.
2. F. Wang, W. B. Tan, Y. Zhang, X. P. Fan, M. Q. Wang, *Nanotechnology*, 2006, **17**, R1-R13.
3. R. T. Ranasinghe, T. Brown, *Chem. Commun.*, 2005, 5487-5502.
4. H. M. O'Hare, K. Johnsson, A. Gautier, *Curr. Opin. Struct. Biol.*, 2007, **17**, 488-494.
5. M. R. Webb, *Mol. BioSys.*, 2007, **3**, 249-256.
6. D. P. Bratu, B. J. Cha, M. M. Mhlanga, F. R. Kramer, S. Tyagi, *Proc. Natl. Acad. Sci. U.S.A.*, 2003, **100**, 13308-13313.
7. A. A. Marti, S. Jockusch, N. Stevens, J. Ju, N. J. Turro, *Acc. Chem. Res.*, 2007, **40**, 402-409.
8. S. Tyagi, D. P. Bratu, F. R. Kramer, *Nat. Biotechnol.*, 1998, **16**, 49-53.
9. S. Tyagi, F. R. Kramer, *Nat. Biotechnol.*, 1996, **14**, 303-308.
10. *Fluorescent Energy Transfer Nucleic Acid Probes - Design and Protocols*, (Ed.: V. V. Didenko) Humana Press, Totowa, NJ 07512 2006.
11. T. Förster, *Naturwissenschaften*, 1946, **33**, 166-175.
12. M. Kosuge, M. Kubota, A. Ono, *Tetrahedron Lett.*, 2004, **45**, 3945-3947.
13. G. Tong, J. M. Lawlor, G. W. Tregear, J. Haralambidis, *J. Am. Chem. Soc.*, 1995, **117**, 12151-12158.
14. A. Cuppoletti, Y. J. Cho, J. S. Park, C. Strassler, E. T. Kool, *Bioconjug. Chem.*, 2005, **16**, 528-534.

15. P. J. Hrdlicka, B. R. Babu, M. D. Sorensen, N. Harrit, J. Wengel, *J.Am.Chem.Soc.*, 2005, **127**, 13293-13299.
16. S. Tyagi, S. A. E. Marras, F. R. Kramer, *Nat.Biotechnol.*, 2000, **18**, 1191-1196.
17. J. R. Lakowicz, *Principles of Fluorescence Spectroscopy*, 3rd ed. Springer, Singapore, 2006.
18. C. J. Yang, H. Lin, W. Tan, *J.Am.Chem.Soc.*, 2005, **127**, 12772-12773.
19. P. Conlon, C. J. Yang, Y. Wu, Y. Chen, K. Martinez, Y. Kim, N. Stevens, A. A. Marti, S. Jockusch, N. J. Turro, W. Tan, *J.Am.Chem.Soc.*, 2008, **130**, 336-342.
20. J. N. Wilson, Y. N. Teo, E. T. Kool, *J.Am.Chem.Soc.*, 2007, **129**, 15426-15427.
21. J. B. Birks, *Photophysics of Aromatic Molecules*, Wiley, New York, 1970.
22. K. Yamana, Y. Fukunaga, Y. Ohtani, S. Sato, M. Nakamura, W. J. Kim, T. Akaike, A. Maruyama, *Chem.Comm.*, 2005, 2509-2511.
23. E. V. Bichenkova, A. Gbaj, L. Walsh, H. E. Savage, C. Rogert, A. R. Sardarian, L. L. Etchells, K. T. Douglas, *Org.Biomol.Chem.*, 2007, **5**, 1039-1051.
24. I. V. Astakhova, A. D. Malakhov, I. A. Stepanova, A. V. Ustinov, S. L. Bondarev, A. S. Paramonov, V. A. Korshun, *Bioconjug.Chem.*, 2007, **18**, 1972-1980.
25. S. M. Langenegger, R. Häner, *Chem.Comm.*, 2004, 2792-2793.
26. A. Okamoto, T. Ichiba, I. Saito, *J.Am.Chem.Soc.*, 2004, **126**, 8364-8365.
27. I. Trkulja, S. M. Biner, S. M. Langenegger, R. Häner, *ChemBioChem*, 2007, **8**, 25-27.
28. K. Fujimoto, H. Shimizu, M. Inouye, *J.Org.Chem.*, 2004, **69**, 3271-3275.
29. H. Maeda, T. Maeda, K. Mizuno, K. Fujimoto, H. Shimizu, M. Inouye, *Chem.Eur.J.*, 2006, **12**, 824-831.
30. H. Zhu, F. D. Lewis, *Bioconjug.Chem.*, 2007, **18**, 1213-1217.
31. E. Kostenko, M. Dobrikov, D. Pyshnyi, V. Petyuk, N. Komarova, V. Vlassov, M. Zenkova, *Nucl.Acids.Res.*, 2001, **29**, 3611-3620.
32. P. L. Paris, J. M. Langenhan, E. T. Kool, *Nucl.Acids Res.*, 1998, **26**, 3789-3793.
33. M. Masuko, H. Ohtani, K. Ebata, A. Shimadzu, *Nucl.Acids Res.*, 1998, **26**, 5409-5416.
34. U. B. Christensen, E. B. Pedersen, *Helv.Chim.Acta*, 2003, **86**, 2090-2097.
35. H. Kashida, H. Asanuma, M. Komiyama, *Chem.Comm.*, 2006, 2768-2770.
36. A. A. Marti, X. X. Li, S. Jockusch, Z. M. Li, B. Raveendra, S. Kalachikov, J. J. Russo, I. Morozova, S. V. Puthanveetil, J. Y. Ju, N. J. Turro, *Nucl.Acids Res.*, 2006, **34**, 3161-3168.

37. S. M. Langenegger, R. Häner, *Bioorg.Med.Chem.Lett.*, 2006, **16**, 5062-5065.
38. F. Samain, V. L. Malinovskii, S. M. Langenegger, R. Häner, *Bioorg.Med.Chem.*, 2008, **16**, 27-33.
39. V. Looser, S. M. Langenegger, R. Häner, J. S. Hartig, *Chem.Commun.*, 2007, 4357-4359.
40. H. Langhals, *Helv.Chim.Acta*, 2005, **88**, 1309-1343.
41. F. Würthner, *Chem.Commun.*, 2004, 1564-1579.
42. E. E. Neuteboom, S. C. J. Meskers, E. W. Meijer, R. A. J. Janssen, *Macromolecular Chemistry and Physics*, 2004, **205**, 217-222.
43. W. Wang, W. Wan, H. H. Zhou, S. Q. Niu, A. D. Q. Li, *J.Am.Chem.Soc.*, 2003, **125**, 5248-5249.
44. W. Wang, J. J. Han, L. Q. Wang, L. S. Li, W. J. Shaw, A. D. Q. Li, *Nano Letters*, 2003, **3**, 455-458.
45. S. Bevers, S. Schutte, L. W. McLaughlin, *J.Am.Chem.Soc.*, 2000, **122**, 5905-5915.
46. Y. Zheng, H. Long, G. C. Schatz, F. D. Lewis, *Chem.Commun.*, 2005, 4795-4797.
47. Y. Zheng, H. Long, G. C. Schatz, F. D. Lewis, *Chem.Commun.*, 2006, 3830-3832.
48. C. Wagner, H. A. Wagenknecht, *Org.Lett.*, 2006, **8**, 4191-4194.
49. N. Rahe, C. Rinn, T. Carell, *Chem Commun.*, 2003, 2119-2121.
50. F. D. Lewis, L. G. Zhang, R. F. Kelley, D. McCamant, M. R. Wasielewski, *Tetrahedron*, 2007, **63**, 3457-3464.
51. S. M. Langenegger, R. Häner, *Helv.Chim.Acta*, 2002, **85**, 3414-3421.
52. N. Berova, L. Di Bari, G. Pescitelli, *Chem.Soc.Rev.*, 2007, **36**, 914-931.
53. N. Berova, K. Nakanishi, R. W. Woody, *Circular Dichroism - Principles and Applications*, 2nd ed. Wiley-VCH, New York 2000.
54. F. M. Winnik, *Chem.Rev.*, 1993, **93**, 587-614.
55. V. L. Malinovskii, F. Samain, R. Häner, *Angew.Chem.Int.Ed.Engl.*, 2007, **46**, 4464-4467.
56. I. Trkulja, R. Häner, *Bioconjug.Chem.*, 2007, **18**, 289-292.
57. I. Trkulja, R. Häner, *J.Am.Chem.Soc.*, 2007, **129**, 7982-7989.
58. N. Venkatesan, Y. J. Seo, B. H. Kim, *Chem.Soc.Rev.*, 2008, *First published on the web 17th January 2008*.

Chapter 5. Formation of a One- and a Two-Dimensional DNA Scaffold Containing Pyrene Units

5.1 Abstract

Two different DNA scaffolds containing pyrene building blocks were constructed for studying molecular self-assembly. One scaffold consists of a one-dimensional DNA assembly along a double strand containing pyrene building blocks. The second which is a two dimensional DNA framework, consists in a three-way junction with three branches of different lengths and different numbers of pyrene moieties per strand. Here, we report the synthesis and the spectroscopic properties of these DNA mimics containing multiple pyrene building blocks.

5.2 Introduction

Self-assembly is often one of the key approaches discussed when debating future methods for building nanostructures and nanodevices.¹ Self-assembly procedures for the production of some non-biological systems are commonly used and have in some cases found commercial applications. These include self-assembled monolayers for the immobilization of compounds and materials on surface. However, these structures are typically polydisperse and only nanoscaled in one dimension. Formation of more complex monodisperse and two- or three-dimensional nanostructures consisting of multiple building blocks requires precise control over each interaction when the structure undergoes self-assembly. The self-assembly of oligonucleotides is a versatile and a powerful tool for the construction of objects on the nanoscale. The strictly information driven pairing of DNA fragments can be used to rationally design and build nanostructures with planned topologies and geometries. The geometrical structures of branched nucleic acid molecules and the effect of a branched point on the thermodynamic stability of these molecules have been studied in detail in the last few years.²⁻⁵ Many of these branched molecular structures, such as four- and three-way junctions

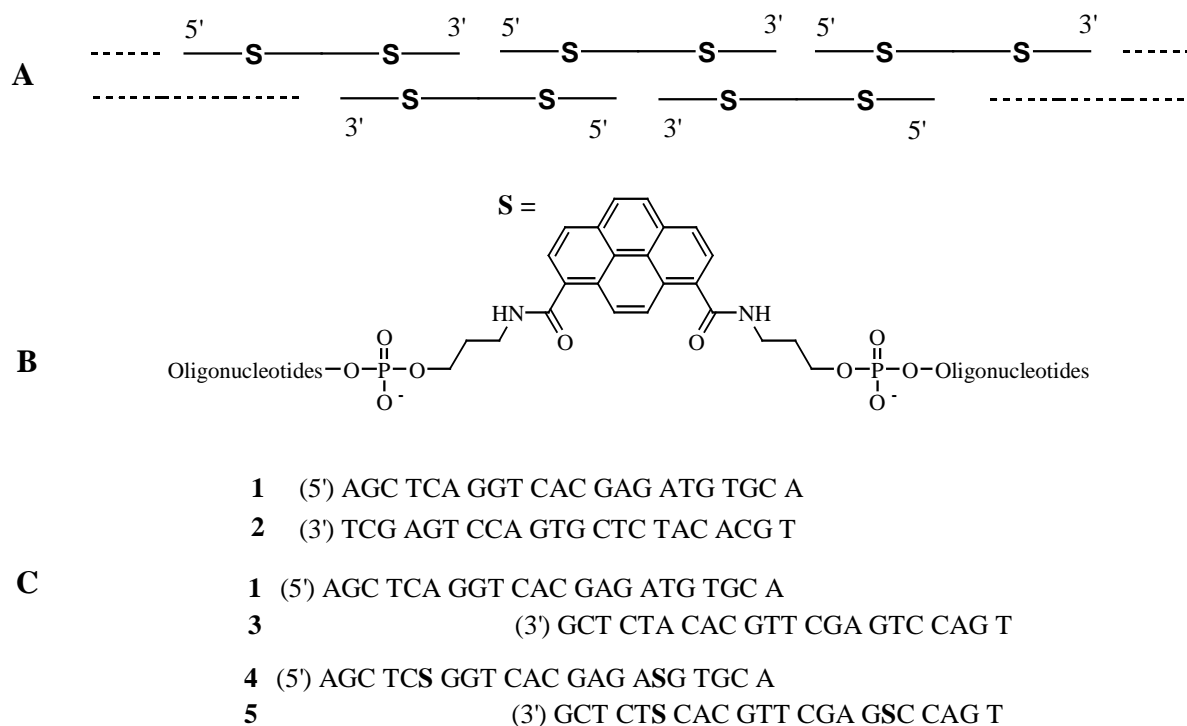
and bulged duplexes, correspond to important biological structures. The main biological relevance of branched DNA species lies in their proposed role as possible intermediates in molecular rearrangements, repair and recombination. Fluorescence resonance energy transfer (FRET) has proved to be a powerful technique for investigating the structures of DNA/RNA molecules, especially when applied to a set of identical branched structures with dye attached to different permuted positions.⁶⁻¹¹ Recently, we reported the synthesis and the properties of a pyrene based building blocks which was incorporated into DNA for its stacking properties and for its capability to form excimer. Pyrene is a strong fluorophore and a good intercalator for DNA that is why we used it for multiple incorporation into DNA.¹²⁻¹⁴ Here, we report the synthesis and the spectroscopical properties of a one- and a two-dimensional DNA scaffold. One scaffold consists of a one-dimensional DNA assembly along a double strand containing two pyrene building blocks per strand. The second which is a two dimensional DNA framework consists in a three-way junction with three branches of different lengths and different numbers of pyrene moieties per strand.

5.3 Results and Discussion

The pyrene phosphoramidite was obtained according to a procedure reported in the literature.¹²⁻¹⁴ The building block was incorporated into oligonucleotides. Assembly of the different oligonucleotides involved the standard phosphoramidite procedure. Deprotection (conc. NH₃, 50°C), followed by standard HPLC purification yielded oligonucleotides **1-8** (*Table 5.3*).

5.3.1 One-Dimensional DNA Scaffold Containing Pyrene Building Blocks

Here, the idea was to design a scaffold which is able to be extended in one dimension along a double strand. For this study, we used pyrene moieties as fluorophore to detect the extension of the duplex. Pyrene building blocks are placed in opposite position to each other along the double strand (*Scheme 5.1*). In this case, pyrene moieties should form excimer which can be observed. Oligonucleotides **1-5** were used for this one-dimensional DNA scaffold. **1** and **2** are in normal duplex form, **1** and **3** as well as **4** and **5** are shifted to give an extended duplex.



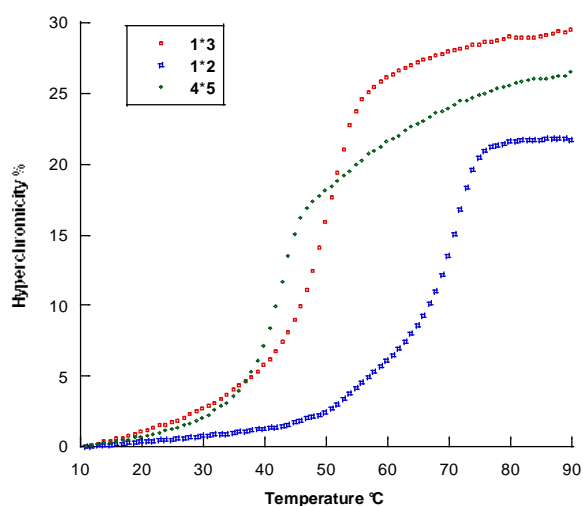
Scheme 5.1. (A) Linear assembly. (B) Pyrene building block. (C) Different sequences used for this project.

The effect of the pyrene building block on duplex stability was analysed by thermal denaturation experiments (*Table 5.1*). The natural duplex **1*2** (T_m 71.2°C) which is entirely hybridised and the natural duplex **1*3** (T_m 50.2°C) which is shifted, are used as controls. A decrease in stability is observed for the hybrid **4*5** (ΔT_m -8.7°C) compare to the natural hybrid **1*3** (*Fig. 5.1*). Effectively, in this duplex system, two A-T base pairs were replaced by four pyrene units and this decrease is due to the lack of four bases.

Table 5.1. Hybridization data of different oligonucleotide duplexes containing pyrene-based building blocks.

Oligo #	Duplex	T _m [°C]	ΔT _m [°C]
1	(5') AGC TCA GGT CAC GAG ATG TGC A	71.2	-
2	(3') TCG AGT CCA GTG CTC TAC ACG T		
1	(5') AGC TCA GGT CAC GAG ATG TGC A	50.2	-
3	(3') GCT CTA CAC GTT CGA GTC CAG T		
4	(5') AGC TCS GGT CAC GAG ASG TGC A	41.5	-8.7 ^{a)}
5	(3') GCT CTS CAC GTT CGA GSC CAG T		

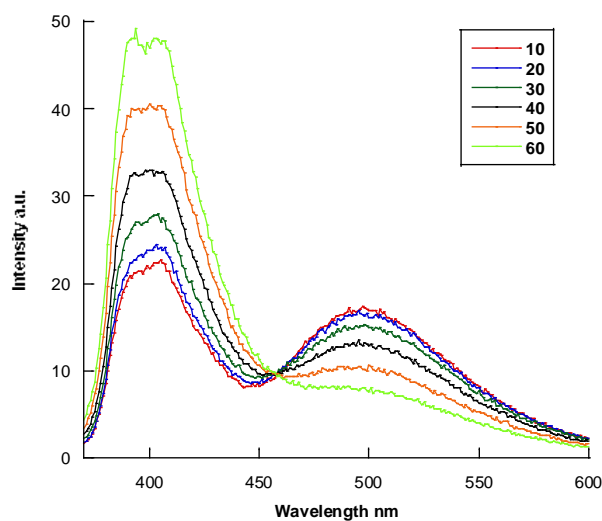
Conditions: 1.0 μM oligonucleotide concentration (each strand), 10 mM phosphate buffer (pH 7.4) and 100 mM NaCl. a) relative to **1*3**.

**Figure 5.1** Melting curves of different duplex hybrids. Conditions: 1.0 μM oligonucleotide concentration (each strand), 10 mM phosphate buffer (pH 7.4) and 100 mM NaCl.

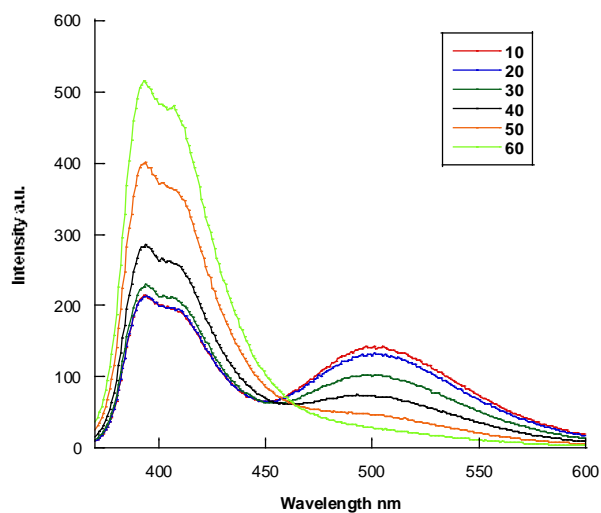
Temperature-dependent fluorescence experiments were achieved for single strands **4**, **5** and for the **4*5** hybrid (*Fig. 5.2*). The behaviour of single strands **4** (a) and **5** (b) are similar in temperature-dependent fluorescence spectra. At low temperature we observed the same kind of monomer and excimer ratio for **4** and for **5** and at high temperature monomer is predominant and no excimer was observed for single strands **4** and **5**. An explanation of this phenomenon can be that the two pyrene building blocks within single strand can form static excimer at low temperature which is not stable at high temperature.

The temperature-dependent fluorescence spectrum of hybrid **4*5** (c) shows a important excimer signal at low temperature which decreases progressively with an increase of the temperature. After 40°C we observe only monomer emission which is in agreement with the thermal melting experiments where we observed a T_m of 41.5°C for the hybrid **4*5**. This experiment led us to the conclusion that the extended duplex is formed due to the strong excimer and low monomer signal for hybrid **4*5** at low temperature.

(a)



(b)



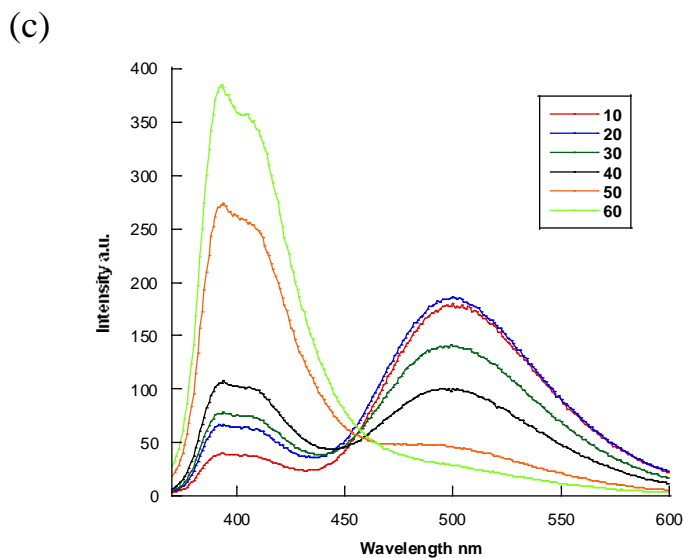


Figure 5.2. Temperature-dependent fluorescence spectra of single strands **4** (a), **5** (b) and of hybrid **4*5** (c). Conditions: 1.0 μM oligonucleotide concentration (each strand), 10 mM phosphate buffer (pH 7.4) and 100 mM NaCl.

Gel electrophoresis experiments were performed to see if we really have an extension of the **1*3** and the **4*5** duplex or if we only formed the partial duplex (*Fig. 5.3*). The first experiment (*Fig. 5.3 left*) shows that hybrid **1*2** has a higher mobility than hybrids **1*3** and **4*5** which show the same migration. This means that if we only formed the partial duplex with **1*3** or with **4*5** we should have the same mobility as with **1*2**. This is not what we observed, therefore we can claim the presence of an extended duplex for hybrid **1*3** and **4*5**, as proposed before. The second experiment (*Fig. 5.3 right*) was done to compare the mobility of hybrids **1*3** and **4*5**. We observed the same mobility for both hybrids but a really defined band is observed for hybrid **4*5** and a smeared band over the whole gel is observed for **1*3**. An explanation can be that there are different kind of lengths for hybrid **1*3** but only very long length for hybrid **4*5**. For the moment we are not able to assign the length of these extended hybrids.

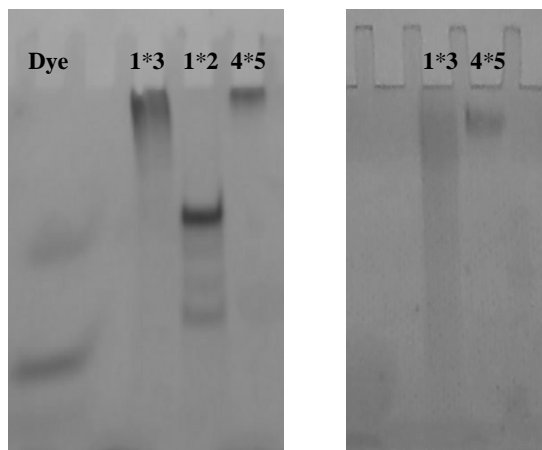


Figure 5.3. Nondenaturing 20% polyacrylamide gel of hybrids **1*3**, **1*2** and **4*5** (left) and of **1*3** and **4*5** (right). Conditions: Tris borate buffer, pH 7, 100V, 10mA, 5h (left) and 300V, 10 mA, 10h (right).

Circular dichroism (CD) spectral analysis of hybrid **4*5** is consistent with an overall *B*-conformation (Fig. 5.4). Temperature-dependent CD spectrum of hybrid **4*5** shows that we have exciton coupled CD below 40°C and above 40°C this phenomenon is no more observed. This is due to the melting of the duplex around 40°C ($T_m = 41.5^\circ\text{C}$). We have a helical arrangement which comes from the intense bisignate signal from the pyrene band centered at 367 nm, with a positive Cotton effect at 385 nm, followed by a minimum at 349 nm.

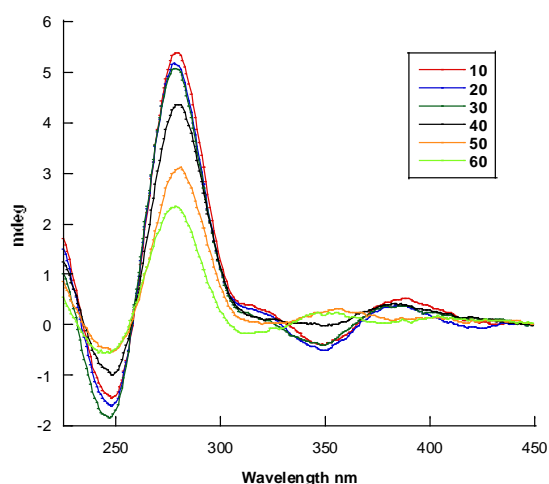


Figure 5.4 Temperature-dependent CD spectrum of duplex **4*5**. Conditions: 1.0 μM oligonucleotide concentration (each strand), 10 mM phosphate buffer (pH 7.4) and 100 mM NaCl.

Temperature-dependent UV-absorbance was achieved for hybrid **4*5** (Fig. 5.5). Interaction between pyrene and nucleobases can be observed in the temperature-dependent experiments. Increasing temperatures are associated with an increase in absorbance as well as a blue-shift in maximum absorbance in the range 300-400 nm, which corresponds to pyrene absorbance. The gradual change in temperature leads to an isosbestic point at 370 nm.

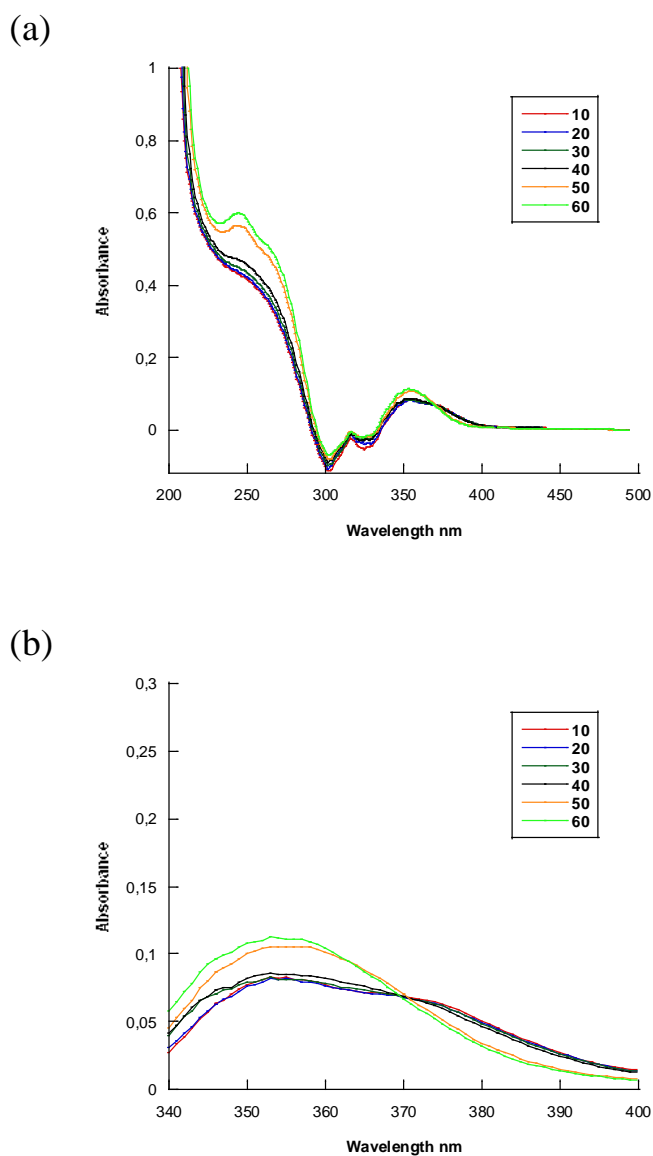
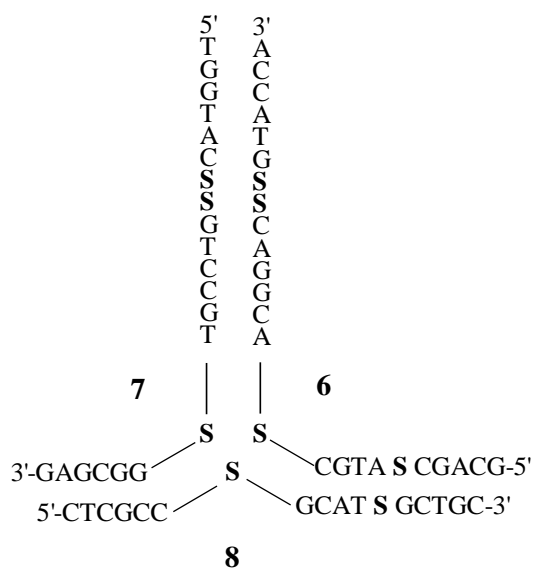


Figure 5.5. Temperature-dependent UV-absorbance of the hybrid **4*5** (a) showing an isosbestic point at 370 nm (b). Conditions: 1.0 μ M oligonucleotide concentration (each strand), 10 mM phosphate buffer (pH 7.4) and 100 mM NaCl.

5.3.2 Two-Dimensional DNA Scaffold Containing Pyrene Building Blocks

Oligonucleotides **6-8** were used for a two-dimensional DNA scaffold; single strands **6**, **7** and **8** were used to form a 3-way junction (*Scheme 5.2*). Our sequences were designed to have different number of nucleotides : 2×12 complementary bases for hybrid **6*7**, 2×9 for hybrid **6*8** and 2×6 for hybrid **7*8**. We decided to place two and two pyrene moieties in the middle of the long branch, one and one in the middle of the medium one and no pyrene in the short one to avoid destabilization. Three pyrene moieties were furthermore placed at the branch point of the structure.



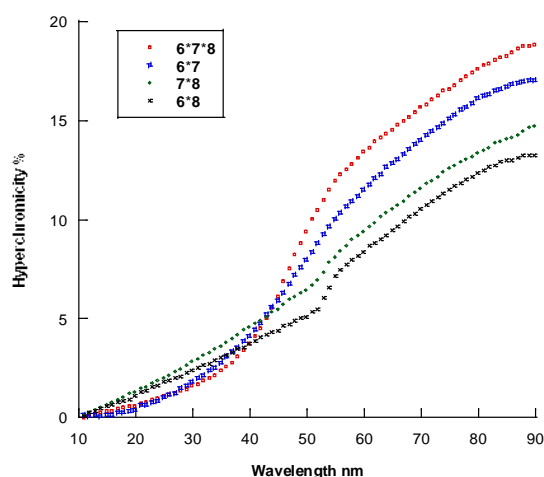
Scheme 5.2. 3-way junction containing pyrene building blocks.

The stability of the 3-way junction **6*7*8** and of its partial duplexes **6*7**, **7*8** and **6*8** was investigated (*Table 5.2* and *Fig. 5.6*). For hybrid **6*7** a transition was observed with a T_m of 49.5°C . For hybrids **7*8** and **6*8** no transitions are observed because the number of nucleotides for hybridization is probably too small. For the hybrid **6*7*8** a transition is observed with a T_m of 47.5°C . This transition is different from the hybrid **6*7** and the melting curve of **6*7*8** is more sharpened. This probably means that to be in the three-way form, the hybridization of **6** and **7** with its 12 complementary bases should be the driving force to form the first part of the three-way junction and that **8** should hybridize with the partial duplex **6*7** only when this one is already formed.

Table 5.2. Hybridization data of different oligonucleotide duplexes containing pyrene-based building blocks.

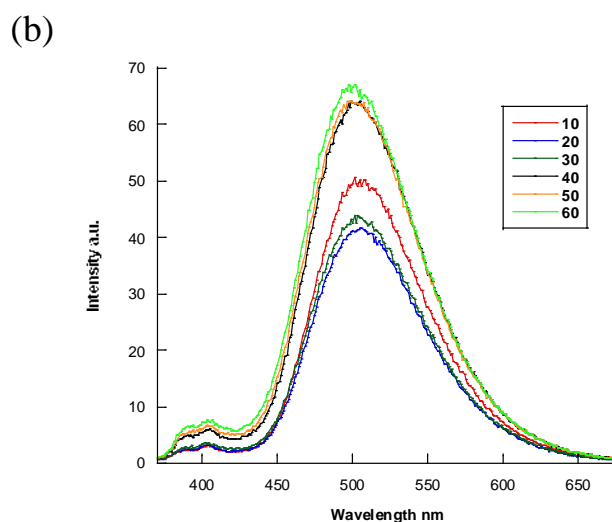
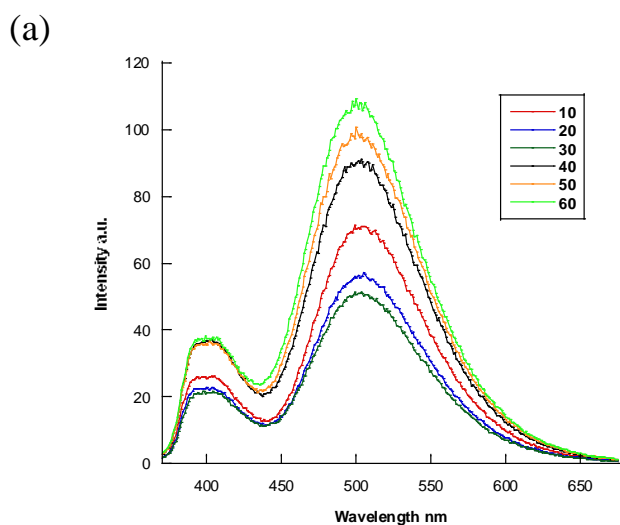
Oligo #	Duplex	T _m [°C]
6	(5') GCA GCS ATG CSA CGG ACS SGT ACC A	49.5
7	(5') TGG TAC SSG TCC GTS GGC GAG	
7	(5') TGG TAC SSG TCC GTS GGC GAG	- ^{a)}
8	(5') CTC GCC SGC ATS GCT GC	
6	(5') GCA GCS ATG CSA CGG ACS SGT ACC A	- ^{a)}
8	(5') CTC GCC SGC ATS GCT GC	
6	(5') GCA GCS ATG CSA CGG ACS SGT ACC A	
7	(5') TGG TAC SSG TCC GTS GGC GAG	47.5
8	(5') CTC GCC SGC ATS GCT GC	

Conditions: 1.0 μ M oligonucleotide concentration (each strand), 10 mM phosphate buffer (pH 7.4) and 100 mM NaCl; 0.5°C/min; absorbance measured at 260 nm. a) No clear transition observed.

**Figure 5.6** Melting curves of different duplex hybrids. Conditions: 1.0 μ M oligonucleotide concentration (each strand), 10 mM phosphate buffer (pH 7.4) and 100 mM NaCl.

Temperature-dependent fluorescence experiments were performed with single strands **6**, **7** and **8** (Fig. 5.7). Strand **6** (a) contains four pyrene units where two of them are adjacent. We should observe monomer from the two pyrene units which are far in space and excimer from the two pyrene units which are adjacent. As expected, a strong excimer band with a maximum emission at 503 nm and a monomer band around 400 nm are observed. Strand **7** (b) contains three pyrene units where two of them are adjacent. We should observe monomer from one pyrene unit and excimer from the two pyrene units which are adjacent. As expected, a strong excimer band with a maximum of emission at 504 nm and a monomer band around

400 nm are observed. We notice that the signal of the monomer of **7** is smaller than the signal of the monomer of **6**. This happens because **6** contains two pyrenes which show monomer and **7** only one and also because in strand **7** one of the pyrene unit is next to a guanine which is known to have quenching properties. Strand **8** (c) contains two pyrene units which are far in space. We should only observe monomer from these two pyrenes. As expected, a monomer band around 400 nm is observed. The signal is rather weak because each pyrene unit is next to a guanine.



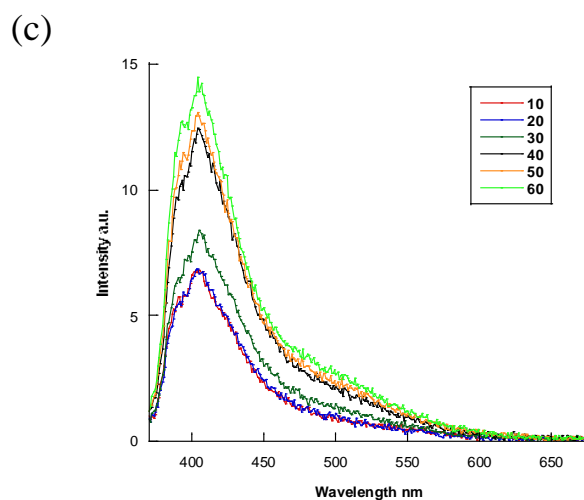


Figure 5.7. Temperature-dependent fluorescence spectra of single strands **6** (a), **7** (b) and **8** (c). Conditions: 1.0 μM oligonucleotide concentration (each strand), 10 mM phosphate buffer (pH 7.4) and 100 mM NaCl.

Temperature-dependent fluorescence experiments were carried out for hybrids **6*7**, **7*8**, **6*8**, and **6*7*8** (Fig. 5.8). Hybrid **6*7** (a) shows a weak signal of monomer, an important excimer signal at 511 nm and at high temperature a blue shift is observed at 500 nm which is characteristic to the denaturation of a duplex containing pyrene moieties (T_m 49.5°C). Hybrids **7*8** (b) and **6*8** (c) don't show the same behaviour as hybrid **6*7**. The signal of hybrid **7*8** is the sum of the signals of **7** and **8** and the signal of hybrid **6*8** is the sum of the signals of **6** and **8**. No melting temperature were obtained for these two hybrids and the fluorescence experiments confirm here that we are in single strand forms for hybrids **7*8** and **6*8**. Hybrid **6*7*8** (d) shows a weak signal of monomer and an important excimer signal at 510 nm at high temperature a blue shift is observed at 499 nm (T_m 47.5°C). The temperature-dependent spectra of hybrid **6*7** and **6*7*8** look similar but we can still notice a difference in the reduction of the signal with the temperature. Effectively, the signal of hybrid **6*7** decreases from 10°C till 40°C with a important jump at 50°C and the signal of hybrid **6*7*8** stay constant till 40°C with then the same important jump at 50°C. The difference of intensity at 40°C between hybrids **6*7** and **6*7*8** corresponds to 40 units. These results let us think that a three-way junction is formed by hybrid **6*7*8**.

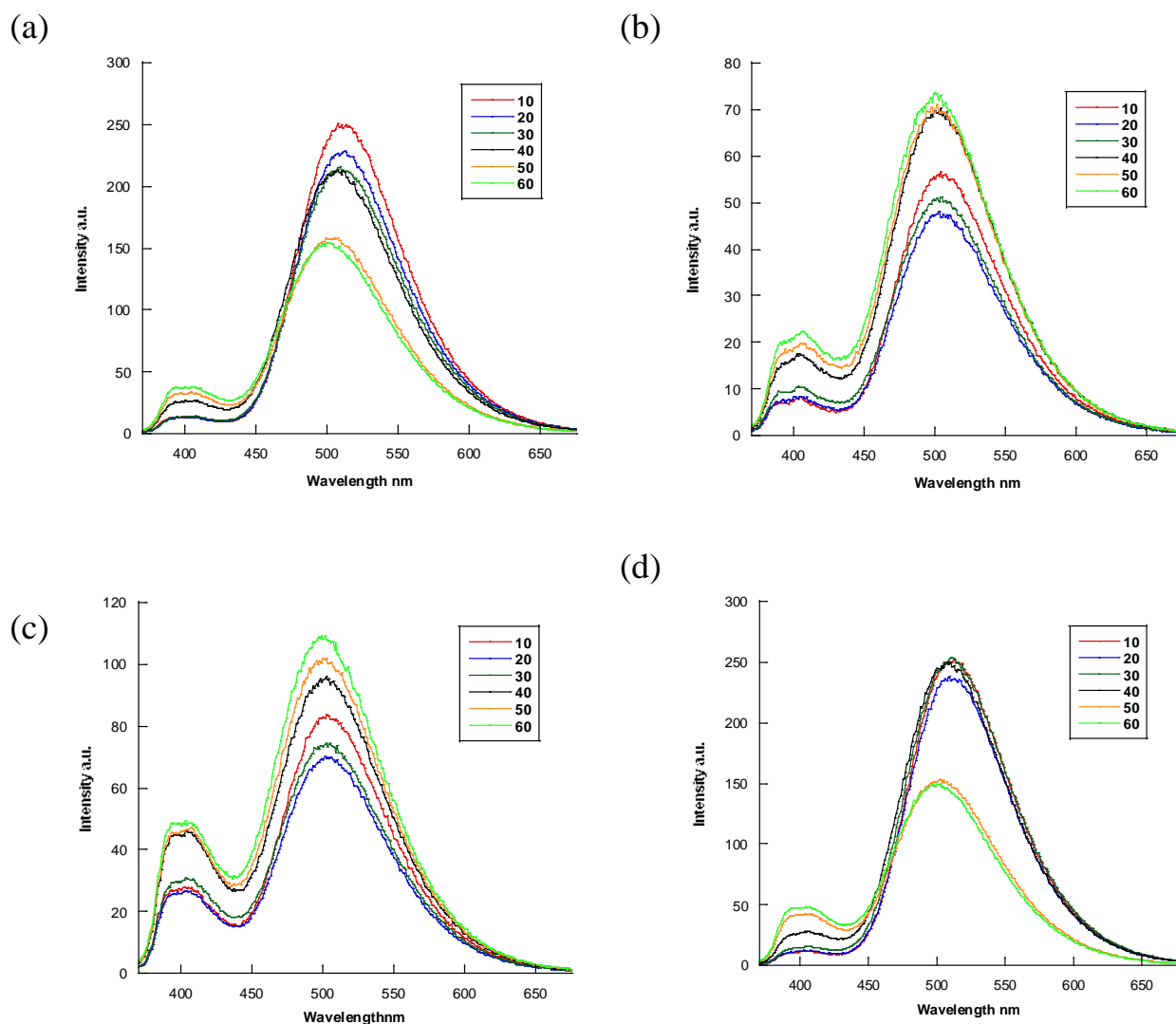


Figure 5.8. Temperature-dependent fluorescence spectra of hybrid **6*7** (a), **7*8** (b), **6*8** (c), and **6*7*8** (d). Conditions: 1.0 μM oligonucleotide concentration (each strand), 10 mM phosphate buffer (pH 7.4) and 100 mM NaCl.

Gel electrophoresis was performed to complete this study (Fig. 5.9). We observed a single band for **6**, **7** and **8** which corresponds to single strands. For hybrid **6*7**, we observed a single band which corresponds to a duplex. For hybrids **7*8** and **6*8**, we observed 2 bands which correspond to 2 single strands because no duplex was formed. For **6*7*8**, we observed the band of the three way junction which has a lower mobility than the other hybrids. This experiment strongly suggests that the 3-way junction was formed.

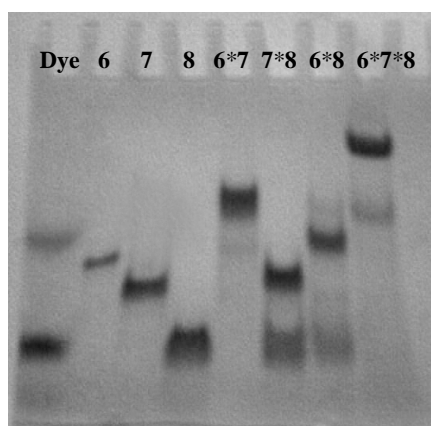


Figure 5.9. Nondenaturing 20% polyacrylamide gel of single strands **6**, **7**, **8** and of hybrids **6*7**, **7*8**, **6*8** and **6*7*8**. Conditions: Tris borate buffer, pH 7, 100V, 10mA, 5h.

Circular dichroism (CD) spectral analysis of hybrid **6*7*8** is consistent with an overall *B*-conformation (Fig. 5.10). Temperature-dependent CD spectrum of hybrid **6*7*8** shows that we have exciton coupled CD in the pyrene absorption area below 40°C. Above 40°C, the three-way junction starts to melt ($T_m = 47.5^\circ\text{C}$). We have a helical arrangement that is illustrated by the intense bisignate signal from the pyrene band centered at 357 nm, with a positive Cotton effect at 365 nm, followed by a minimum at 332 nm.

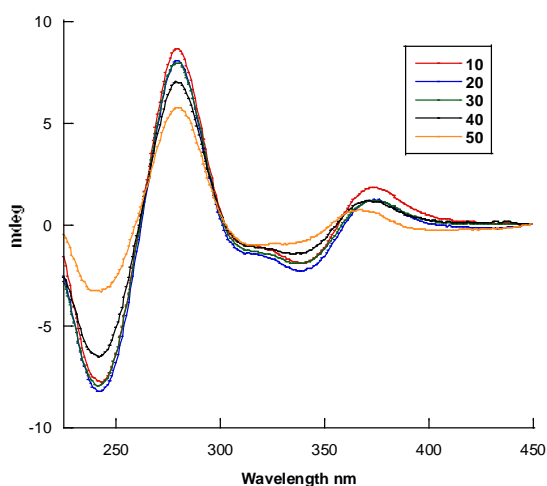


Figure 5.10. Temperature-dependent CD spectrum of duplex **6*7*8**. Conditions: 1.0 μM oligonucleotide concentration (each strand), 10 mM phosphate buffer (pH 7.4) and 100 mM NaCl.

Temperature-dependent UV-absorbance was achieved for hybrid **6*7*8** (Fig. 5.11). Interaction between pyrene and nucleobases can be observed in the temperature-dependent experiments. Increasing temperatures are associated with an increase in absorbance as well as a blue-shift in maximum absorbance in the range 300-400 nm, which corresponds to pyrene absorbance. The gradual change in temperature leads to an isosbestic point at 368 nm.

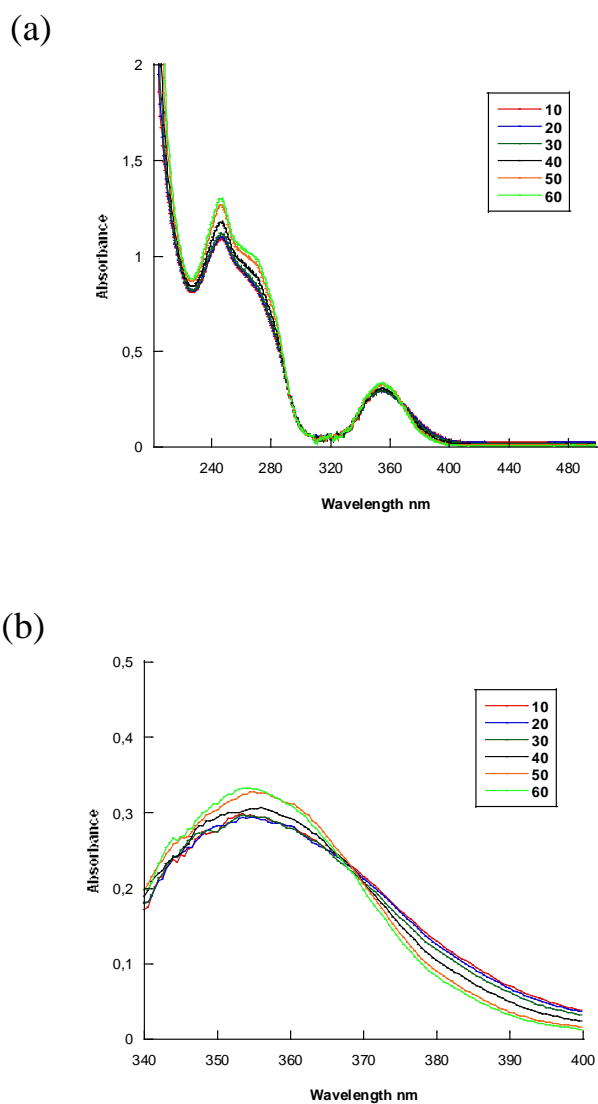


Figure 5.11. Temperature-dependent UV-absorbance of the hybrid **6*7*8** (left, full spectrum) showing an isosbestic point at 368 nm (right). Conditions: 1.0 μ M oligonucleotide concentration (each strand), 10 mM phosphate buffer (pH 7.4) and 100 mM NaCl.

5.4 Conclusions

Two different DNA scaffolds containing pyrene building blocks were constructed for DNA self-assembly. The one-dimensional framework containing pyrene moieties shows assembly along the double strand by fluorescence experiments and by gel electrophoresis. For the moment we are not able to know the length of this extended duplex. The design of the three-way junction was a success. Effectively, the length of the branches and the different numbers of pyrene units per branch was an advantage for our study. The long partial duplex seems to be the driving force of the formation of the three-way junction. By fluorescence experiments we were able to follow the formation of partial duplexes and also the formation of the three-way junction. Gel electrophoresis experiments confirm our hypothesis. This study might be useful to guide the future design of DNA nanostructure which is important in order to achieve sophisticated structures and potential technological applications, such as nanofabrications¹⁵⁻¹⁶ and organizing nano-electronic devices.¹⁷⁻²⁰

5.5 Experimental part

General. - Reactions were carried out under N₂ atmosphere using anhydrous solvents. Flash column chromatography was performed using silica gel 60 (63-32 μM, *Chemie Brunschwig AG*). If compounds were sensitive to acid, the silica was pre-treated with solvent containing 1% Et₃N. All NMR spectra were measured at room temperature on a *Bruker AC-300* spectrometer. ¹H-NMR spectra were recorded at 300 MHz. Chemical shifts (δ) are reported in ppm relative to the residual undeuterated solvent (CDCl₃: 7.27 ppm). Multiplicities are abbreviated as follows: *s* = singlet, *d* = doublet, *t* = triplet, *q* = quadruplet, *m* = multiplet. ¹³C-NMR spectra were recorded at 75 MHz. Chemical shifts are reported in ppm relative to the residual non-deuterated solvent (CDCl₃: 77.00 ppm). ³¹P-NMR spectra were recorded at 122 MHz. Chemical shifts are reported in ppm relative to 85% H₃PO₄ as an external standard. Electron impact mass spectra (EI-MS) was performed.

Synthesis of the pyrene building block. The required pyrene building block with a three carbon linker was synthesized according to the published procedure.

Synthesis and analysis of oligonucleotides. Cyano phosphoramidites from *Transgenomic* (Glasgow, UK) were used for oligonucleotide synthesis. Oligonucleotides **5-10** were prepared via automated oligonucleotide synthesis by a standard synthetic procedure ('trityl-off' mode) on a 394-DNA/RNA synthesizer (*Applied Biosystems*). Cleavage from the solid support and final deprotection was done by a treatment with 33% NH_4OH at 50°C for 8 hours. All oligonucleotides were purified by reverse phase HPLC (LiChrospher 100 RP-18, 5 μm , Merck, *Bio-Tek instrument Autosampler 560*); eluent A = $(\text{Et}_3\text{NH})\text{OAc}$ (0.1 M, pH 7.4); eluent B = 80 % of MeCN + 20 % of eluent A; gradient 5-35% B over 20 min at 25°C . ESI-MS (negative mode, $\text{CH}_3\text{CN}/\text{H}_2\text{O}/\text{TEA}$) of oligonucleotides was performed with a *Sciex QSTAR pulsar*, (hybrid quadrupole time-of-flight mass spectrometer, *Applied Biosystems*); data of oligomers **1-8** are given in *Table 5.3*.

Table 5.3. Mass spectrometry data (molecular formula, calc. average mass, and obtained).

<i>N</i> ^o	<i>Oligonucleotides</i>	<i>Molecular formula</i>	<i>Calc. mass</i>	<i>Found</i>
1	(5') AGC TCA GGT CAC GAG ATG TGC A	$\text{C}_{215}\text{H}_{269}\text{N}_{88}\text{O}_{128}\text{P}_{21}$	6784.5	6786
2	(3') TCG AGT CCA GTG CTC TAC ACG T	$\text{C}_{213}\text{H}_{271}\text{N}_{78}\text{O}_{132}\text{P}_{21}$	6686.4	6687
3	(3') GCT CTA CAC GTT CGA GTC CAG T	$\text{C}_{213}\text{H}_{271}\text{N}_{78}\text{O}_{132}\text{P}_{21}$	6686.4	6688
4	(5') AGC TCS GGT CAC GAG ASG TGC A	$\text{C}_{243}\text{H}_{290}\text{N}_{85}\text{O}_{128}\text{P}_{21}$	7099.4	7101
5	(3') GCT CTS CAC GTT CGA GSC CAG T	$\text{C}_{241}\text{H}_{292}\text{N}_{75}\text{O}_{132}\text{P}_{21}$	7001.3	7003
6	(5') GCA GCS ATG CSA CGG ACS SGT ACC A	$\text{C}_{299}\text{H}_{347}\text{N}_{93}\text{O}_{144}\text{P}_{24}$	8289.8	8292
7	(5') TGG TAC SSG TCC GTS GGC GAG	$\text{C}_{248}\text{H}_{290}\text{N}_{76}\text{O}_{126}\text{P}_{20}$	6970.1	6972
8	(5') CTC GCC SGC ATS GCT GC	$\text{C}_{191}\text{H}_{230}\text{N}_{56}\text{O}_{102}\text{P}_{16}$	5437.3	5438

Thermal denaturation experiments were carried out on a *Varian Cary-100 Bio-UV/VIS* spectrometer equipped with a *Varian Cary-block* temperature controller and data were collected with *Varian WinUV* software at 260 nm (cooling-heating-cooling cycles in the temperature range of $10\text{-}90^\circ\text{C}$, temperature gradient of $0.5^\circ\text{C}/\text{min}$). Experiments were carried

out for 1.0 μM oligonucleotide concentration (each strand), 10 mM phosphate buffer and 100 mM NaCl at pH 7.4. Data were analyzed with *Kaleidagraph software* from *Synergy software*. Melting temperature (T_m) values were determined as the maximum of the first derivative of the smoothed melting curve.

Temperature dependent UV/VIS spectra were collected in the range of 210-500 nm at 10-90 $^{\circ}\text{C}$ with a 10 $^{\circ}\text{C}$ interval on *Varian Cary-100 Bio-UV/VIS* spectrophotometer equipped with a *Varian Cary-block* temperature controller. All experiments were carried out at 1.0 μM oligonucleotide concentration (each strand) in phosphate buffer (10 mM) and NaCl (100 mM) at pH 7.4.

Fluorescence data were collected for 1.0 μM oligonucleotide solutions (1.0 μM of each strand in case of double strands) in phosphate buffer (10 mM) and NaCl (100 mM) at pH 7.4 on a *Varian Cary Eclipse* fluorescence spectrophotometer equipped with a *Varian Cary-block* temperature controller (excitation at 354 nm, excitation and emission slit width 10 and 5nm, respectively).

CD spectra were recorded on a *JASCO J-715* spectrophotometer using quartz cuvettes with an optical path of 1 cm.

Gel electrophoresis experiments. *BIORAD Mini-protean*, Power supply EPS 3500 XL, *Life technologies*, vertical gel electrophoresis glass plates were used. Non-denaturing 0.75 mm thick 20% polyacrylamide gels were prepared using acrylamide/bisacrylamide (19:1). A 10 \times TB buffer was prepared (90 mM Tris buffer, 90 mM boric acid) and the pH was adjusted to 7.0 using concentrated HCl. To 5 ml of this solution 5 μl of ammonium peroxide disulfate (10% in mQ H_2O) and 5 μl of N, N, N', N'-tetramethyldiamine (TEMED) were added. The gel was then poured between the plates and polymerized for at least 30 minutes. TB 1x buffer was used as electrophoresis buffer. The quantity of the loaded samples was about 900 pmol for each oligonucleotide. The oligomers were dried at speed vac and taken up in 10 μl of loading buffer (7% glycerol in TB buffer). The samples were then heated to 90 $^{\circ}\text{C}$ for 2 min, cooled down slowly to room temperature and then put on ice-water 0 $^{\circ}\text{C}$ for 5 minutes. Bromophenol blue was used as marker: 1 μg was dissolved in 1ml formamide; 2.5 μl of this solution was then added to 10 μl loading buffer. After conditioning of the gel (1 h at 100 V)

the samples were loaded onto the gel and electrophoresis was performed at 1) pH 7.0, 10 mA, 100 V and 300V for 5 h at 4 °C (Figure 5.3) or 2) pH 7.0, 10 mA, 100 V for 5 h at 4 °C (Figure 5.9). Bands were detected by UV shadowing on a TLC plate at 254 and 354 nm.

References

1. Whitesides G. M. and Grybowski B., *Science*, **2002**, 295, 2418-2421.
2. Altona C., Pikkemaat J. A., Overmarks F.J.J., *Curr. Opin. Struct. Biol.*, **1996**, 6, 305-316.
3. Lilley D. M. J., Clegg R. M., *Q. Rev. Biophys.*, **1993**, 26, 131-175.
4. Lilley D. M. J., Clegg R. M., *Annu. Rev. Biophys. Biomol. Struct.*, **1993**, 26, 131-175.
5. Seeman N. C., Kallenbach N.R., *Annu. Rev. Biophys. Biomol. Struct.*, **1994**, 53-86, *Ann. Rev. Inc., Palo Alto*.
6. Clegg R. M., Murchie A. I. H., Zechel A., Carlberg C., Diekmann S., Lilley D. M. J., *Biochemistry*, **1992**, 31, 4846-4856.
7. Cooper J. P., Hagerman P. J., *Biochemistry*, **1990**, 29, 9261-9268.
8. Eis P. S., Millar D. P., *Biochemistry*, **1993**, 32, 13852-13860.
9. Millar D. P., *Curr. Opin. Struct. Biol.*, **1996**, 6, 322-326.
10. Murchie A. I. H., Clegg R. M., von Kitzing E., Dukett D. R., Dieckmann S., Lilley D. M. J., *Nature*, **1989**, 341, 763-766.
11. Tuschl T., Gohlke C., Jovin T. M., Westhof E., Eckstein F., *Science*, **1994**, 266, 785-789.
12. Samain F., Malinovskii V. L., Langenegger S. M., Häner R., *Bioorg. Med. Chem.*, **2007**, in press (doi:10.1016/j.bmc.2007.04.052).
13. Malinovskii V. L., Samain F., Häner R., *Angew. Chem. Int. Ed.*, **2007**, 46, 4464-4467.
14. Langenegger S. M., Häner R., *Chem. Commun.*, **2004**, 2792-2793.
15. Braun E., Eichen Y., Sivan U., Ben-Yoseph G., *Nature*, **1998**, 391, 775-778.
16. Deng Z., Mao C., *Angew. Chem. Int. Ed.*, **2004**, 43, 4068-4070.
17. Alivisatos A. P., Johnsson K. P., Peng X., Wilson T. E., Loweth C. J., Bruchez, M. P., Schultz P. G., *Nature*, **1996**, 382, 609-611.
18. Mirkin C. A., Letsinger L., Mucic R. C., Storhoff J. J., *Nature*, **1996**, 382, 607-609.

19. Niemeyer C. M., Sano T., Smith C. L., Cantor C. R., *Nucleic Acids Res.*, **1994**, 22, 5530-5539.
20. Deng Z., Tian Y., Lee S. H., Ribbe A. E., Mao C., *Angew. Chem. Int. Ed.*, **2005**, 44, 3582-3585.

Chapter 6. Conclusions and Outlook

This work presents a study of three non-nucleosidic base surrogates: tetrathiafulvalene, anthraquinone and perylene diimide which were synthesized and incorporated into DNA as potential electro-donor or electro-acceptor building blocks. Another study was performed for a one- and a two- dimensional DNA scaffold containing pyrene units.

Four isomeric anthraquinone building blocks differing in the site of linker attachment were synthesized and incorporated into oligodeoxynucleotides. The site of linker attachment was found to have a strong influence on duplex stability. Effectively, a pair of the 2,6-isomer shows an increase in stability for DNA duplex. On the other hand, hybrids containing a pair of the 1,4-, 1,5- and 1,8-isomers led to a substantial reduction in stability. Molecular models suggest that the positive effect of the 2,6-isomer is a result of interstrand stacking interactions between the two anthraquinones. In the case of the other isomers investigated, such stacking interactions seem much less favourable. These anthraquinone derivatives represent useful building blocks for diagnostic tools or for applications in DNA-based nanomaterials.

Non-nucleosidic tetrathiafulvalene building block suitable for oligonucleotide synthesis under standard protocol was prepared. TTF-modified oligonucleotides form stable hybrids. Furthermore, photo-induced electron transfer was demonstrated by fluorescence quenching in TTF/pyrene modified heterohybrids. Finding shown in this study represent a setting for the development of TTF-oligonucleotide based redox-active and optical sensors for diagnostic. Study of electrochemical properties of TTF containing oligonucleotides attached to gold surface is under progress.

Oligonucleotides containing one or two incorporations of non-nucleosidic perylene diimide building block form stable duplexes. Fluorescence spectroscopy shows that two PDI opposite to two pyrene units are a powerful quencher for pyrene excimer. It was interesting to observe that a strong fluorophore like the PDI in the presence of DNA and water environment is not fluorescent. On the other hand, in the presence of another fluorophore like the pyrene which is able to form excimer the PDI is able to quench completely the signal of this excimer.

A possible further work in our group can be the design of a molecular beacon containing pyrene and PDI units. Molecular beacon probe assays utilize single-stranded hybridization probes that form a stem-and-loop structures (*Fig. 6.1*). A fluorophore is attached to one end of the oligonucleotide and a non-fluorescent quencher moiety is attached to the other end of the oligonucleotide. The stem hybrid brings the fluorophore and the quencher in close proximity, allowing energy from the fluorophore to be transferred directly to the quencher through contact quenching. At assay temperatures, when the probe encounters a target DNA or RNA molecule it forms a probe-target hybrid that is longer and more stable than the stem hybrid. At this moment the fluorescence is restored.

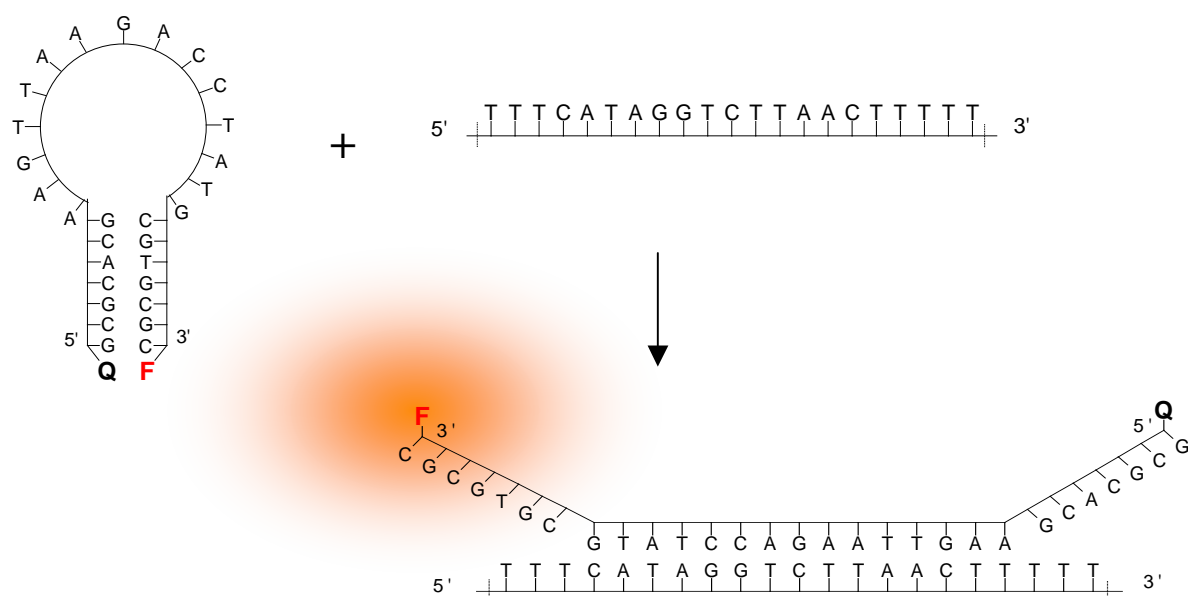


Figure 6.1 Principle of a molecular beacon.

Effectively, PDI and pyrene moieties are promising building blocks. Pyrene is able to form excimer and PDI is able to quench completely the fluorescence of this excimer. So two pyrene units opposite to two PDI units (same system as in chapter 4) can be used for molecular beacon type probes.

Annexes

Annexe 1: Chemical Synthesis of Oligonucleotides



Figure A.1. Nucleic Acid Synthesizer

Oligonucleotide synthesis is a remarkably simple process that has far reaching implications. Oligonucleotide synthesis is extremely useful in laboratory procedures (*Fig. A.1*). It is used to make primers crucial in methods such as PCR replication. Making a custom oligonucleotide is additionally useful because they will only bind to the region of DNA that is complementary to your custom oligonucleotide sequence. This allows specific segments of DNA to be amplified. In addition, custom oligonucleotide synthesis allows other sequences, such as restriction sites, to be added on to the desired oligonucleotide. Custom oligonucleotides are generally 15-20 bases in length which can limit how many additional sequences can be added on to the desired primer sequence.

Step 1: De-blocking

The first base, which is attached to the solid support, is at first inactive because all the active sites have been blocked or protected. To add the next base, the DMT group protecting the 5'-hydroxyl group must be removed. This is done by adding a base, either dichloroacetic acid (DCA) or trichloroacetic acid in dichloromethane (DCM), to the reaction column. The 5'-hydroxyl group is now the only reactive group on the base monomer. This ensures that the addition of the next base will only bind to that site. The reaction column is then washed to remove any extra acid and by-products (BioSource, 2003).

Step 2: Base Condensation

The next base monomer cannot be added until it has been activated. This is achieved by adding tetrazole to the base. Tetrazole cleaves off one of the groups protecting the phosphorus linkage (IDT, 2000). This base is then added to the reaction column. The active 5'-hydroxyl group of the preceding base and the newly activated phosphorus bind to loosely join the two bases together. This forms an unstable phosphite linkage. The reaction column is then washed to remove any extra tetrazole, unbound base and by-products (BioSource, 2003).

Step 3: Capping

When the activated base is added to the reaction column some does not bind to the active 5'-hydroxyl site of the previous base. If this group is left unreacted in a step it is possible for it to react in later additions of different bases. This would result in an oligonucleotide with a deletion. To prevent this from occurring, the unbound, active 5'-hydroxyl group is capped with a protective group which subsequently prohibits that strand from growing again. This is done by adding acetic anhydride and N-methylimidazole to the reaction column (IDT, 2000). These compounds only react with the 5'-hydroxyl group. The base is capped by undergoing acetylation. The reaction column is then washed to remove any extra acetic anhydride or N-methylimidazole (BioSource, 2003).

Step 4: Oxidation

In step 2 the next desired base was added to the previous base, which resulted in a unstable phosphite linkage. To stabilize this linkage a solution of dilute iodine in water, pyridine, and tetrahydrofuran is added to the reaction column (IDT, 2000). The unstable phosphite linkage is oxidized to form a much more stable phosphate linkage.

Repeat

Steps one through four are repeated until all desired bases have been added to the oligonucleotide (Fig. A.2). Each cycle is approximately 98/99% efficient (IDT, 2000).

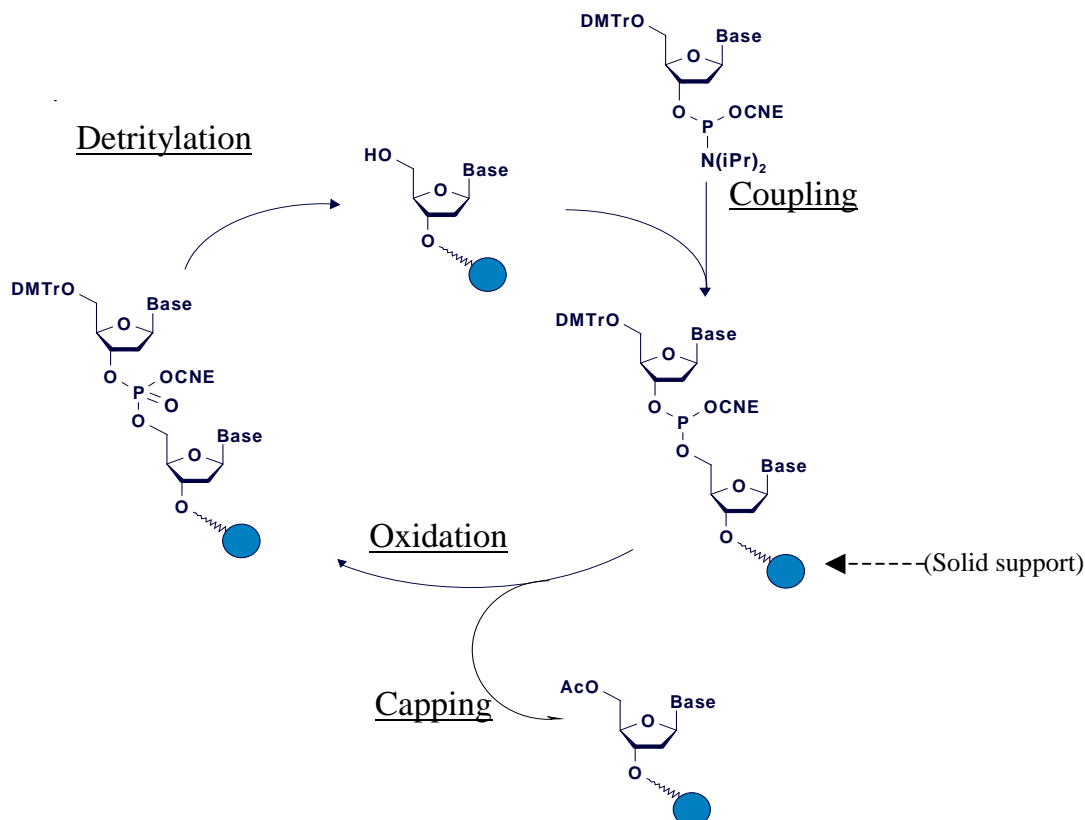


Figure A.2. Chain elongation cycle during automated DNA synthesis

Post Synthesis

After all bases have been added the oligonucleotide must be cleaved from the solid support and deprotected before it can be effectively used. This is done by incubating the chain in concentrated ammonia at a high temperature for an extended amount of time. All the protecting groups are now cleaved, including the cyanoethyl group, the heterocyclic protection groups, and the DMT group on the very last base (BioSource, 2003).

Final Product

The final product is a mixture of the sought after oligonucleotide, cleaved protective groups and oligonucleotides with internal deletions . This mixture of wanted and unwanted species is what the oligonucleotide synthesis companies send to the recipient. To obtain a solution only containing the desired oligonucleotide, the recipient must desalt the heterogeneous mixture.

Desalting

Desalting is done to purify the solution. It removes any species that may interfere with future reactions. The major problematic ingredient in the heterogeneous mixture is the ammonium ion. To filter the solution of the ammonium ions three different methods can be utilized. They are ethanol precipitation, size-exclusion chromatography, or reverse-phase chromatography (BioSource, 2003).

References:

BioSource International. 2003 Feb 10. BioSource home page. <http://www.biosource.com>

Integrated DNA Technologies. Copywrite 2000. IDT home page. <http://www.idtdna.com>

Purves, W., Sadava, D., Orians, G., Heller, H. 2001. Life: The Science of Biology. 6th ed. Sinauer Associates, Inc. p. 210-217.

Häner R., Oligonucleotide Technology – A Research Platform for Chemical Biology, Chimia 2001, 55, No.4.

Annexe 2 : DNA Single Strands Containing Pyrene Units

During the project of the two-dimensional DNA-scaffold, we made an interesting observation with the CD-spectra of two single strands containing pyrene units. Strands **1** and **2** contain four and three pyrene units placed at different positions.

Both strands show exciton coupling in the pyrene area (300-400 nm) which is characteristic to an association of some pyrene units (*Fig. A.2* and *Fig. A.3*). Exciton coupling was most of the time observed for duplexes and we never observed such an intense signal for single strands before. For single strand **1** and **2**, we observed a helical arrangement illustrated by the intense bisignate signal of the pyrene band centered at 353 nm, with a positive Cotton effect at 369 nm, followed by a minimum at 340 nm. The intensity of the signal of single strand **1** in the pyrene area is the same as the intensity of the signal in the B-DNA region (240-300 nm). For single strand **2**, the intensity of the signal in the pyrene region is lower but a band is more pronounced at 252-254 nm than for single strand **1**.

1 5'-GCAGC-Py-ATGC-Py-ACGGAC-PyPy-GTACCA-3'

2 5'-TGGTAC-PyPy-GTCCGT-Py-GGCGAG-3'

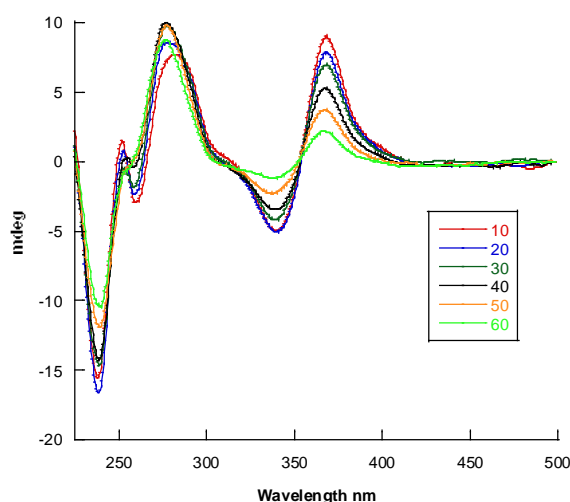


Figure A.2. Temperature-dependent CD spectrum of single strand **1**. Conditions: 2.0 μ M oligonucleotide concentration (each strand), 10 mM phosphate buffer (pH 7.4) and 100 mM NaCl.

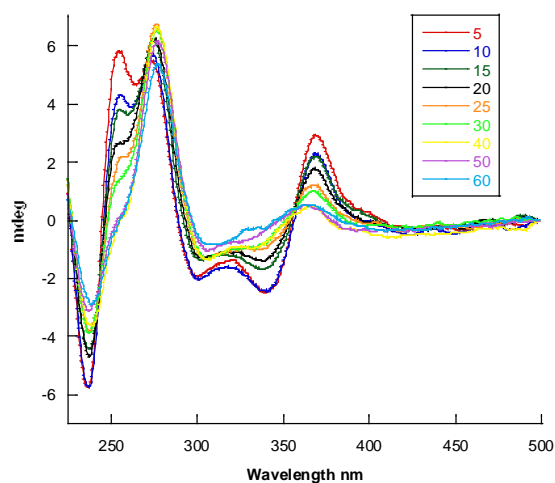


Figure A.3. Temperature-dependent CD spectrum of single strand **2**. Conditions: 2.0 μM oligonucleotide concentration (each strand), 10 mM phosphate buffer (pH 7.4) and 100 mM NaCl.

Thermal melting experiments were performed for single strands **1** and **2** (Table A.1, Fig. A.4 and Fig. A.5). T_m values were obtained for single strands **1** and **2** at 245 nm which is characteristic to pyrene absorption (T_m **1** = 68.9°C and T_m **2** = 69.4°C). At 350 nm where pyrene also absorbs, a transition was obtained for both but we were not able to see the plateau and to determine a T_m value. A reduction of salt concentration will probably show nice transitions for single strands **1** and **2**. At 260 nm (DNA absorption) no T_m value was obtained the curve is pretty linear for single strands **1** and **2**.

Table A.1. Thermal melting experiments of single strand **1** and **2** at 245, 260 and 350 nm.

oligonucleotide	T_m at 245 nm	T_m at 260 nm	T_m at 350 nm
1	68.9°C	-	n. d.
2	69.4°C	-	n. d.

Conditions: 2.0 μM oligonucleotide concentration (each strand), 10 mM phosphate buffer (pH 7.4) and 100 mM NaCl.

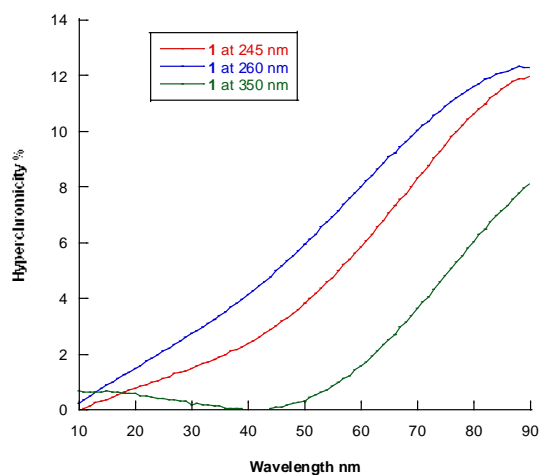


Figure A.4. Thermal melting experiments of single strand **1**. Conditions: 2.0 μM oligonucleotide concentration (each strand), 10 mM phosphate buffer (pH 7.4) and 100 mM NaCl.

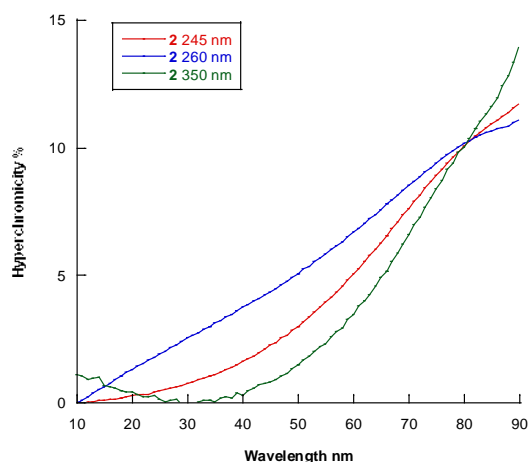


Figure A.5. Thermal melting experiments of single strand **2**. Conditions: 2.0 μM oligonucleotide concentration (each strand), 10 mM phosphate buffer (pH 7.4) and 100 mM NaCl.

These single strands cannot be self-complementary for duplex or partial duplex formation. An explanation of this phenomenon could be that a secondary structure is formed within single strands which means that pyrene units are probably forming aggregates in an organized way. Another explanation could be that pyrene units are stacked on DNA-bases (G for example : PyPy next to G for **1** and **2**) and then an organized system is formed.

Other experiments will be achieved to understand the existence of these exciton coupling and why a transition is obtained at 245 and 350 nm for single strand **1** and **2**.

Some new oligonucleotides have to be synthesized as reference :

For exemple for single strand 1:

5'-GCAGC-**Py**-ATGC-**Py**-ACGGAC-**PyPy**-GTACCA-3'

- by removing 1 pyrene unit at different places:

5'-GCAGCATGC-**Py**-ACGGAC-**PyPy**-GTACCA-3'

5'-GCAGC-**Py**-ATGCACGGAC-**PyPy**-GTACCA-3'

5'-GCAGC-**Py**-ATGC-**Py**-ACGGAC-**Py**-GTACCA-3'

- by removing 2 pyrenes units at different places :

5'-GCAGCATGCACGGAC-**PyPy**-GTACCA-3'

5'-GCAGCATGC-**Py**-ACGGAC-**Py**-GTACCA-3'

5'-GCAGC-**Py**-ATGCACGGAC-**Py**-GTACCA-3'

5'-GCAGC-**Py**-ATGC-**Py**-ACGGACGTACCA-3'

- by keeping pyrene units and by changing neighbouring bases :

5'-GCAG**C**-**Py**-**A**TGC-**Py**-**A**CGGAC-**PyPy**-**G**TACCA-3'

CURRICULUM VITAE

BOUQUIN Nicolas
Bahnhöheweg 40
3018 Bern
Born 31/12/1980 in Strasbourg
Nationality : French
Telephone number : +41764903112
Email : nicolas.bouquin@hotmail.fr



Current position: 4th year of PhD : Department of Chemistry and Biochemistry (Bern).
Person in charge : Prof. Dr. R. Häner.

EDUCATIONAL BACKGROUND

- 2004-2008 :** **Thesis in organic and bioorganic chemistry** at the University of Bern.
- 2003-2004 :** **DEA in organic chemistry** at the ECPM and at the University Louis Pasteur (Strasbourg).
- 2002-2004 :** **Engineering School** in chemistry at the ECPM (Strasbourg).
- 2001-2002 :** **Maîtrise de Chimie** at the University Louis Pasteur (Strasbourg) equivalent to MSc in Chemistry.
- 2000-2001 :** **Licence de Chimie** at the University Louis Pasteur (Strasbourg) equivalent to BSc in Chemistry.
- 1998-2000 :** **IUT Robert Schumann** (Strasbourg) equivalent to Higher National Diploma in Chemistry.
- 1997-1998 :** **General certificate of Education at Advanced Level.** A level in Maths, Physics, Chemistry and Technology.

PROFESSIONAL EXPERIENCE

- 2004-2008 :** **4 years' PhD in Organic Chemistry and Biochemistry** at the Department of Chemistry and Biochemistry of Bern. Person in charge: **Prof. Dr. R. Häner.** *Assembly of DNA-like structures containing Anthraquinone, Perylene diimide and Tetrathiafulvalene building blocks.*
- 2004 :** **6 months' training period at the ECPM** (Strasbourg). Specialized in Organic Synthesis. Person in charge: **Dr. F. Colobert.** *Synthèse du motif biarylique à chiralité axiale de la (-)-stéganacine.*
- 2003 :** **4 months' training period at CIBA** (Grenzach-Wyhlen – Germany). Organic Synthesis in research and development. Person in charge: **Dr. H. Hermann.**
- 2001-2002 :** **1 and 3 months' training period at the University Louis Pasteur** (Strasbourg). Specialized in Organic and Coordination Chemistry. Person in charge : **Prof. Dr. M.W. Hoesseni.** *Synthèse et caractérisation de ligands organiques dérivés de l'hexafluoroacétylacétonate.*
- 2000 :** **3 months' training period at the Institut Charles Sadron** (Strasbourg). Assistant lab in the polymers department. Persons in charge : **Dr. Y. Frère and Dr. L. Danicher.** *Synthèse de capsules biocompatibles.*

SKILLS

- Synthesis** **Organic synthesis** : advanced level.
Inorganic synthesis : good level.
Polymer synthesis : basic knowledge.
- Techniques** NMR (1D and 2D), MS spectrometry, IR, HPLC (normal phase, reverse phase and ion exchange), Fluorescence spectroscopy, CD spectroscopy, UV-vis spectroscopy, Gel electrophoresis, Synthesis of oligonucleotides.
- Informatic** **Laboratory software** : KaleidaGraph, Hyperchem, ChemOffice, Isis Draw, Spartan, Cambridge Data Base and Microsoft Office.
Bibliographic software :SciFinder, Beilstein.
- Other** **Engineering skills** : advanced level.

LANGUAGES

- French** : mother tongue.
English : advanced level. Diploma of TOEIC.
German : good level.

PUBLICATIONS

1. N. Bouquin, V. L. Malinovskii and R. Häner, **Anthraquinones as Artificial DNA Building Blocks**, *E. J. Org. Chem.*, **2008**, in press.
2. N. Bouquin, V. L. Malinovskii, Xavier Guégano, Shi-Xia Liu, Silvio Decurtins and R. Häner, **TTF-Modified DNA**, submitted.
3. N. Bouquin, V. L. Malinovskii and R. Häner, **Highly efficient quenching of excimer fluorescence by perylene diimide in DNA**, *Chem. Comm.*, **2008**, accepted.

MISCELLANEOUS

- Driving licence** : B.
Sport : fitness, tennis and ski.

REFEREES

Prof. Dr. Robert Häner
Department für Chemie und Biochemie
Universität Bern
Freiestrasse 3 CH-3012
Tel : +41 31 631 43 82
Email : robert.haener@ioc.unibe.ch

Dr. Françoise Colobert
ECPM
25, rue Becquerel
67087 Strasbourg
Tel : +333 90 24 27 77
Email : fcolober@chimie.u-strasbg.fr